UNIVERSITÄTSKLINIKUM HAMBURG-EPPENDORF

Zentrum für Geburtshilfe, Kinder- und Jugendmedizin
Klinik für Geburtshilfe und Pränatalmedizin

Prof. Dr. med. Kurt Hecher

The impact of prenatal stress on fetal lung development and its association with asthma in mice

Dissertation

zur Erlagung des Doktorgrades Dr. rer. biol. Hum. / PhD
an der Medizinischen Fakultät der Universität Hamburg.

vorgelegt von:

Dimitra Zazara
aus Athen (Griechenland)

Hamburg 2020

Angenommen von der
Medizinischen Fakultät der Universität Hamburg am: 12.02.2020

Veröffentlicht mit Genehmigung der
Medizinischen Fakultät der Universität Hamburg.

Prüfungsausschuss, der/die Vorsitzende: Prof. Dr. Petra Arck

Prüfungsausschuss, zweite/r Gutachter/in: Prof. Dr. Udo Schumacher

Prüfungsausschuss, dritte/r Gutachter/in: Prof. Dr. Udo Markert

Table of contents

1 Introduction

1.1 Fetal programming

The concept of fetal programming, also known as "the developmental origins of health and disease", underpins the role of intrauterine life as a crucial determinant of postnatal health (1, 2). Maternal exposure to adverse environmental conditions during pregnancy influences the intrauterine environment thereby interfering with normal fetal development and subsequently increasing the risk for diseases later in life (3-5). This concept is supported by numerous epidemiological studies revealing links between distinct prenatal challenges and altered risk for specific diseases in postnatal life. For example, poor maternal nutritional habits during pregnancy, including under-, over- or malnutrition, can increase the risk for obesity and hypertension in the offspring, whereas prenatal exposure to air pollutants or maternal smoking has been linked with a higher susceptibility to respiratory diseases, such as asthma, in childhood (6-9). Among other challenges, an enhanced risk for asthma, allergies and infections can also be seen in children that were prenatally exposed to an increased maternal stress perception (10-12), although the mechanisms underlying such connections remain largely elusive.

Strikingly, recent evidence highlights a constantly rising incidence of such chronic non-communicable diseases, including cardiovascular and allergic disorders (13, 14). This trend cannot be merely justified by genetic predisposition; it may largely be attributed to prenatal insults that program postnatal health. Therefore, insights into the mechanisms linking intrauterine challenges with poor postnatal health are required in order to identify the causes for the increasing onset of chronic diseases and, subsequently, to design preventive strategies and optimize therapeutic options.

1.2 Prenatal stress and fetal programming

For the successful progression and completion of pregnancy, maternal immune system adaptation takes place. In order to avoid rejection of the semi-allogeneic fetus that carries maternal and paternal, thus foreign to the mother, antigens, the maternal immune system undergoes modifications in cell phenotypes, counts and functions thereby acquiring a tolerogenic phenotype while, at the same time, largely maintaining intact defense capabilities (3, 15). Exogenous and endogenous factors can challenge the adaptational processes thereby disrupting normal fetal growth and development and, in turn, increasing offspring's postnatal susceptibility to chronic diseases such as cardiovascular, metabolic and immune disorders (4). Prenatally occurring environmental challenges that may interfere with maternal immune

adaptation and result in poor fetal development, include nutritional insults, such as overnutrition or lack of nutrients (16, 17), maternal viral infections (18-20), medication (21, 22), as well as high maternal stress perception (23, 24).

The role of maternal stress during pregnancy as a determinant of fetal growth and postnatal health is well recognized. Epidemiological studies underline an association between prenatal stress exposure and adverse pregnancy as well as birth outcomes, evident as decreased length of gestation and intrauterine growth restriction (25). Similarly, impaired fetal growth was also observed in a mouse model of mid-gestational stress challenge (26).

Interestingly, apart from its effects on birth outcome, prenatal exposure to maternal stress may have long-term consequences on the offspring's health. For example, the prenatally stress challenged offspring are more likely to develop mental disorders, including depression, schizophrenia and autism (27-31), cardiovascular and metabolic diseases (32-34) as well as diabetes mellitus type 1 (35). Strikingly, the prenatal stress-related susceptibility to most of these diseases is higher in the male offspring (36-38), although prenatally stress-challenged girls may also exhibit an increased risk for diabetes mellitus type 1(35).

Furthermore, mounting evidence indicates that prenatal stress exposure may predispose the offspring to poor immunity, manifested as an increased risk for infectious diseases (11, 12) as well as atopic disorders including asthma, allergic rhinitis and dermatitis (10, 39, 40) later in life. This association between prenatal stress challenge and an increased susceptibility to an asthmatic phenotype was supported by studies in mice showing enhanced airway hyperresponsiveness and inflammation in response to experimental asthma induction in prenatally stress challenged adult offspring (41). In humans, a higher risk for asthma and atopic dermatitis was observed in 14-year old children born to mothers that had been exposed to adverse life events during late pregnancy (10). Similarly, studies in Mexico and USA reported a link between maternal stress during pregnancy and wheezing in childhood (42, 43). Interestingly, sex specificity was also observed in this context, with most of the studies showing that female children are more susceptible to prenatally programmed asthma and wheezing following maternal stress during pregnancy (42, 44-46).

Despite the well-documented link between prenatal stress challenge and poor postnatal health, the mechanisms underlying the programming effect of maternal stress are not completely elucidated. As discussed previously, maternal stress exposure interferes with the maternal immune adaptation to pregnancy at the fetomaternal interface, thereby favoring the acquisition of a pro-inflammatory rather than a tolerogenic immune phenotype (26, 47, 48). Additionally, maternal progesterone, a hormone crucially involved in initiation and successful completion of

pregnancy as well as normal fetal growth and development (23), is decreased upon stress exposure (26). A reduction of placental blood flow is also observed in stress-challenged pregnancies, an effect compromising fetal nutrition and oxygen supply, thereby causing fetal oxidative stress due to high reactive oxygen species production (49). An oxidative environment may in turn affect the developing fetal tissues and increase the risk for atopy later in life (39, 50).

Along with these alterations, maternal exposure to stress may directly interfere with fetal development. High maternal stress perception leads to maternal hypothalamic-pituitary-adrenocortical (HPA) axis activation with a subsequent high secretion of glucocorticoids. In mammalian pregnancies, glucocorticoids are essential for normal fetal growth. The development and maturation of organs like the fetal lung, intestine, brain and liver is driven by glucocorticoids (51). Despite their central role in prenatal development, fetal exposure to maternal glucocorticoids needs to be tightly regulated. To this end, the placenta acts as a barrier preventing excessive glucocorticoid transfer from the mother to the fetus, through the actions of 11β-hydroxysteroid dehydrogenase type 1 (11β-HSD1) and type 2 (11β-HSD2). While the former converts inactive cortisone to cortisol in humans or 11-deoxycorticosterone to corticosterone in rodents, the latter inactivates glucocorticoids and therefore, is a major regulator of transplacental glucocorticoid flow (52).

However, elevated maternal circulating glucocorticoids, secreted due to stress or administered as treatment to maternal conditions like asthma, manage to overcome the placental barrier and enter the fetal circulation (53). High circulating glucocorticoids interfere with the development of the fetal endocrine system and alter the expression of several growth factors, hormones and hormone receptors in fetal tissues (54). Such an endocrine imbalance and altered glucocorticoid-mediated signaling pathways may be detrimental for fetal organs such as the lung, which depend on glucocorticoids for their growth and maturation.

Several studies attribute the fetal programming effect of prenatal maternal stress on epigenetics. The term “epigenetics” describes distinct heritable changes in gene activity and expression without alterations in DNA sequence. The main epigenetic modifications include DNA methylation, histone modification and microRNA-mediated gene silencing (55). Although epigenetic modifications are crucially involved in normal fetal development and tissue differentiation, recent studies suggest that intrauterine challenges, such as increased maternal stress perception, may induce distinct epigenetic modifications and thus, long-term changes in gene function, thereby programming postnatal health and disease (56-58).

1.3 Asthma

Asthma is one of the most common health problems affecting >300 million people worldwide. Most cases of asthma begin in childhood and are associated with atopy (59). The reported global prevalence of childhood asthma is approximately 14% and is constantly increasing (9, 60, 61). However, asthma is not constant throughout life. Remission of the existing disease or relapse in adulthood may occur (62). Similarly, apart from the early-onset allergic asthma, adult-onset non-allergic forms of the disease are reported (63), but they exceed the purpose of this work and will not be further discussed. An additional determinant of the prevalence of the disease is sex. Whereas asthma is more common among preadolescent boys, this trend reverses in puberty and adulthood, when females seem to be more frequently affected (64).

Although effective treatments are broadly available, asthma-related morbidity is high. Children with asthma experience a poor quality of life associated with decreased exercise tolerance as well as frequent hospitalization and subsequent chronic school absenteeism (65). The absence of curative strategies might be due to our poor understanding of asthma's etiology and pathogenesis. Although asthma occurs largely due to a crosstalk between genetic and environmental factors, no single gene or environmental factor has been identified as cause of the disease. Since the etiology of asthma appears to be multifactorial, several genes have been associated with asthma, with the most prominent candidate being *ADAM33,* a gene coding for the disintegrin and metalloproteinase domain-containing protein 33. *ADAM33,* expressed in the fetal lung mesenchymal compartment and postnatally in smooth muscle cells of bronchi and pulmonary fibroblasts, was recently identified as an asthma susceptibility gene and seems to play a role in lung development, asthma-related bronchial hyperresponsiveness and airway remodeling (66-68).

Mounting evidence suggests that childhood asthma may have its origin – at least partially- in fetal life. Since the pathogenesis of asthma relies both on immune and lung dysfunction, with current theories identifying the airway epithelium as the key orchestrator of the disease (69), intrauterine challenges interfering with fetal immune system or lung development may be responsible for the fetal programming of asthma.

1.3.1 Hallmarks of asthma

Asthma is defined as a chronic inflammatory disorder of the conducting airways, which tend to contract too fast and intensely either spontaneously or in response to several environmental or endogenous factors. In acute asthma exacerbations, exposure to allergens results in a quick

bronchoconstriction and airway narrowing with subsequently severe airflow reduction. Mast cells are critical effectors of this allergen-triggered reaction. Specifically, upon immunoglobulin E (IgE)-mediated stimulation, mast cell degranulation results in the secretion of mediators such as histamine, tryptase, leukotrienes, and prostaglandins that directly cause airway smooth muscle contraction (70). Such a bronchoconstrictor response can be elicited by a wide variety of stimuli and is defined as airway hyperresponsiveness.

Apart from this enhanced airway responsiveness to stimuli, the hallmarks of asthma include acute or chronic airway inflammation, mucus hypersecretion and airway remodeling. The latter refers to permanent structural changes in the airways, including epithelial shedding, basal membrane thickening, goblet cell hyperplasia and increased mucus production, subepithelial fibrosis, airway smooth muscle hypertrophy and hyperplasia as well as angiogenesis and vasodilation (71).

Collectively, all these features account for the heterogeneity of asthma in terms of clinical manifestation and response to treatment, but also point toward a multifaceted pathogenesis of the disease (72). Although once defined as a pure allergic disorder relying on Th2 immune responses, increasing evidence reveals a pathogenic role for the airway epithelium that appears to prepare the ground for a persistent inflammatory phenotype, which, in turn, due to defective local injury-repair pathways, results in airway remodeling (69). Additional exposure to environmental factors such as allergens and pollutants perpetuates the ongoing pathogenic processes and ensures disease chronicity.

1.3.2 Pathogenesis of asthma

Airway inflammation, a fundamental component of asthma pathogenesis, is mainly based on Th2 immune responses orchestrated by several immune cell populations, including, apart from CD4+T cells, eosinophils, neutrophils, mast cells and macrophages, with eosinophilia being the most prominent feature (64, 73). While early-stage inflammation affects only the conducting airways, both small airways and alveoli are infiltrated in later stages due to disease progression.

A crucial role in the initiation of inflammation in asthma plays the airway epithelium, which can recognize environmental antigens and secrete cytokines that drive the Th2 immune cascade. Subsequently, dendritic cells located in the airways capture and process the inhaled allergens and ultimately, migrate to secondary lymphoid tissues where presentation of antigens to T lymphocytes is performed (74). With this step, allergen sensitization is established and a subsequent allergen-specific immune response commences (75).

Upon sensitization, T cells, and especially Th2 cells, infiltrate the airways and facilitate the secondary recruitment of macrophages, basophils and eosinophils that accumulate locally and sustain inflammation. The eosinophils predominate in the inflammatory sites and can also be found in the sputum and bronchoalveolar lavage (BAL) fluid of asthmatic individuals (76). Overall, eosinophils are crucially involved in the perpetuation of the allergic inflammation while, in parallel, contributing to airway hyperresponsiveness, mucus hypersecretion and airway remodeling. Following activation of eosinophils, degranulation occurs and chemical mediators, such as eosinophil peroxidase, major basic protein and eosinophil cationic protein, are released from small granules located in the cytoplasm of eosinophils. Secreted leukotrienes as well as cytokines such as IL-13 promote airway hyperresponsiveness and mucus hypersecretion, two main hallmarks in asthma pathogenesis, by acting on airway smooth muscle cells or enhancing goblet cell differentiation, respectively (77, 78). By secreting highly charged basic proteins with cytotoxic effects, eosinophils exert tissue damaging effects that result in chronic aberrant activation of repair pathways and ultimately, contribute to the asthma-related airway remodeling.

Although eosinophils are, undoubtedly, in the center of asthma pathogenesis, high numbers of macrophages are also found in the asthmatic lung, suggesting that these cells have a critical role in the development of lung pathology in asthma. Two main subtypes of macrophages can be found in the lung tissue, namely the alveolar macrophages (alvMac), which comprise the most abundant macrophage population and are located in the alveoli and the airway lumen, and the interstitial macrophages (intMac) that inhabit the interstitium (79). However, mainly the alvMac have been implicated in the development and progression of asthma. Studies in humans and mice report a dual immunomodulatory role for alvMac in asthma. On the one hand, alvMac perpetuate airway inflammation and underlying tissue injury by releasing pro-inflammatory cytokines including tumor necrosis factor (TNF), IL-1, and IL-8, as well as reactive oxygen intermediates, but on the other hand, they perform immunosuppressive functions by secreting anti-inflammatory mediators such as IL-10, IL-12 and nitric oxide in an effort to prevent excessive inflammation and maintain tissue homeostasis (80).

Apart from alvMac, regulatory T cells (Tregs) are also critically involved in sustaining tissue homeostasis, with the secretion of the anti-inflammatory cytokine IL-10 likely playing a central role in their immunosuppressive function (81, 82). Tregs are defined as $CD4^+CD25^+$ and are characterized by the expression of the forkhead/winged-helix transcription factor FOXP3 (83). An implication of Tregs in allergic disorders was first suggested by human studies showing that FOXP3 mutations are responsible from the immune dysregulation, polyendocrinopathy,

enteropathy, and X-linked inheritance syndrome, with affected patients also suffering from atopic dermatitis (84). Subsequent studies highlighted an association between decreased Treg frequency in the peripheral blood or impaired immunosuppressive function with the manifestation of an allergic disease (85-87). Interestingly, a study focusing on pediatric asthma demonstrated that, in asthmatic children, pulmonary Tregs are low in number and unable to suppress Th2 immune responses. However, upon inhaled corticosteroid treatment, this quantitative and functional deficit is restored (88). Overall, published evidence links asthma with Treg decrease and dysfunction and identifies this cellular population as a potential therapeutic target.

Apart from aberrant immune responses, the airway epithelium emerges as a key player in asthma pathogenesis (69). Under normal conditions, the airway epithelium serves as a tightly regulated impermeable barrier that strictly controls interactions with the environment. The barrier function of the airway epithelium relies mainly on the formation of tight junctions, which are apical intercellular complexes consisting of several proteins including claudins, zonula occludens-1 (ZO-1) and transmembrane adhesion proteins (89). Apart from tight junctions, cell-to-cell and cell-to-extracellular matrix interactions through desmosomes, E-cadherin and hemidesmosomes contribute to epithelial barrier integrity (90). However, in asthma, disruption of tight junctions and desmosome structures compromises the integrity of the barrier and increases the permeability of the airway epithelium thereby facilitating the passage of inhaled environmental pollutants and allergens to underlying airway tissue (91). This high vulnerability of the asthmatic airway epithelium is further aggravated by an existing impairment of the antioxidative defense mechanisms that facilitates a state of chronic damage (92). Overall, these defects in airway barrier function and defense perpetuate airway inflammation, aberrant repair and remodeling. Interestingly, bronchial biopsies from asthmatic children and adults show signs of extensive epithelial damage together with upregulation of epidermal growth factor receptors and impaired cellular proliferation (69, 93-95). These findings relate the onset and progress of asthma with an underlying vicious circle of chronic epithelial injury and incomplete repair.

1.3.3 Developmental origin of asthma

Numerous studies have demonstrated that the origin of asthma lies –at least partially- in fetal and early postnatal life. The developmental origin of asthma is further supported by evidence linking low birth weight with a higher risk for asthma and impaired lung function later in life (96, 97). Low birth weight may imply poor fetal development as it can be the consequence of

growth adaptation processes commencing upon exposure to adverse intrauterine conditions (4). Apart from low birth weight, fetal growth adaptation in response to adversities may also affect the developing lung, resulting in narrow airways and reduced lung volume, features that collectively increase the risk for asthma in childhood (98-101). Intrauterine exposure to adverse conditions, including maternal smoking, nutrition and increased stress perception may compromise fetal development and initiate fetal growth adaptation processes, thereby subsequently leading to an increased risk for poor respiratory health and asthma later in life.

Exposure to maternal smoking, one of the most common challenges of pregnancy in western societies, is known to impair fetal growth thereby leading to low birth weight and reduced lung size and volume (102). Importantly, studies in humans and mice identified a strong association between prenatal tobacco smoke exposure and lung function impairment that is present at birth and persists throughout child- and adulthood (103, 104). Due to its effect on both lung growth and function, prenatal exposure to tobacco smoke results in a higher risk of wheezing phenotypes and asthma in childhood (105-109). Similarly, prenatal air pollution exposure exerts detrimental effects on the developing lung and has been linked with childhood wheeze, asthma as well as persistent lung function alterations (110, 111), especially in boys. Animal studies corroborate these observations by linking prenatal air pollution exposure with impaired lung development, postnatal airway hyperresponsiveness, enhanced airway inflammation and increased IgE levels (112-115).

Although the mechanisms by which intrauterine exposure to tobacco smoke and air pollution programs postnatal lung function and disease remain unknown, mounting evidence suggests that epigenetic modulations may be involved. Maternal exposure to tobacco smoke or air pollution favors the induction of maternal systemic oxidative stress and, through epigenetic modifications, drives the release of proinflammatory cytokines, such as IL-6 and IL-8, in maternal peripheral tissues (116). Such a highly oxidative proinflammatory maternal environment compromises placental and endothelial function thereby inducing fetal oxidative stress, which, in turn, may be detrimental for fetal development by altering gene expression and interfering with crucial milestones for lung and immune system maturation (115, 117-119). Indeed, human studies revealed an association among prenatal tobacco smoke or air pollution exposure, distinct alterations in global and gene-specific DNA methylation patterns in fetal tissues as well as asthma development in the offspring (120-123). Interestingly, in response to prenatal smoke exposure, a sex-specific severity of asthma-like symptoms has been observed in the offspring, along with an impaired lung development. Based on recent studies in mice, these sex-specific effects may be attributed to tobacco smoke-induced epigenetic modifications

in promoter methylation of insulin-like growth factor 1 and its receptor (*Igf1* and *Igf1r*), two key promoters of pre- and postnatal mouse development (124). Specifically, a downregulation of *Igf1* and *Igf1r* in the female lung may indicate poor postnatal lung development, especially in the female offspring (125, 126).

A crucial determinant of postnatal health is maternal nutrition during pregnancy. Interestingly, an association between maternal high-fibre diet during pregnancy and a lower risk for allergic airway disease in the murine offspring was recently reported (16). Similarly, human studies demonstrated that increased maternal vitamin D intake during pregnancy may lower the risk for wheezing phenotypes in early childhood (127), whereas folic acid supplementation in late pregnancy as well as low maternal vitamin E and zinc intake were associated with a higher susceptibility to childhood asthma (128-130).

Interestingly, high maternal stress perception during pregnancy has also been associated with increased susceptibility to wheezing phenotypes during childhood. Recent epidemiological studies reported that disaster-induced maternal stress during pregnancy increases the risk for asthma only in girls (44). Similarly, high maternal progesterone levels in the first trimester of pregnancy were linked to a lower risk for asthma only in the female offspring (45). Since prenatal stress is known to decrease maternal progesterone during pregnancy, low progesterone may account for a higher risk for asthma in girls. In a second pregnancy cohort performed in Mexico, pre- and postnatal maternal stress aggravated the risk for wheezing phenotypes in boys and girls respectively (43), whereas cumulative stress across both prenatal and postnatal periods affected mainly the girls and increased their susceptibility to childhood asthma (42).

Despite the well-documented link between maternal stress during pregnancy and increased risk for asthma in childhood, the exact mechanisms as well as the target of prenatal stress in the developing fetus remain unknown. Prenatal exposure to maternal stress during crucial developmental windows may disrupt fetal development, organogenesis and maturation. Given the multifaceted pathogenesis of asthma implicating both the lung and the immune system, one can hypothesize that prenatal stress targets the developing lung or immunity thereby preparing the ground for postnatal manifestation of the disease.

1.4 Fetal development in humans and mice

In order to elucidate the mechanisms underlying the fetal programming of asthma, a good knowledge of fetal immune system and lung development is required.

1.4.1 Fetal immune system development

Fetal immune system development is a highly regulated multistage process that includes sequential steps of hematopoietic stem cell (HSC) production, migration through hematopoietic sites as well as differentiation and final functional and phenotypic maturation. Both in humans and mice, the developmental process starts early in gestation, when hematopoietic progenitors emerge in the first weeks of human pregnancies in close proximity to the ventral wall of the dorsal aorta, in a region called para-aortic splachnopleurae, and in the yolk sac, and between gestational days (gd) 8.5 and 10.5 in mice in the yolk sac, placenta and para-aortic splachnopleurae which later evolves into the aorta-gonad-mesonephros region (131). Shortly after their emergence, immature HSC migrate through the bloodstream into the fetal liver, where hematopoiesis is first detectable from gd 10.5 in mice and the sixth week of pregnancy in humans (131-133). Indeed, the fetal liver serves as the main hematopoietic organ during the first and second trimester in human pregnancies and midgestation in mice (131, 134). Among others, erythro-myeloid progenitors located in the fetal liver give rise to cells of the erythroid and myeloid lineages, while T-cell precursors migrate from the liver to fetal thymus in waves as early as midgestation (5, 133). Starting from gd15.5 in mice, HSC colonize the fetal bone marrow, where active hematopoiesis begins on gd 17.5 and persists postnatally (131, 135). On the other hand, in human pregnancies, bone marrow colonization by fetal-liver derived HSC starts in the first trimester and shortly thereafter, during the second trimester, the bone marrow becomes the primary hematopoietic organ in late fetal and postnatal life (134).

1.4.2 Lung development

The lung emerges as product of a fine well-orchestrated developmental process that occurs both prenatally and postnatally. In both mice and humans, lung development can be divided into five distinct stages, namely the embryonic, pseudoglandular, canalicular, saccular and alveolar stage, that collectively give rise to the tree-like system of conducting airways and the gas exchange area of the lung parenchyma (Figure 1)(136, 137).

During the embryonic stage (gestational weeks 4-7 in humans and gd 9.5-12.5 in mice), the left and right lungs emerge as two independent outpouchings of the foregut. The two lung buds located on the right and left side of the trachea start elongating and, through a repetitive circle of growth and branching in the surrounding mesenchymal tissue, give rise to all future airways. This process, also known as branching morphogenesis, occurs mainly during the pseudoglandular stage (gestational weeks 5-17 in humans and gd 12.5-16.5 in mice) (138). The first future airways formed during this stage are lined by high columnar epithelial cells which, towards the terminal branches, are replaced by a cuboidal epithelium. During the canalicular

stage (gestational weeks 16-25 in humans and gd 16.5-17.5), branching morphogenesis is completed with the formation of the distal airways. Importantly, this stage comprises the differentiation of the epithelia that allows a distinction between conducting and respiratory airways. Specifically, the immature cuboidal epithelial cells lining the terminal branches and future alveolar ducts give rise to the immature alveolar epithelium. In the next stage, also known as saccular stage (gestational weeks 24-38 in humans and gd 17.5- postnatal day (pd) 5 in mice), the terminal airways grow in length and width thereby forming the so-called sacculi. The expansion of the gas exchange region results in decomposition of the surrounding mesenchyme with subsequent thinning down of the intersaccular and future interalveolar walls. An additional milestone reached in this stage is the appearance of mature type I and type II alveolar epithelial cells (AEC). The former cover most of the inner surface area of the alveolar ducts and, together with the endothelium of the capillaries, form the air-blood barrier thereby performing gas exchange after birth (139). Expression of aquaporin 5 (*AQP5*) serves as a type I AEC differentiation marker since it is a prominent characteristic of mature type I AEC (140). On the other hand, type II AEC are sparsely located in the alveolar walls and are responsible for surfactant production, which begins in this developmental stage (141, 142). Surfactant is a lipoprotein complex that consists mainly of phospholipids and surfactant proteins (SFTPA, SFTPB, SFTPC and SFTPD) and reduces surface tension in the alveoli thereby preventing alveolar collapse at the end of expiration (143). *SFTPA* and *SFTPC* expression characterizes type II AEC and serves as an indicator of their differentiation (144). During the last developmental phase, the alveolar stage (gestational week 38- young adulthood in humans and pd5-pd30 in mice), existing terminal airspaces are subdivided by the formation of new walls, named septa. This process, also known as alveolarization, results in the formation of alveoli, the functional respiratory units of the lung. Gradual formation of secondary septa gives rise to many smaller alveoli, thereby increasing the gas exchange surface area as well as lung parenchyma complexity.

Lung development is tightly regulated by developmental factors that ensure fine orchestration of the series of events. For example, the transcription factors SOX9 (SRY-related high-mobility group [HMG] box 9), NMYC and ID2 are expressed in the distal lung epithelium and play a key role in maintaining a fine balance between epithelial cell proliferation and differentiation thereby ensuring a smooth transition from branching morphogenesis to terminal airspace formation (145-148). *Sox9* expression at the distal branching lung epithelium decreases gradually starting on gd 16.5, when terminal differentiation of type I and II AEC begins. Of note, SOX9 deficiency in early developmental stages results in disrupted branching

morphogenesis with inappropriate epithelial differentiation and cystic terminal airspaces in mice (146). Similarly, IGF1 signaling through its receptor IGF1R is crucially involved in fetal lung growth and organogenesis as it was shown to promote epithelial cell differentiation and vascular maturation in later stages of mouse fetal lung development (149). Importantly, studies in mice associated IGF1 signaling deficiency with lung hypoplasia, disrupted lung structure with collapsed airspaces, delayed mesenchymal decomposition as well as impaired epithelial and vascular maturation (150, 151).

Since lung development occurs mostly prenatally, the developing lung appears as a potential target of adverse maternal conditions during pregnancy. While available studies demonstrate that prenatal exposure to maternal smoking or air pollution directly interfere with fetal lung development thereby resulting in poor respiratory health after birth (136, 152, 153), little is known about the impact of prenatal stress challenge on the developing lung and its association with postnatal lung dysfunction and increased risk for asthma in early life.

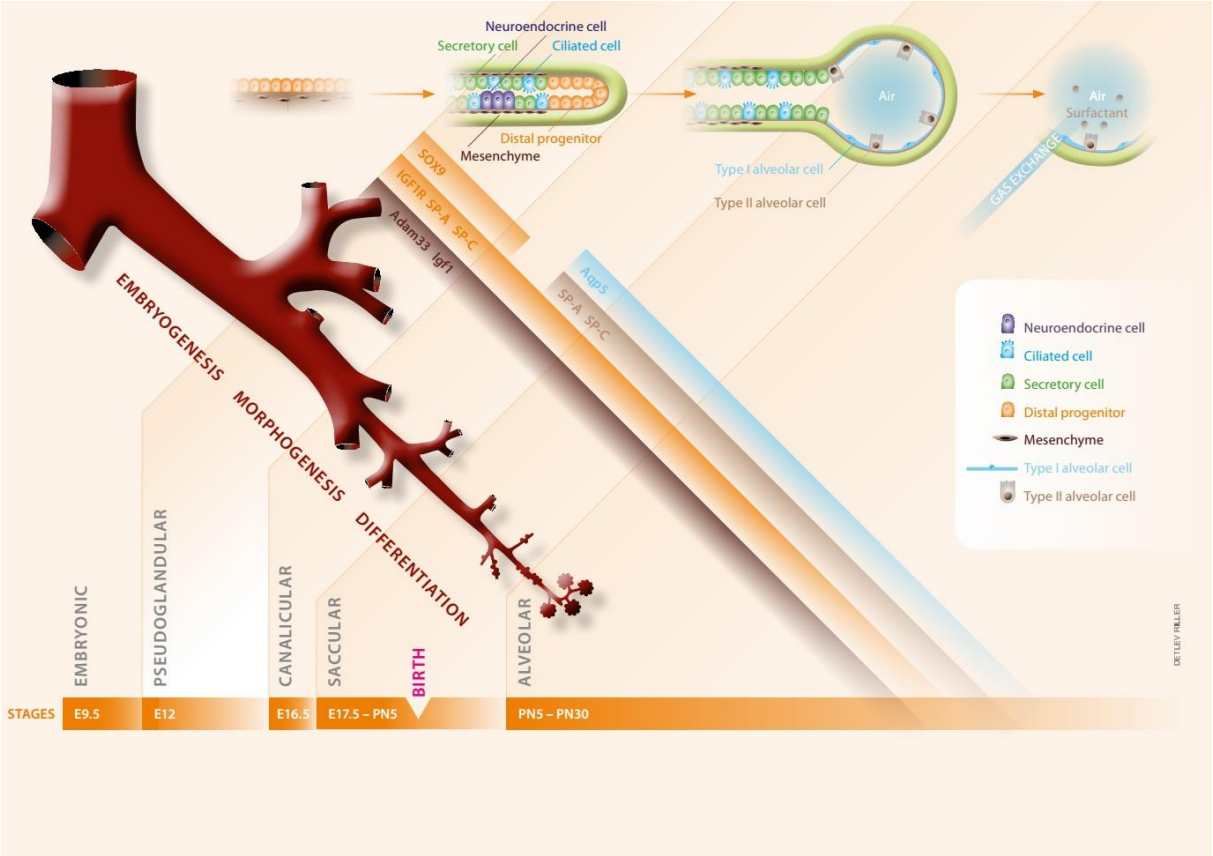

Figure 1. Lung development in mice. Murine lung development is a multistage process that starts *in utero* and is completed within the first month of life. Through five distinct stages, the primary lung buds branch and expand giving rise to airways and, after birth, to alveoli. In parallel, distinct cellular populations residing in the pulmonary tissue proliferate and differentiate into mature cells comprising the bronchial and alveolar epithelium. While secretory and ciliated epithelial cells are mainly found in the former, the latter consists of mature type I and II alveolar cells which express aquaporin (AQP5) or surfactant proteins A and C (SFTPA/SP-A, SFTPC/SP-C) and are responsible for postnatal gas exchange and surfactant production, respectively. Some of the factors involved in the developmental process are insulin-like growth factor 1 and its receptor (IGF1 and IGF1R), the transcription factor

SOX9 (SRY-related high-mobility group [HMG] box 9) and the disintegrin and metalloproteinase glycoprotein ADAM33, which is expressed by fetal mesenchymal cells and is related to postnatal asthma manifestation. (E, gestational days; PN, postnatal days)

1.5 Objectives of this thesis

Mounting evidence suggests that prenatal stress can increase the risk for asthma during childhood (10). However, insights into the mechanisms underlying the programming effect of prenatal stress challenge on postnatal health and disease are missing. This thesis intends to address this lack of knowledge and elucidate the impact on prenatal stress challenge on fetal development and its association with poor health later in life. Specifically, our hypothesis is that prenatal stress challenge results in an increased susceptibility to asthma in the offspring by interfering with fetal lung development.

In order to address this hypothesis we aim to:

1. Identify the programming effect of prenatal stress challenge on postnatal lung function and susceptibility to asthma
2. Determine the developmental target of prenatal stress challenge by distinguishing the effect of a prenatally stress challenged lung or immune system on postnatal asthma manifestation
3. Investigate the impact of prenatal stress challenge on fetal development

These findings will provide valuable insight into the stress-mediated fetal programming and pathogenesis of asthma and will complement the long-term aim to identify early markers and signs pointing to an increased risk for asthma development later in life.

2 Materials and Methods

2.1 Materials

2.1.1 Chemicals

All standard chemicals for buffer, solution or medium preparation were acquired from Sigma-Aldrich Chemie GmbH (Munich, Germany), Merck Millipore (Darmstadt, Germany) and Gibco/ThermoFisher Scientific (Waltham, MA, USA). Chemicals for special applications are listed in Table 1.

Table 1: Chemicals

Name	Company
Albumin from chicken egg (Ovalbumin) grade V	Sigma-Aldrich Chemie GmbH, Munich, Germany
Albumin from chicken egg (Ovalbumin) grade VI	Sigma-Aldrich Chemie GmbH, Munich, Germany
Bovine serum albumin (BSA)	Sigma-Aldrich Chemie GmbH, Munich, Germany
Citrate buffer	DCS, Hamburg, Germany
Collagenase D	Roche Diagnostics GmbH, Mannheim, Germany
CompBeads (anti-rat/anti-hamster/anti-mouse Ig κ and negative control compensation particles)	BD Bioscience, Heidelberg, Germany
Cotrim K (240 mg/5 ml Cotrimoxazol = 200 mg/5 ml Sulfamethoxazol, 40 mg/ 5 ml Trimethoprim)	Ratiopharm GmbH, Ulm, Germany
DNase I	Sigma-Aldrich Chemie GmbH, Munich, Germany
Eosin	Waldeck GmbH & Co. KG, Münster, Germany
Ethanol (99%), denatured	Th. Geyer GmbH & Co. KG, Renningen, Germany
Eukitt medium	O. Kindler GmbH, Freiburg, Germany
Fetal calf serum (FCS)	Gibco/ThermoFisher Scientific, Waltham, MA, USA
Forene (100% isoflurane)	Abbvie, North Chicago, IL, USA
Formaldehyde solution	Sigma-Aldrich Chemie GmbH, Munich, Germany
Giemsa stock solution	Carl Roth GmbH & Co. KG, Karlsruhe, Germany

Goldner 1 (azophloxine solution)	Sigma-Aldrich Chemie GmbH, Munich, Germany
Goldner 2 (phosphotungstic acid)	Merck Millipore, Darmstadt, Germany
Goldner 3 (light-green SF solution)	Merck Millipore, Darmstadt, Germany
Hematoxylin	Ventana, Hoffmann-La Roche, Basel, Switzerland
Imject alum adjuvant (aluminium hydroxide)	ThermoFisher Scientific, Waltham, MA, USA
Ketamine 10%	WDT eG, Germany
L-Glutamine 200mM (100x)	Gibco/ThermoFisher Scientific, Waltham, MA, USA
NaCl (0.9 %)	B. Braun Melsungen AG, Melsungen, Germany
Normal rat serum (NRS)	Jachson ImmunoResearch Laboratories, West Grove, PA, USA
May Grünwald's eosine-methylene blue solution	Carl Roth GmbH & Co. KG, Karlsruhe, Germany
Acetyl-β-methylcholine chloride	Sigma-Aldrich Chemie GmbH, Munich, Germany
Mowiol 4-88	Carl Roth GmbH & Co. KG, Karlsruhe, Germany
Pacific Orange™ Succinimidyl Ester (PacO)	ThermoFisher Scientific, Waltham, MA, USA
Pancuronium bromide	Sigma-Aldrich Chemie GmbH, Munich, Germany
Paraffin	DCS, Hamburg, Germany
Paraformaldehyde (PFA)	Biochemica, Billingham, UK
Penicillin (10.000 units)/ Streptomycin (10 mg/ml)	Sigma-Aldrich Chemie GmbH, Munich, Germany
Periodic acid	Sigma-Aldrich Chemie GmbH, Munich, Germany
Potassium dihydrogen phosphate ("Weisesche Pufferlösung")	Provided inhouse
Proteinase K	Roche Diagnostics GmbH, Mannheim, Germany
QIAzol Lysis Reagent	Qiagen, Venlo, Netherlands
Red blood cell (RBC) lysis buffer	eBioscience, San Diego, CA, USA
RNAlater	Qiagen, Venlo, Netherlands
Schiff's reagent	Merck Millipore, Darmstadt, Germany
Sucrose	Sigma-Aldrich Chemie GmbH, Munich, Germany

TaqMan Universal PCR Master Mix	Life Technology, Carlsbad, CA, USA
Terbutaline hemisulfate salt	Sigma-Aldrich Chemie GmbH, Munich, Germany
Tissue Tek (OCT)	Sakura Finetek Europa
Trypan Blue Stain (0.4%)	Gibco/ThermoFisher Scientific, Waltham, MA, USA
Triton-X-100	Merck Millipore, Darmstadt, Germany
Weigert's iron hematoxylin (equal ratio of Ferric Hematoxylin solution A and B)	Waldeck, Münster, Germany
Rompun 2%	Bayer, Leverkuzen, Germany
Xylene	Greyer, Renningen, Germany
Xylol replacement medium [Xylolersatzmedium (XEM)] HS200	DiaTec Diagnostics GmbH, Dortmund, Germany

2.1.2 Kits

Table 2: Kits

Name	Company
DNase elimination	Amgen, Thousand Oaks, CA, USA
DNeasy Kit	Qiagen, Venlo, Netherlands
Foxp3Fixation/Permeabilization Concentrate and Diluent	eBioscience, San Diego, CA, USA
RNeasy Plus Universal Mini Kit	Qiagen, Venlo, Netherlands
Superscript	Invitrogen, Carlsbad, CA, USA

2.1.3 Media, buffers and solutions

Table 3: Media, buffers and solutions

Name	Composition	Company
FACS buffer	Dulbecco's Phosphate-Buffered Saline (PBS) 0.5% BSA	Gibco/ThermoFisher Scientific, Waltham, MA, USA
complete RPMI (cRPMI)	Roswell Park Memorial Institute (RPMI) 1640 10% FCS 1% Penicillin/Streptomycin 1% L-Glutamine	Gibco/ThermoFisher Scientific, Waltham, MA, USA

Blocking solution (immunofluorescence)	0.1% Triton-X-100 in 1x PBS 10% FCS 3% BSA	
Citrate buffer (pH=6)	1L H_2O 2.1g Sodium Citrate	

2.1.4 Plastic and other materials

Consumables were purchased from Sarstedt AG & Co. (Nümbrecht, Germany), Greiner Bio-One International GmbH (Kremsmünster, Austria), Nunc GmbH & Co. KG (Langenselbold, Germany), GE Healthcare (Little Chalfont, UK) and Eppendorf AG (Hamburg, Germany), if not stated otherwise (Table 4).

Table 4: Plastic and other materials

Name	**Company**
Cell strainer (40µm nylon)	Falcon Brand Products, Corning, NY, USA
Tissue-Tek III Blue biopsy cassettes	Sakura Finetek Europe
Embedding cassettes "Macro"	Carl Roth GmbH & Co. KG, Karlsruhe, Germany
Standard microscope slides	Carl Roth GmbH & Co. KG, Karlsruhe, Germany
SuperFrost Plus microscope slides	ThermoFisher Scientific, Waltham, MA, USA
BD Venflon needle protected intravenous cannula 20G, 1x32mm	BD, Becton, Dickinson and Company, Sweden
BD Micro-fine+ Insulin syringes U100 0,3x8 mm	BD, Becton, Dickinson and Company, Sweden
Syringes (1ml, 5ml, 10 ml)	B. Braun Melsungen AG, Hessen, Germany
Polystyrene, round-bottom FACS tube (5 ml)	Falcon Brand Products, Corning, NY, USA
Syringe needle 27G x ½'' 0,4x12mm	B. Braun Melsungen AG, Hessen, Germany
Syringe needle 26G x ½'' 0.45 x 12mm	B. Braun Melsungen AG, Hessen, Germany
Syringe needle 21G x ½'' 0.80 x 40mm	B. Braun Melsungen AG, Hessen, Germany

2.1.5 Antibodies

Antibodies used in flow cytometry and immunofluorescence are listed in Table 5 and 6, respectively.

Table 5: Antibodies for flow cytometry

Antigen	Conjugated fluorochrome	Clone	Dilution	Company
CD45.1	FITC	A20	1:400	BioLegend, San Diego, CA, USA
CD45.2	APC-Cy7	104	1:100	BioLegend, San Diego, CA, USA
CD45	APC-Cy7	30-F11	1:400	BD Bioscience, Heidelberg, Germany
CD103	PerCP-Cy5.5	2E7	1:100	BioLegend, San Diego, CA, USA
CD11b	BV605	M1/70	1:50	BD Bioscience, Heidelberg, Germany
CD11c	Pe-Cy7	N418	1:100	BioLegend, San Diego, CA, USA
Siglec-F	PE	E50-2440	1:50	BD Bioscience, Heidelberg, Germany
Gr-1	BV650	RB6-8C5	1:200	BioLegend, San Diego, CA, USA
MHCII	APC	M5/114.15.2	1:200	BioLegend, San Diego, CA, USA
F4/80	BV421	BM8	1:100	BioLegend, San Diego, CA, USA
CD3	PE eFluor®610	145-2C11	1:100	eBioscience, San Diego, CA, USA
CD4	Alexa Fluor® 700	GK1.5	1:200	BioLegend, San Diego, CA, USA
CD8α	BV650	53.7.7	1:100	BioLegend, San Diego, CA, USA
CD25	PE-Cy7	PC61	1:200	BD Bioscience, Heidelberg, Germany
FoxP3	PE	FJK-16s	1:200	eBioscience, San Diego, CA, USA
CD44	Pacific Blue	IM7	1:200	BioLegend, San Diego, CA, USA
CD62L	BV711	MEL-14	1:100	BioLegend, San Diego, CA, USA

Table 6: Antibodies for immunofluorescence

Antigen	Origin	Dilution	Company
Anti-ZO-1	Rabbit polyclonal	1:100	Invitrogen, ThermoFisher Scientific, Waltham, MA, USA

anti-Rabbit IgG (H+L) Secondary Antibody, Alexa Fluor 568	Donkey polyclonal	1:1000	ThermoFisher Scientific, Waltham, MA, USA
Hoechst 33258		1:5000	Sigma-Aldrich Chemie GmbH, Munich, Germany

2.1.6 Primers

Primers for polymerase chain reaction (PCR) for fetal sex determination are listed in Table 7 and were purchased from TIB Molbiol (Berlin, Germany).
Gene expression assays for TaqMan® quantitative real-time PCR (qPCR) were purchased from Applied Biosystems (Foster City, CA, USA) (Table 8).

Table 7: Primers for PCR

Primer	**Sequence (5' > 3')**
Sry fw	TGGGACTGGTGACAATTGTC
Sry rev	GAGTACAGGTGTGCAGCTCT
Il3 fw	GGGACTCCAAGCTTCAATCA
Il3 rev	TGGAGGAGGAAGAAAAGCAA

Table 8: TaqMan® gene expression assays

Gene expression assay	**Assay ID**
Adam33	Mm00459691_m1
Aqp5	Mm00437578_m1
Hsd11b1	Mm00476182_m1
Hsd11b2	Mm01251104_m1
Tsc22d3 (Gilz)	Mm00726417_s1
Igf1	Mm00439560_m1
Igf1r	Mm00802831_m1
Nr3c1	Mm00433832_m1
Sftpa1	Mm00499170_m1
Sftpc	Mm00488144_m1

Sox9	Mm00448840_m1
Gapdh	Mm99999915_g1
Atp5b	Mm01160389_g1

2.1.7 Equipment and instruments

Experiments were conducted using standard laboratory equipment. Special instruments used are listed in Table 9.

Table 9: Instruments

Name	**Company**
Flow cytometer LSR Fortessa	BD Bioscience, Heidelberg, Germany
Infinite 200 PRO NanoQuant reader	Tecan, Männedorf, Switzerland
Microtome SM2010R	Leica, Wetzlar, Germany
Rodent repellent device	Conrad Electronics, Germany
Ultrasound rodent repellent device	Weitech, Belgium
StepOne PlusTM Real-Time PCR System	Applied Biosystems, Foster City, CA, USA
QuantStudio 5 Real-Time PCR System	Applied Biosystems, Foster City, CA, USA
Shandon Cytospin 2	Marshall Scientific, USA
Slide scanner Mirax Midi	Carl Zeiss MicroImaging GmbH Germany
PARI BOY® SX	PARI Medical Holding GmbH, Germany
Buxco® FinePointe Resistance and Compliance system	Data Sciences International, New Brighton, MN, USA
CryoStar™ NX70 Cryostat	ThermoFisher Scientific, Waltham, MA, USA
Precellys 24 tissue homogenizer	PeQlab, VWR, Erlangen, Germany
Inverted microscope Axio Vert.A1 FL-LED	Carl Zeiss MicroImaging GmbH Germany
Axiocam 503 color Digital Camera	Carl Zeiss MicroImaging GmbH Germany
Mastercycler® nexus GX2	Eppendorf AG, Hamburg, Germany

Gel documentation system Gel Doc XR	Bio-Rad Laboratories GmbH, München, Germany
Microwave	Robert Bosch GmbH, Germany

2.1.8 Software

Software used for data acquisition and analysis is found in Table 10.

Table 10: Software

Name	Company
GraphPad Prism version 7	GraphPad Software, La Jolla, CA, USA
GraphPad Prism version 8	GraphPad Software, La Jolla, CA, USA
FlowJo version 9.9.5 for Mac	TreeStar, Ashland, OR, USA
FACSDiva™ Software version 8.0.1	BD Bioscience, Heidelberg, Germany
Pannoramic Viewer	3DHISTECH, Budapest, Hungary
ImageJ	National Institutes of Health, Bethesda, Maryland, USA
ZEN 2.3 (blue edition)	Carl Zeiss MicroImaging GmbH Germany
FinePointe Review software version 2.3.1.0	Data Sciences International, New Brighton, MN, USA

2.1.9 Mice

Adult male and female C57BL/6 mice were purchased from Charles River and kept in the animal facility of the University Medical Centre Hamburg-Eppendorf in a 12-hour light/dark circle with ad libitum access to food and water. All animal studies were designed in accordance with institutional guidelines and approved a priori by the respective German authorities (Behörde für Gesundheit and Verbraucherschutz Hamburg; approval numbers: G15/036 and G17/044).

2.2 Methods

2.2.1 Timed pregnancy and prenatal stress challenge

After one week of acclimatization to the animal facility, eight-week old C57BL/6 female mice were mated to C57BL/6 male mice. The presence of a vaginal plug in the morning indicated gestational day (gd) 0.5. On gd 7.5 and 9.5 the mice were weighed and pregnancy was confirmed by a 1.5-2 g body weight increase relative to gd 0.5. To challenge the pregnancy, pregnant dams were exposed to sound stress for 24 hours on gds 10.5, 12.5 and 14.5. The sound stress was induced by two rodent repellent devices located inside the stress cage, with one emitting sound of 88dB at a frequency of 1200 Hz in intervals of 15 sec and the other emitting ultrasound waves constantly. Pregnant dams that were not disturbed during pregnancy except for weight documentation on gd 11.5, 13.5 and 15.5 served as controls.

2.2.2 Experimental asthma induction in the offspring

For experimental asthma induction in the offspring, an ovalbumin (OVA)-based mouse model of allergic airway inflammation was used (154, 155). Specifically, prenatally stress challenged and control mice, either at the age of 6 or 16 weeks in the case of bone marrow chimeras, were sensitized to OVA on days 1, 14 and 21 with three intraperitoneal (i.p.) injections of 10 μg OVA (grade VI) and 150 μg aluminium hydroxide (Imject alum adjuvant) in sterile PBS. Acute allergic airway inflammation was subsequently achieved by challenging the mice with 20-minute exposure to OVA (grade V) aerosol (1% w/v in PBS) on days 26, 27, and 28. Control mice were sensitized and challenged with i.p. PBS injection and PBS aerosol, respectively.

2.2.3 Metacholine challenge test

24 hours after the last challenge with OVA aerosol, airway response to increasing concentrations of aerosolized methacholine (MCh) was assessed using the Buxco® FinePointe Resistance and Compliance system, as described elsewhere (154, 155). Briefly, after anesthesia induction with i.p. injection of ketamine [90mg/kg bodyweight (BW)] and xylazine (10 mg/kg BW), mice were tracheotomized and mechanically ventilated with 150 μl/breath. To block spontaneous neuromuscular activity, pancuronium bromide (0.5 mg/kg BW) was administered i.p. After a 5-minute acclimation period, MCh challenge test started with the administration of 1x PBS aerosol, followed by increasing concentrations of aerosolized MCh in 1x PBS (3.125, 6.25, 12.5, 25 and 50 mg/ml). Each challenge lasted for 30 sec, with a subsequent observation time of 270 sec. Transpulmonary pressure and airflow in the presence of increasing MCh concentrations were documented and analyzed with the FinePointe Review software (version

2.3.1.0), which subsequently determined airway resistance (RI) (cm H_2O/ml/s). Following the last measurement, terbutaline hemisulfate (180 ng/20 g BW) was administered i.p. to induce bronchodilation and therefore, facilitate the subsequent collection of lung tissues.

2.2.4 Bone marrow transplantation (BMT)

For generation of bone marrow chimeras, bone marrow cells were isolated from eight-week old prenatally stress challenged and control C57BL/6 CD45.1$^+$ donor mice. Donor mice were anaesthetized with CO_2 and subsequently sacrificed by cervical dislocation. Subsequently, femurs and tibiae were collected and flushed with complete RPMI in sterile conditions. After centrifugation at 600 g for 8 min at 4°C, the cell pellet was resuspended in 1x PBS using a 21G syringe and cells were then counted using a hemocytometer. Subsequently, $10x10^6$ bone marrow cells in 100 µl 1x PBS were injected intravenously (i.v.), via the retro-bulbar plexus, in ten-week old prenatally stress challenged and control C57BL/6 CD45.2$^+$ recipients under isoflurane-induced anesthesia, 12 hours after total-body irradiation (10 Gy), as described elsewhere (156). For protection against infections, recipient mice received Cotrimoxazol (0.4 mg/ml) in drinking water, starting 3 days prior to irradiation until 2 weeks post BMT. One mouse was not engrafted (sentinel) and was observed until moribund between days 5 and 15 post irradiation. To determine whether immune reconstitution was successfully completed in the recipients, the frequency of CD45.1$^+$ and CD45.2$^+$ immune cells in peripheral blood was analyzed by flow cytometry 5 weeks post BMT.

2.2.5 Tissue collection

Fetal and neonatal tissues

On gds 13.5, 15.5 and 18.5, pregnant dams were anaesthetized with CO_2 inhalation and subsequently sacrificed by decapitation. Pregnancy outcome (number of implantations and abortions, fetal weight) was documented. Fetuses were isolated and sacrificed by immediate decapitation. For subsequent fetal sex determination by PCR, tail biopsies were collected and stored at -20 °C. Half of the fetuses were then embedded in OCT by using dry ice and stored at -80°C for subsequent histological analysis. Fetal lungs from the rest of the fetuses were harvested and preserved in RNAlater for subsequent RNA isolation and gene expression analysis. On postnatal days 1, 5 and 30, mice were euthanized by cervical dislocation. Subsequently, 10 ml cold 1x PBS were injected into the right ventricle until lungs were cleared of blood. Lungs from half of the mice were harvested and stored in RNAlater at -20°C until use. For subsequent histological analysis, lungs were inflated with intratracheal delivery of 700µl OCT/4% Paraformaldehyde (PFA) solution (1:3), collected in 4% PFA and placed at

4°C. 24 hours later, the lungs were transferred in tubes containing sucrose 30% in 1x PBS. On the following day, the lungs were embedded in OCT with the use of dry ice and stored at -80°C for future use.

Adult tissues

Adult mice were anaesthetized with CO_2 inhalation and subsequently euthanized by cervical dislocation. A large incision was made up to the neck of the mouse and perfusion of the lungs was performed via the right ventricle. Blood was collected from the abdominal vena cava. The lung-draining lymph nodes were recognized and harvested in complete RPMI for flow cytometry. After carefully removing the skin and surrounding tissues, the trachea was exposed and the lungs were rinsed with 1 ml 1x PBS containing 2% fetal calf serum (FCS) to collect bronchoalveolar lavage fluid (BAL). Subsequently, the left bronchus was ligated and the left lung was extracted and divided into two pieces, which were then placed in complete RPMI for flow cytometry or in RNAlater for subsequent gene expression analysis, respectively. To isolate the right lung, the forceps was placed under the trachea to separate the trachea from the oesophagus. Inflation of the right lung was then performed by intratracheal delivery of 500 µl 4 % PFA dissolved in 1x PBS. Gently, the right lung was finally dissected, dropped into 50 ml conical tube with a large volume of 4 % PFA and left at 4 °C overnight.

2.2.6 Single cell isolation from mouse organs

To perform flow cytometry, single-cell suspensions of lungs, spleen and lung-draining lymph nodes were generated. Following perfusion with PBS, lungs were collected in complete RPMI, minced and digested using 10 µl collagenase D (working concentration: 2 mg/ml) and 3 µl DNase I (10 U/µl) dissolved in 1x PBS. Following incubation at 37 °C for 30 min, the digested lung tissues were passed through a 40-µm cell strainer. Similarly, single-cell suspensions of spleen and lung-draining lymph nodes were generated by passing the tissue through a 40-µm cell strainer. To ensure lysis of erythrocytes, spleen cells were subsequently incubated with red blood cell lysis buffer for 5 min. After centrifugation at 450g for 8 min at 4 °C, the cell pellet was resuspended in 1x PBS and cells were counted using a hemocytometer.

2.2.7 Quantification of gene expression in the lung

The mRNA expression of genes associated with lung development (*Adam33, Igf1, Igf1r, Sox9*), cellular differentiation (*Aqp5, Sftpc, Sftpa*), and glucocorticoid signaling [*Hsd11b1, Hsd11b2, Nr3c1, Tsc22d3 (Gilz)]* in the lungs of prenatally stress challenged and control mice was

examined at several prenatal and postnatal time points. To this end, quantitative real-time PCR (qPCR) was performed.

RNA isolation

In order to evaluate the mRNA expression of the above-mentioned genes, RNA was first isolated from lung homogenates of prenatally stress challenged and control mice using the RNeasy Plus Universal Mini Kit. Before RNA isolation, lung tissue samples stored in RNAlater were put into micro packaging vials containing ceramic beads (1.4 mm) together with 700 µl QIAzol Lysis Reagent and were homogenized using the Precellys 24 tissue homogenizer. DNA was then eliminated via a DNase treatment with 100 µl gDNA Eliminator Solution. After incubation with 180 µl chloroform for 3 min at room temperature (RT), the samples were centrifuged (12000 rpm, 15 min, 4 °C) and the upper aqueous phase was then placed into a new tube with 70% ethanol. Subsequently, the solution was pipetted to a spin column and centrifuged at 8000g for 15 sec at RT. After discarding the flow-through, the column was washed with washing buffer and next transferred into a new tube. 40 µl RNase free water were then added to the spin column membrane and centrifuged at 8000 g for 1min. Finally, the spin column was discarded and the remaining eluate with RNA was transferred into a new tube. The Infinite 200 PRO NanoQuant reader was used for RNA concentration measurement and the RNA was subsequently stored at -20 °C.

cDNA synthesis

To remove DNA and increase RNA purity, DNA digestion via DNase treatment of the RNA was performed. Specifically, 5 µg RNA were incubated with 10×DNase I Buffer, rDNase I and RNase Inhibitor (RNase OUT) for 30 min at 30 °C. After addition of DNase Inactivation Reagent and incubation for 2 min at RT, the samples were centrifuged at 10000 g for 1.5 min at 4 °C and 30 µl of the supernatant were transferred into a new tube. For cDNA synthesis, 1 µg RNA was incubated with dNTPs and random primers (0.25 µg/µl) at 65°C for 5 min and then shortly chilled on ice. Next, each sample was incubated with 8 µl of a master mix consisting of 5×First-Strand buffer, RNase OUT (40 U/µl), 0.1 M DTT and Superscript II RT (200 U/µl). The incubation steps were the following: 25 °C for 10 min, then 42 °C for 50 min and, as a last step, 70 °C for 15 min. Measurement of the cDNA concentration was subsequently performed using the Infinite 200 PRO NanoQuant reader.

qPCR

For the quantification of mRNA expression levels, the StepOnePlus or the QuantStudio 5 Real-Time PCR System and the corresponding software were used. For the reaction, 100 ng cDNA were used as template in a final volume of 20 μl and amplifications were performed using the 2×TaqMan Universal PCR Master Mix. The reaction was performed using the following standard cycling conditions:

- 50 °C for 2 min
- 95 °C for 10 min
- 95 °C for 15 sec
- 60 °C for 60 sec

All experiments were performed in triplicates and quantifications were normalized to the expression of two housekeeping genes, *Gapdh* and *Atp5b*. Relative transcript levels for each gene of interest were determined using the equation described previously (157). In all experiments, the relative expression level of each gene of interest in control mice was set equal to 1.

2.2.8 Polymerase Chain Reaction (PCR) for fetal sex determination

For fetal sex determination, genomic DNA was isolated from fetal tail biopsies using the DNeasy Blood and Tissue Kit of Qiagen following the manufacturer's instructions. Subsequently, fetal sex was defined by PCR using two sets of primers specific for *Sry* and *Il-3*, two genes that are found on chromosomes Y and 11, respectively. Therefore, when both the *Sry*-specific [402 base pairs (bp)] and the *Il-3*-specific (544bp) bands were detected, the fetuses were identified as males. On the other hand, female sex was indicated by the appearance of a single *Il-3*-specific band. The reaction was performed using the following program:

- 94°C for 10 min
- 94°C for 40 sec (33 cycles)
- 50°C for 1 min
- 72°C for 1 min
- 72°C for 5 min

The bands were detected by agarose gel electrophoresis under UV light using the gel documentation system Gel Doc XR.

2.2.9 Flow cytometry

Flow cytometry has emerged as a critical tool for the characterization of immune function and immunophenotyping of distinct cell populations. This method allows identification of distinct

cell types based on their physical properties (size, shape and granularity) and the expression of surface markers or intracellular cytokines and transcription factors.

Extracellular and intracellular staining

For flow cytometry, $1x10^6$ cells from lung or lung-draining lymph nodes were used, respectively. To block unspecific binding, cells were incubated with rat anti-mouse CD16/CD32 Mouse Fragment Crystallizable Block (1:200) and normal rat serum (1:100) in 50 µl FACS buffer for 15 min at 4 °C. Subsequently, the cells were incubated with the respective antibodies for extracellular staining for 30 min at 4 °C in the dark. To identify dead cells, the fixable dead/life stain Pacific Orange™ (1:1000) was added to the antibody mix. Next, the cells were washed with FACS buffer (450 g, 8 min, 4 °C) to remove unbound antibodies and were then directly used for flow cytometry or stained intracellularly. For intracellular staining, the cells were fixed and permeabilized with the Foxp3 Fixation/ Permeabilization Concentrate and Diluent. After washing with 1x PBS, the cells were incubated with the respective antibodies for intracellular staining for 30 min at RT in the dark. Following incubation, the cells were washed again and resuspended in 250 µl FACS buffer. To determine the optimal concentration for each antibody, titration was performed prior to staining. Data were acquired using a BD LSR/Fortessa II flow cytometer and analyzed using FlowJo software.

Data analysis

As a first step in analyzing the data acquired with the BD LSR/Fortessa II flow cytometer, cell populations were distinguished based on their size using the forward scatter (FCS) and their granularity with the side scatter (SSC). Next, after excluding doublets and dead cells with the help of the dead/life stain, living single cells were detected. Subsequently, $CD45^+$ cells were identified and different immune cell types were further distinguished within this population. For example, cell populations orchestrating the innate immune response were identified in lung and BAL. Specifically, eosinophils were characterized as $CD45.1^+CD11c^{neg}CD11b^+SiglecF^+$), alveolar macrophages were identified as $CD45.1^+CD11c^+CD11b^{neg}SiglecF^+$, whereas neutrophils were described as $CD45.1^+CD11b^+MHCII^{neg}Gr1^{hi}$ (158, 159). Importantly, the adaptive immune response was also examined in lung and lung-draining lymph nodes. To this end, $CD4^+$ and $CD8^+$ T cells were identified as $CD45^+CD3^+CD4^+$ or $CD8^+$ cells, respectively. Regulatory T cells were characterized as $CD4^+Foxp3^+CD25^+$.

Compensation of spectral overlay

Before sample acquisition, compensation of spectral overlay of the fluorochromes used in each panel was performed as described previously. Specifically, each antibody was coupled with anti-mouse/rat/hamster Ig Kappa (κ) beads based on the host in which the antibody was generated. The beads were incubated with the respective antibody for 20 min at RT in the dark, then washed with FACS buffer and centrifuged (450 g, 5 min, 4 °C). Antibody volumes were determined empirically and varied from 0.1 to 1.25 μl per sample. For a single stained cell viability sample, 1x 10^6 spleen cells, half of which were killed at 70 °C for 5 min before the incubation with the antibody, were used. To detect auto-fluorescence, unstained beads and cells were used. The measurement of the samples was performed using the LSR/Fortessa II flow cytometer in the Compensation Setup mode of the FACSDiva software and the compensation values were automatically calculated. To further correct compensation post measurement, if needed, "fluorescence minus one" (FMO) samples were measured. FMO samples are cells stained with all fluorescent antibodies in the respective panel except for one antibody.

2.2.10 Cytology and histology

Preparation of cytocentrifugal specimens

Following the MCh challenge test (as described in 2.2.3), lungs were rinsed with 1 ml PBS containing 2% FBS and total cell number in the BAL was determined with a hemocytometer. Subsequently, 5 × 10^4 BAL cells were transferred into cytospin carriers and cytocentrifugal specimens were generated after centrifugation at 800 rpm for 8 min.

Preparation of histological slides

Lungs were collected as described in 2.2.5. For preparation of cryosections, after overnight fixation in 4% PFA, the harvested lungs inflated with OCT/PFA solution were transferred in tubes containing sucrose at 30% dissolved in 1x PBS. On the following day, the lungs were embedded in OCT with the use of dry ice. Frozen control and stress challenged lungs, as well as snap frozen fetuses, were sectioned at 7μm using the CryoStar™ NX70 Cryostat.

Lungs isolated from adult mice were transferred in tubes containing 1x PBS, following overnight fixation in 4% PFA. For histological sectioning, the lungs were subsequently embedded in paraffin. To this end, the tissues were first dehydrated by immersion in increasing concentrations of ethanol resulting in water and formalin removal. Next, the lungs were cleared from ethanol by xylene, which allows paraffin infiltration thereby resulting in embedding the tissues in a paraffin block. The paraffin-embedded tissue blocks were then cooled down to -12 °C for 30 minutes before they were sectioned at 4μm using the microtome SM2010R. The sections were mounted on glass slides and finally dried overnight at 37 °C.

Dehydration and infiltration were performed according to the following protocol:

- Ethanol 70 % for 1 h
- Ethanol 80 % for 1 h
- Ethanol 90 % for 1 h
- Ethanol 95 % for 1 h
- Ethanol 100 % for 1 h
- Ethanol 100 % for 1.5 h
- Xylene I for 1 h
- Xylene II for 1 h
- Paraffin type 3, 58 °C for 1 h
- Paraffin type 3, 58° C for 1 h
- Paraffin type 3, 58 °C for 1 h

Before staining, deparaffinization and rehydration of the slides were performed following the established protocol:

- Xylene, 3 x 5 min
- Ethanol 100 %,2 x 5 min
- Ethanol 96 % for 2 min
- Ethanol 90 % for 2 min
- Ethanol 80% for 2 min
- Ethanol 70% for 2 min
- Washing in ddH_2O for 5 min

May-Grünwald Giemsa (MGG) staining

MGG staining allows the differentiation and count of different blood cell populations on cellular preparations. MGG consists of two neutral stains, namely the May-Grünwald stain and the Giemsa stain. The former is composed of eosin and methylene blue whereas the latter is a mixture of eosin, methylene blue and azure B. Overall, MGG stains nuclei purple to violet, the cytoplasm of lymphocytes and monocytes blue, eosinophilic granules red to dark violet, thrombocytes violet and erythrocytes reddish.

To morphologically differentiate and count cellular populations in BAL, MGG staining of cytocentrifugal BAL specimens was performed following the established protocol:

- May-Grünwald solution for 6 min
- Washing in ddH_2O for 3 min
- Giemsa working solution for 40 min

- Washing in ddH_2O for 3 min
- Mounting of slides with Eukitt medium

The slides were scanned with a Mirax Midi Slide Scanner and images were viewed with the Pannoramic viewer or the ZEN 2.3 (blue edition) software. Distinct cell types were counted as a percentage of 500 cells on the slide based on their morphological characteristics as described above.

Hematoxylin and Eosin (H&E) staining

The hematoxylin and eosin staining is one of the most widely used staining methods in histology. Hematoxylin is a basic dye that stains the nucleus blue or purple whereas eosin is acidic and stains the cytoplasm red or pink.

Cryosections as well as deparaffinized lung sections were stained following the established protocol:

- 4% PFA dissolved in 1xPBS for 10 min
- Washing in ddH_2O for 5 min
- Hematoxylin solution for 8 min
- Tap water washing for 2 min
- Eosin G solution 1% for 60 sec
- Ethanol 70%, 3 dips
- Ethanol 80%, 3 dips
- Ethanol 90%, 3 dips
- Ethanol 96%, 3 dips
- Ethanol 100%, 2 x 2 min
- Xylene, 2 x 5 min
- Mounting of slides with Eukitt medium

The slides were scanned with a Mirax Midi Slide Scanner and images were viewed with the Pannoramic viewer or the ZEN 2.3 (blue edition) software.

Periodic acid-Schiff (PAS) staining

PAS staining is commonly used for the detection of polysaccharides, such as glycogen, and mucosubstances, such as glycoproteins and mucins, in tissues. The reaction of these molecules with periodic acid results in the formation of dialdehydes, which in turn react with the Schiff's reagent and give a purple/magenta color.

After deparaffinization and rehydration (see above), lung tissue sections were stained according to the established protocol:

- 1% periodic acid dissolved in ddH_2O for 10 min
- Tap water washing for 10 min
- Washing in ddH_2O, 2 x 2 min
- Schiff's reagent for 20 min
- Washing in warm tap water for 5 min
- Hematoxylin for 5 min
- Tap water washing for 10 min
- Ethanol 70%, 3 dips
- Ethanol 80%, 3 dips
- Ethanol 90%, 3 dips
- Ethanol 96%, 3 dips
- Ethanol 100%, 2 x 2 min
- Xylene, 2 x 5 min
- Mounting of slides with Eukitt medium

Masson's trichrome staining

Masson's trichrome staining is used to detect connective tissues, particularly collagen, in tissue sections. Following the standard staining protocol, collagen is stained blue/green, nuclei are stained dark red/brown, muscle tissue is stained red and cytoplasm appears pink.
Following deparaffinization and rehydration, lung tissue sections were stained according to the established Masson's trichrome staining protocol:

- Weigert's iron hematoxylin staining solution (equal amounts of Ferric Hematoxylin solution A and B) for 8 min
- Washing in ddH_2O for 2 min
- HCl-Alcohol 1% for 10 sec
- Washing in ddH_2O for 2 min
- Tap water washing for 10 min
- Washing in ddH2O for 2 min
- Goldner solution 1 for 8 min
- Washing in 1 % ethanoic acid, 2 x 30 sec
- Goldner solution 2 for 9 min (until destaining of the connective tissue)
- Washing in 1 % ethanoic acid,3 x 30 sec

- Goldner solution 3 for 3 min
- Washing in 1% ethanoic acid, 2 x 30 sec
- Ethanol 70%, 3 dips
- Ethanol 80%, 3 dips
- Ethanol 90%, 3 dips
- Ethanol 96%, 3 dips
- Xylene, 2 x 5 min
- Mounting of slides with Eukitt medium

Immunofluorescence

For immunofluorescent staining, a rabbit polyclonal anti- ZO-1 (Zonula occludens-1) antibody was used. The primary antibody was then detected by a secondary donkey polyclonal anti-rabbit antibody containing the Alexa Fluor 568 dye. No primary antibody was applied on sections that served as isotype controls. Prior to staining, heat-induced retrieval of epitopes was performed. Specifically, the deparaffinized lung tissue sections were placed in a microwaveable vessel containing 0.1 M sodium citrate buffer (pH 6.0) and boiled in a microwave (900W for 2 min and then 250 W for 7 min). The citrate-based solution allows the retrieval of antigens and enhances staining intensity by breaking the protein cross-links that are generated due to formalin fixation and mask the antigenic sites in the tissue thereby. After antigen retrieval and cooling down of the slides, immunofluorescence was performed following the established protocol:

First day

- Washing with 1x PBS for 2 min
- Cold 4% PFA for 10 min
- Washing with 1x PBS, 3 x 2 min
- 0.3% Triton-X-100 dissolved in 1x PBS for 5 min
- Washing with 1x PBS, 3 x 2 min
- Blocking solution at RT for 1h
- Incubation with primary antibody diluted (1/100) in blocking solution at 4°C, overnight

Second day

- Washing with 1x PBS, 3 x 2 min
- Incubation with secondary antibody diluted (1/1000) in blocking solution at RT for 1h
- Washing with 1x PBS, 3 x 2 min
- Incubation with Hoechst 33258 diluted (1/5000) in 1x PBS at RT for 5 min

- Washing with 1x PBS, 3 x 2 min
- Mounting of slides with Mowiol

2.2.11 Histological analysis

Lung morphometry

Frozen lung sections from control and stress challenged fetuses and pups were stained with hematoxylin and eosin and scanned with a Mirax Midi Slide Scanner. Images were obtained at a 15x magnification with Pannoramic Viewer and analysis was conducted using NIH Image J software. As indicators of fetal lung development on gd 18.5, the volume fraction of terminal sac spaces and the mean alveolar thickness were assessed. For estimation of the former, a point counting grid (7 horizontal and 12 vertical lines/84 points) was superimposed on the images of lung parenchyma fields. The volume fraction of the terminal sac spaces was then equal to P_i/P_t, where P_i indicates the number of points on the structure of interest, namely on terminal sac spaces, and P_t is the total number of points on the reference field, which in this case is the lung parenchyma (160). Therefore, the volume fraction of terminal sac spaces was expressed as a percentage of the whole lung parenchyma. The mean alveolar wall thickness (TD) was defined as alveolar tissue volume per surface area and was assessed by intersection and point counting. To calculate TD, the following formula was used: $TD= (ASF \times L_r)/2I_o$, where ASF indicates the volume fraction of alveolar walls, estimated again by point counting as described earlier, L_r is the length of the test line and I_o is the number of intersections of the alveolar walls with the test line (161). Eight randomly selected fields from three distinct levels of the lung parenchyma were assessed, and five test lines per field (in total forty lines) were used to determine TD.
Postnatal lung development was assessed on postnatal days 1, 5 and 30 based on the mean linear intercept (MLI). MLI is a parameter of distal lung structure and describes the mean free distance between airspace walls. In mice, during the first month of life, the last part of lung development, alveolarization, takes place. Specifically, airspaces gradually divide giving rise to the smaller alveoli thereby increasing the complexity of the lung parenchyma. Measurement of MLI offers insight into the complexity of the lung structure and allows an assessment of the ongoing alveolarization and lung development. To assess MLI, a point counting grid (7 horizontal and 12 vertical lines/84 points) was again superimposed on ten randomly selected fields from three levels of the distal lung parenchyma. Fields with vessels or airways were avoided. For each field, the number of times the alveolar walls intercepted each of five distinct lines (each 468.27 μm long) was determined. Using this information, MLI was then estimated by dividing the length of the line by the respective number of counted intercepts (162).

Quantification of peribronchial inflammation

To quantify the peribronchial inflammation after experimental asthma induction, lungs from prenatally stress-challenged and control mice were harvested, fixed, embedded in paraffin and sectioned as described above. Based on the previously described protocol, 4-µm thick sections were then stained for hematoxylin and eosin. Subsequently, the slides were scanned using Mirax Midi Slide Scanner and images were viewed with the ZEN 2.3 (blue edition) software. Semiquantitative assessment of the severity of peribronchial inflammation for twenty airways in two levels of lung parenchyma for each mouse was performed, based on the following scoring scale (163):

- 0: no peribronchial inflammatory infiltration
- 1: few inflammatory cells around the bronchus
- 2: an 1-cell-layer thick ring of inflammatory cells around the bronchus
- 3: a 2–4-cell layer thick ring of inflammatory cells around the bronchus
- 4: a >4-cell layer thick ring of inflammatory cells around the bronchus

Quantification of mucus production

For quantification of bronchial mucus production, PAS-stained lung sections were scanned with Mirax Midi Slide Scanner and semiquantitative analysis was performed using the ZEN 2.3 (blue edition) software. In total, thirty airways from two distinct levels of the lung parenchyma for each mouse were examined. The abundance of PAS-positive mucus-containing cells in each airway was scored as follows (163):

- 0: < 0.5% PAS+ cells
- 1: 5-25% PAS+ cells
- 2: 25-50% PAS+ cells
- 3: 50-75% PAS+ cells
- 4: > 75% PAS+ cells

Quantification of peribronchial fibrosis

After Masson's trichrome staining, lung sections were scanned and images were viewed as previously described. Thirty airways from two distinct levels of the lung parenchyma per mouse were semiquantitatively evaluated. The numerical scores for peribronchial fibrosis for each airway were the following:

- 0: no visible peribronchial collagen deposition
- 1: sparse peribronchial collagen deposition

- 2: 1-layer deep peribronchial collagen deposition
- 3: ≥ 2-layer deep peribronchial collagen deposition

Assessment of tight junction integrity in the bronchial epithelial barrier

The integrity of tight junctions in the bronchial epithelium was assessed by immunofluorescent staining of lung sections with the anti-ZO-1 antibody, based on the protocol described above. The slides were observed with the inverted microscope Axio Vert.A1 FL-LED and pictures were acquired using the Axiocam 503 color Digital Camera.

ZO-1, also known as tight junction protein-1, is located on the cytoplasmic membrane surface of intercellular tight junctions and mediates signal transduction via cell-cell junctions. In average, twenty airways from two levels of the lung parenchyma were examined for each mouse. The abundance of ZO-1+ cells in each airway indicated the tight junction integrity of the bronchial epithelial barrier and was scored as follows:

- 0: 100% ZO-1+ cells
- 1: 80-95% ZO-1+ cells
- 2: 50-80% ZO-1+ cells
- 3: 25-50% ZO-1+ cells
- 4: 5-25% ZO-1+ cells
- 5: <5% ZO-1+ cells

2.2.12 Statistics

Animals were allocated to different groups by alternation. Histological analysis was performed by two independent investigators. The results shown represent mean ± SEM. Comparisons between two groups were performed using student's t-test or Mann-Whitney test, depending on the normality of distribution. Differences in means between multiple groups were examined by one-way or two-way ANOVA with Bonferroni post-hoc tests, as stated in each figure legend. P values were considered statistically significant when <0.05 (*:$p \leq 0.05$; **: $p \leq 0.01$; ***: $p \leq 0.001$; ****:$p \leq 0.0001$). All statistical analyses were done and plots were created using GraphPad Prism versions 7.0 and 8.0.

3 Results

3.1 The impact of prenatal stress challenge on susceptibility to asthma and disease severity in the murine offspring

To identify the impact of prenatal stress challenge on postnatal lung function and susceptibility to asthma in adult mice, we used a well-established mouse model of prenatal stress challenge followed by postnatal induction of experimental allergic asthma (Figure 2A). Specifically, pregnant C57BL/6 mice were challenged with sound stress for 24h on gestational days (gd) 10.5, 12.5 and 14.5, whereas control mice were left undisturbed throughout pregnancy. For postnatal experimental asthma induction, six-week old male and female prenatally stress challenged and control offspring were sensitized and subsequently challenged with ovalbumin (OVA) (Figure 2A). PBS-sensitized and challenged mice served as controls. The successful establishment of the asthmatic phenotype in OVA-sensitized and challenged mice was verified by the significantly higher airway hyperresponsiveness (AHR) upon exposure to increasing doses of metacholine (MCh), as compared to PBS-treated mice (data not shown).

Interestingly, prenatal stress challenge resulted in an overall increased AHR upon MCh provocation, with only female prenatally stress challenged mice exhibiting a significantly increased AHR, as compared to the respective controls (Figure 2B, 2C).

Besides AHR, OVA-induced allergic airway inflammation, a second hallmark of asthma, was also exacerbated following prenatal stress challenge. Specifically, analysis of leukocyte differentials in cytospin preparations of bronchoalveolar lavage fluid (BAL), after May-Grünwald Giemsa staining, revealed increased accumulation of eosinophils in the lungs of prenatally stress challenged mice. Similarly to AHR, female prenatally stress challenged mice exhibited significantly enhanced eosinophil and neutrophil airway recruitment as well as increased peribronchial inflammatory cell infiltration, as compared to the respective controls, as observed in BAL cytospins and lung sections, respectively (Figure 3A-D and 4A, 4D). Additionally, flow cytometry analysis revealed significantly fewer $CD25^{+}FoxP3^{+}CD4^{+}$ regulatory T cells (Tregs) in the lungs and lung draining lymph nodes of female prenatally stress challenged offspring, in contrast to a slightly increased Treg frequency found in the lungs of male mice, potentially as a result of an underlying compensatory mechanism guarding lung homeostasis (Figure 3E-G).

To assess the third hallmark of asthma, airway remodeling, histological analysis of lung sections was performed. Specifically, a semiquantitative scoring analysis of periodic acid-

Schiff (PAS) stained lung sections revealed slightly increased bronchial mucus production in female prenatally stress challenged mice, as compared to the respective controls (Figure 4B, 4D). Similarly, significantly exacerbated peribronchial fibrosis was found in Masson's trichrome stained lungs of male and female prenatally stress challenged mice, as compared to controls (Figure 4C, 4D).

Interestingly, immunofluorescent staining of lung sections for zonula occludens-1 (ZO-1), also known as tight junction protein 1, revealed disruption of the airway epithelial barrier integrity, specifically in the female prenatally stress challenged offspring (Figure 5). This finding goes in line with current theories identifying airway epithelial dysfunction as the key orchestrator of asthma pathogenesis.

Taken together, our findings confirmed a link between prenatal stress challenge and increased asthma severity in the murine offspring. Interestingly, this association was sex-specific, with female prenatally stress challenged mice being more severely affected upon experimental asthma induction.

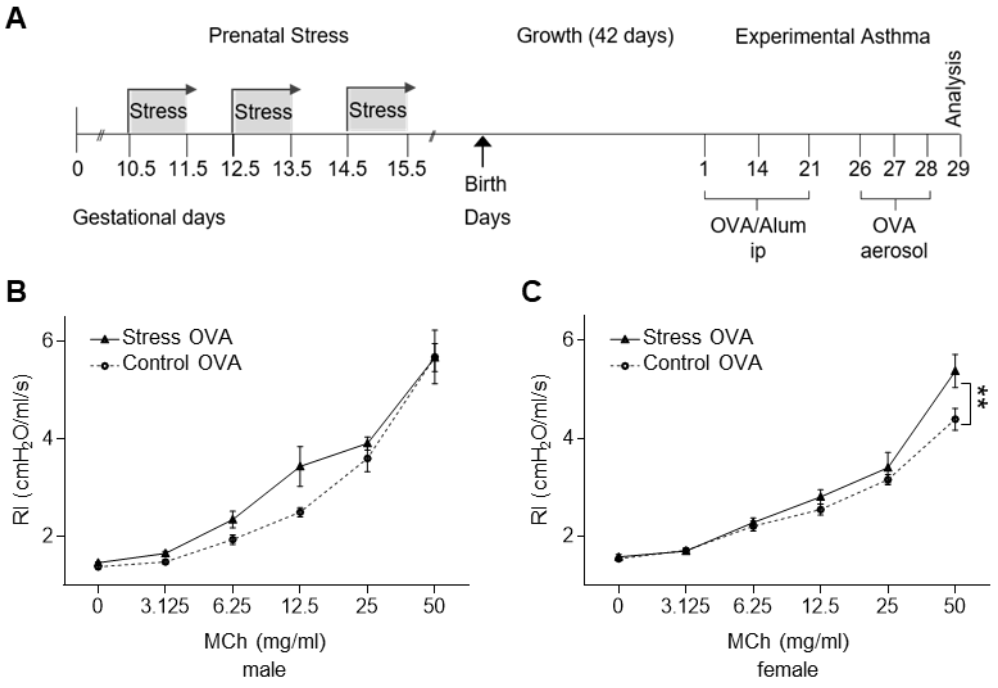

Figure 2. Airway hyperresponsiveness in prenatally stress challenged murine offspring upon experimental asthma induction. (A) Graphic description of the mouse model for prenatal stress challenge and postnatal experimental asthma induction in the adult offspring. (B-C) Airway response to increasing doses of metacholine (MCh) of (B) male and (C) female prenatally stress challenged and control OVA-treated mice. The n numbers used are: male control 8; male prenatally stress challenged 15; female control 17; female prenatally stress challenged 10. Bars represent the mean ± SEM. **:$p \leq 0.01$; as assessed by two-way ANOVA. Non-significant differences ($p > 0.05$) are not explicitly stated. Data were pulished in (171).

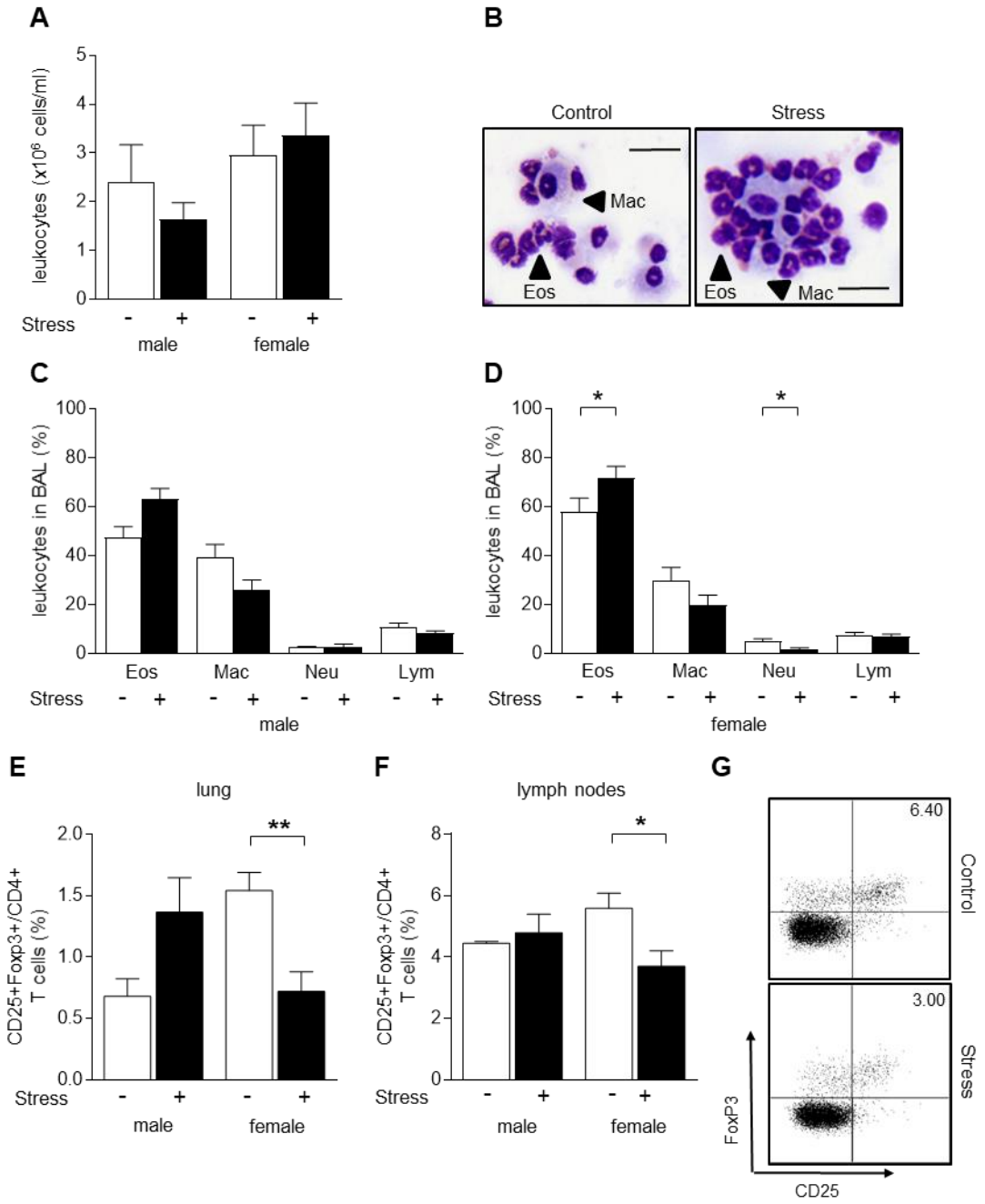

Figure 3. Asthma-related immune response in prenatally stress challenged murine offspring. (A) Total leukocyte numbers found in the BAL of control and prenatally stress challenged mice. (B) Representative images of BAL cells (cytospins) from female control (left) and prenatally stress challenged (right) OVA-treated mice, after May-Grünwald Giemsa staining. Macrophages (Mac) and eosinophils (Eos) are shown with arrow heads. Scale bars: 50 μm. (C,D) Morphological differentiation of leukocytes in BAL cytospins from prenatally stress challenged and control (C) male and (D) female OVA-treated mice. Eos, eosinophils; Mac, macrophages; Neu, neutrophils; Lym, lymphocytes (E-G) Flow cytometric analysis of $CD25^{+}FoxP3^{+}CD4^{+}$ Tregs in (E) lungs and (F) lung draining lymph nodes isolated from male and female, control and prenatally stress challenged OVA- treated mice. (G) Representative dot plots for FoxP3 and CD25 within CD4+ T cells from lung draining lymph nodes of female control (top) and prenatally stress challenged (bottom) OVA−treated mice. The numbers of mice used are: male control 3–6; male prenatally stress challenged 9–13; female control 5–6; female prenatally stress challenged 6–11.Cell frequencies in E and F are provided as percentages within CD4+ T cells. Bars represent the mean ± SEM. *: $p \leq 0.05$;**:$p \leq 0.01$ as assessed by Mann-Whitney U test or two-way ANOVA. Non-significant differences ($p > 0.05$) are not explicitly stated. Data were published in (171).

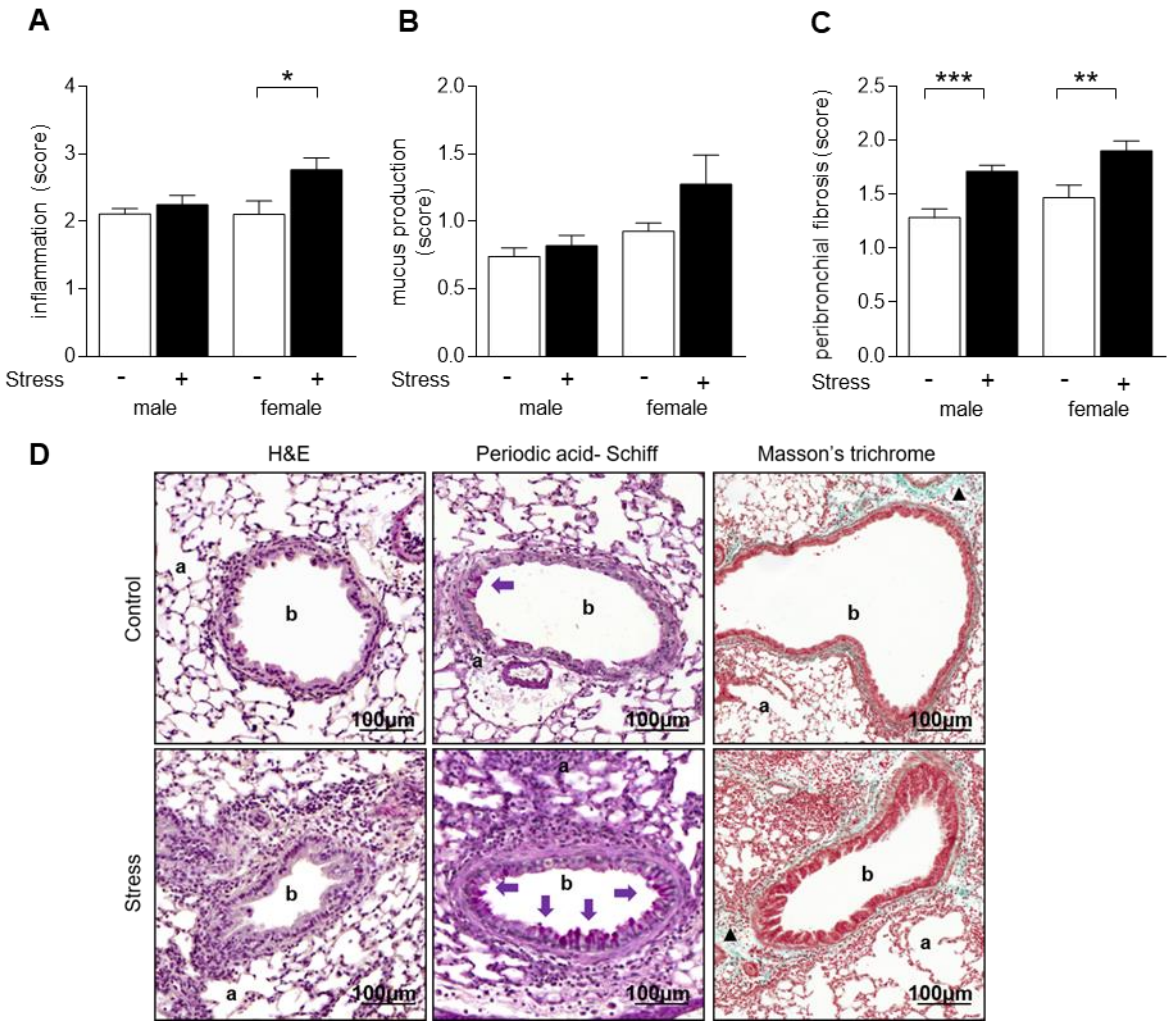

Figure 4. Airway inflammation and remodeling in prenatally stress challenged offspring upon experimental asthma induction. (A-C) Semiquantative analysis of (A) peribronchial immune cell infiltration, (B) the abundance of PAS-positive mucus-containing bronchial cells, and (C) peribronchial fibrosis in the lungs of control and prenatally stress challenged mice. (D) Representative images of lung sections from control (top) and prenatally stress challenged (bottom) female OVA-treated mice. Lung sections were stained with hematoxylin and eosin (H&E) (left) for morphological analysis of peribronchial inflammation, with PAS (middle) for evaluation of mucus production, and with Masson's trichrome (right) for peribronchial fibrosis assessment. Purple arrows show PAS-positive bronchial cells and triangles point to fibrotic areas around the bronchi. a, alveoli; b, bronchi. Sample size: 10 mice/group. Bars represent the mean ± SEM. *: p≤ 0.05;**:p≤ 0.01; ***: p<0.001 as assessed by student´s t-test or Mann-Whitney U test. Non-significant differences (p > 0.05) are not explicitly stated.

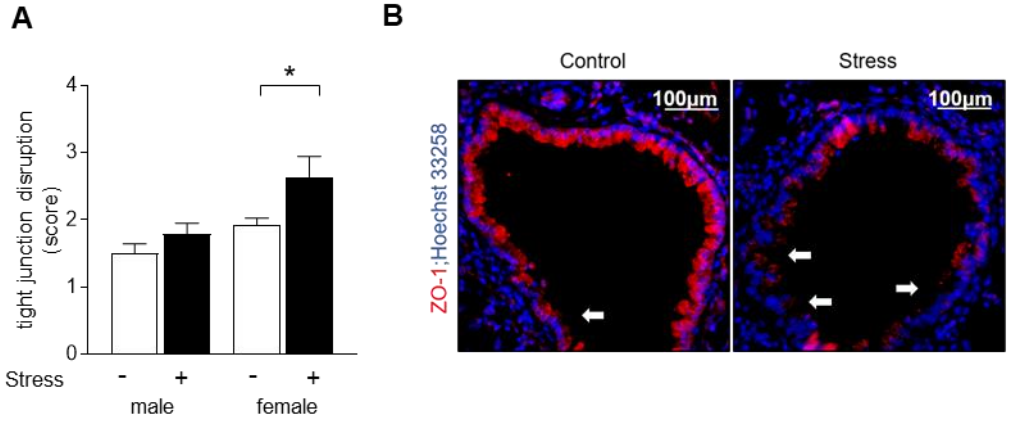

Figure 5. Airway epithelial barrier integrity following prenatal stress challenge and experimental asthma induction in mice. (A) Semiquantative analysis of tight junction disruption in the lungs of male and female control and prenatally stress challenged mice. (D) Representative images of lung sections from control (left) and prenatally stress challenged (right) female OVA-treated mice, after immunofluorescence staining with anti-ZO-1 (red; tight junctions) and Hoechst 33258 (blue; nuclei). Arrows indicate lesions in tight junction barrier within the bronchial epithelium. Sample size: 10 mice/group. Bars represent the mean ± SEM. *: $p \leq 0.05$ as assessed by Mann-Whitney U test. Non-significant differences ($p > 0.05$) are not explicitly stated.

3.2 Investigation of the mechanism underlying the prenatal stress-induced increased risk for asthma in early life

3.2.1 Generation of bone marrow chimeras to identify the target of prenatal stress challenge

After establishing a link between prenatal stress challenge and increased risk as well as severity of asthma in the murine offspring, we aimed to conclusively determine the target of prenatal stress. Since asthma is characterized by both lung and immune dysfunction, prenatal stress may predispose to asthma by affecting either the developing lung, immune system or both. To answer this question, we generated bone marrow chimeras, mice harboring prenatally stress challenged lungs or prenatally stress challenged immune system or both. Following exposure to prenatal stress, as described previously, or undisturbed pregnancy, prenatally stress challenged and control mice were born and left to grow for 10 weeks, respectively. Subsequently, irradiation and bone marrow transplantation (BMT) were performed. $CD45.2^+$ mice served as recipients and $CD45.1^+$ mice were used as donors to generate the following groups (Figure 6A):

1. Male and female mice with stress challenged lungs and bone marrow.
2. Male and female mice with stress challenged lungs and control bone marrow.
3. Male and female mice with control lungs and stress challenged bone marrow.
4. Male and female mice with control lungs and bone marrow.

Immune reconstitution was successfully completed within 5 weeks after BMT, as shown by flow cytometric analysis of peripheral blood from CD45.2$^+$ recipients (Figure 6B). Subsequently, experimental asthma was induced as described previously and the severity of the asthma-like phenotype was assessed.

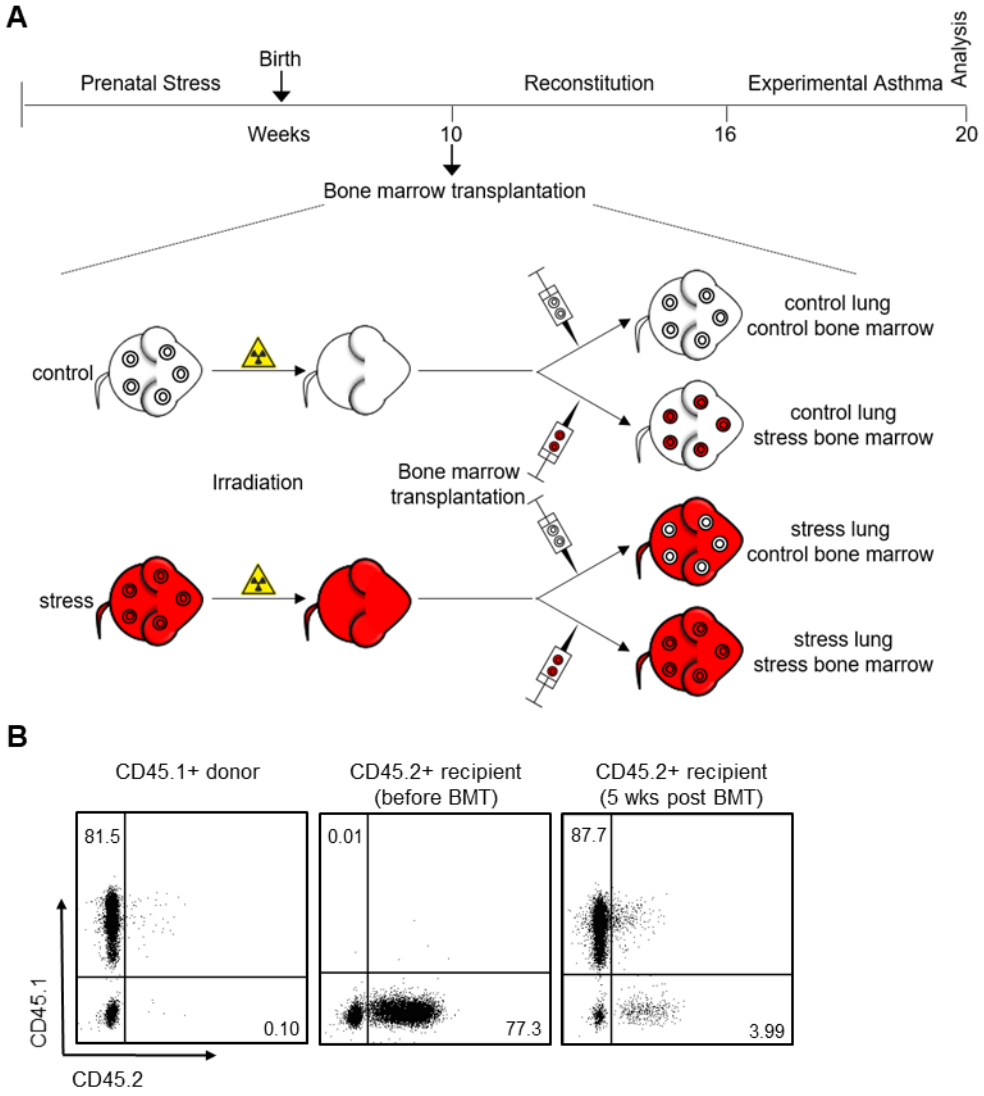

Figure 6. Generation of bone marrow chimeras to uncover the target of prenatal stress challenge. (A) Graphic description of the mouse model for prenatal stress challenge, bone marrow transplantation and postnatal experimental asthma induction in the adult offspring. Ten-week old prenatally stress challenged (red) and control (white) CD45.2$^+$ recipients were irradiated and subsequently transplanted with bone marrow from prenatally stress challenged or control CD45.1$^+$ donors. Following immune reconstitution, experimental asthma was induced, as shown in Figure 1A. (B) Representative dot plots for CD45.1 and CD45.2 within living cells in the peripheral blood of a CD45.1$^+$donor (left), CD45.2$^+$ recipient before (middle) and 5 weeks after bone marrow transplantation (BMT) (right), showing successful completion of immune reconstitution post BMT.

3.2.2 The impact of a prenatally stress challenged immune system on asthma susceptibility and severity in the murine offspring

After bone marrow transplantation and successful immune reconstitution, bone marrow chimeras were sensitized and subsequently challenged with OVA, based on our well-established protocol for experimental asthma induction. PBS-sensitized and challenged mice served as controls.

Interestingly, a prenatally stress challenged immune system alone did not significantly increase asthma susceptibility and severity in the murine offspring. Specifically, mice harboring control lungs and a prenatally stress challenged bone marrow exhibited similar airway hyperresponsiveness upon MCh provocation, compared to mice harboring control lungs and control bone marrow (Figure 7A, 6B).

Additionally, histological analysis of stained lung sections revealed no significant difference in peribronchial immune cell infiltration (Figure 7C, 7F), the abundance of mucus-containing bronchial cells (Figure 7D, 7F) and peribronchial fibrosis (Figure 7E, 7F) between mice harboring control lungs and control or prenatally stress challenged bone marrow. Furthermore, mice harboring a prenatally stress challenged bone marrow did not exhibit enhanced airway recruitment of alveolar macrophages, neutrophils and eosinophils or altered Treg numbers compared to the respective controls, as shown by flow cytometry of lungs and lung draining lymph nodes as well as analysis of leukocytes differentials in BAL cytospins (Figure 8).

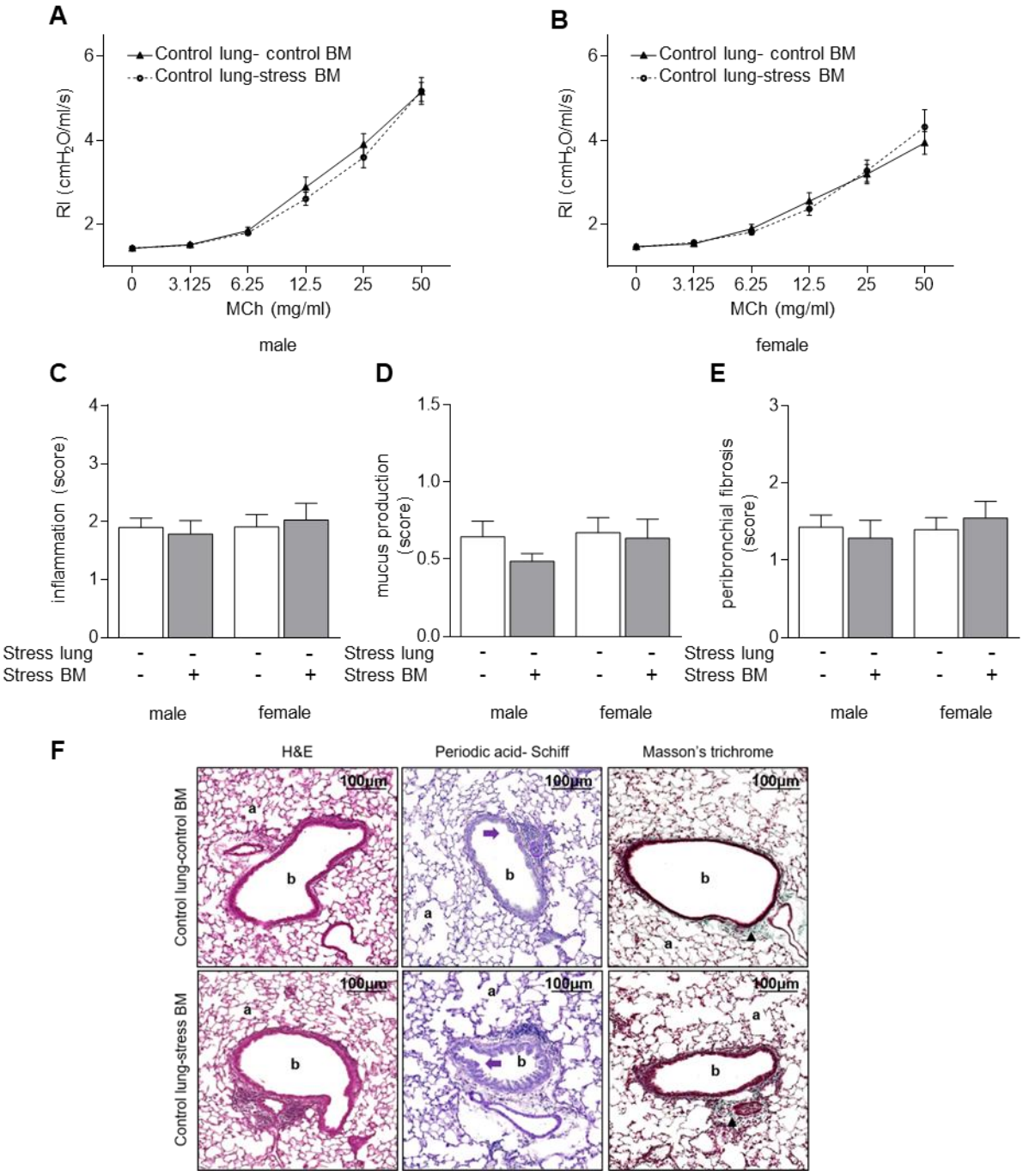

Figure 7. Asthma severity in the presence of a prenatally stress challenged immune system. (A,B) Airway response to increasing MCh doses in (A) male and (B) female OVA-treated mice with control lungs and control or prenatally stress challenged bone marrow (BM). (C-E) Semiquantative analysis of (C) peribronchial inflammation, (D) the abundance of PAS-positive mucus-containing bronchial cells, and (E) peribronchial fibrosis in the lungs of mice harboring control lungs and control or prenatally stress challenged BM. (F) Representative lung sections from OVA-treated mice with control lungs and control (top) or prenatally stress challenged (bottom) BM for analysis of peribronchial inflammation (left), mucus production (middle), and peribronchial fibrosis (right). Purple arrows show PAS-positive bronchial cells and triangles point to fibrotic areas around the bronchi. a, alveoli; b, bronchi. Sample size: 10 mice/group. Bars represent the mean ± SEM. The statistical significance was calculated by student´s t-test or Mann-Whitney U test, no significant differences between groups could be detected.

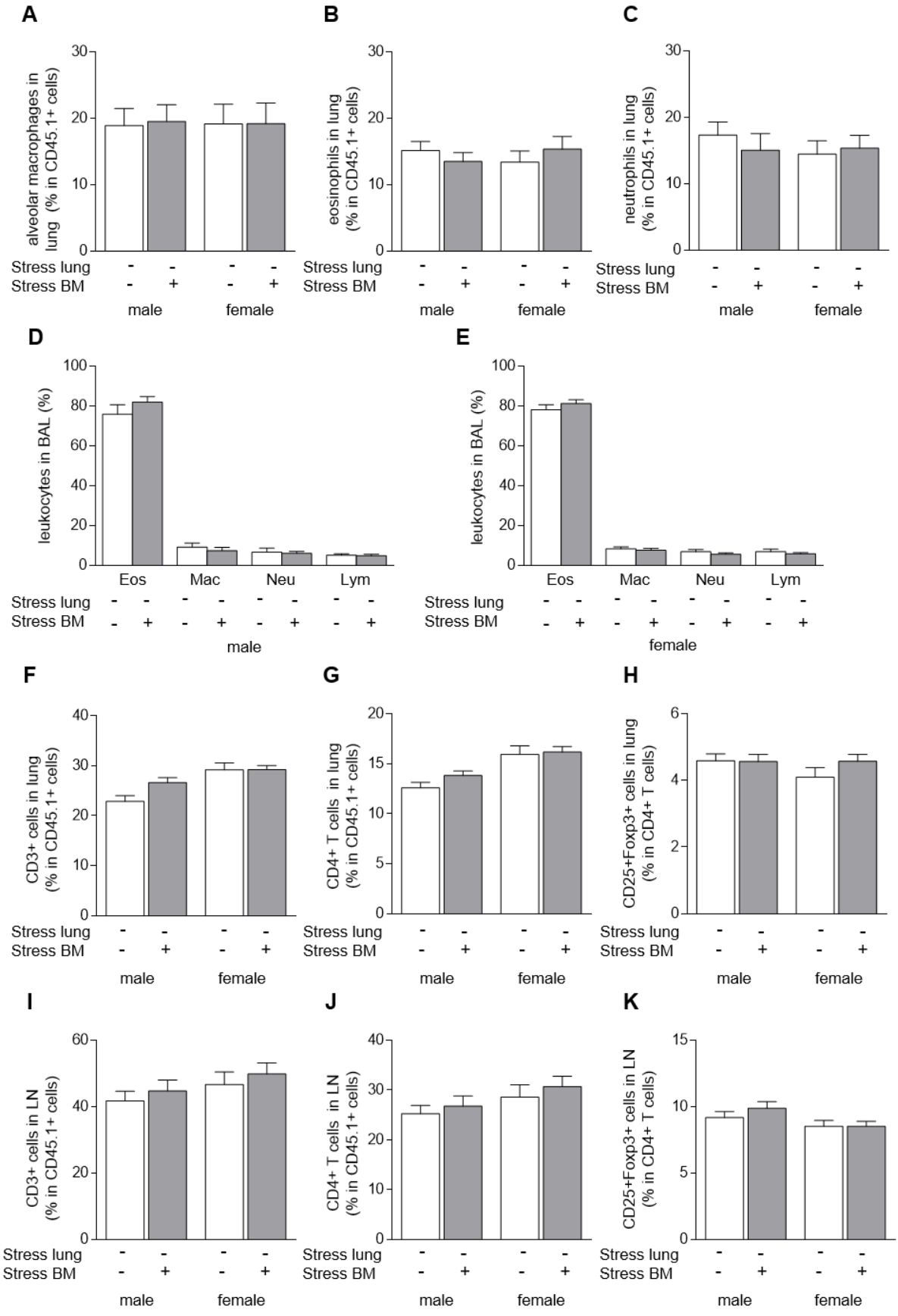
A
alveolar macrophages in lung (% in CD45.1+ cells)
B
eosinophils in lung (% in CD45.1+ cells)
C
neutrophils in lung (% in CD45.1+ cells)
Stress lung
Stress BM
male
female
D
leukocytes in BAL (%)
Eos
Mac
Neu
Lym
E
F
CD3+ cells in lung (% in CD45.1+ cells)
G
CD4+ T cells in lung (% in CD45.1+ cells)
H
CD25+Foxp3+ cells in lung (% in CD4+ T cells)
I
CD3+ cells in LN (% in CD45.1+ cells)
J
CD4+ T cells in LN (% in CD45.1+ cells)
K
CD25+Foxp3+ cells in LN (% in CD4+ T cells)

Figure 8. Influence of a prenatally stress challenged immune system on immune response upon experimental asthma induction. (A-C) Flow cytometric analysis of (A) alveolar macrophages, (B) eosinophils and (C) neutrophils in the lungs of male and female OVA-treated mice with control lungs and control or prenatally stress challenged bone marrow (BM). Cell frequencies are provided as percentages within $CD45.1^+$ cells (D,E) Morphological differentiation of leukocytes in BAL cytospins from (D) male and (E) female OVA-treated mice with control lungs and control or prenatally stress challenged BM. Eos, eosinophils; Mac, macrophages; Neu, neutrophils; Lym, lymphocytes. (F-K) Flow cytometric analysis of (F, I) $CD3^+$ cells, (G,J) $CD4^+$ T cells and (H,K) $CD25^+FoxP3^+CD4^+$ Tregs in the (F,G,H) lungs and (I,J,K) lung draining lymph nodes of male and female OVA-treated mice with control lungs and control or prenatally stress challenged BM. Sample size: 10 mice/group. Cell frequencies are provided as percentages within $CD45.1^+$cells (F,G,I,J) or $CD.4^+$ T cells (H,K). Bars represent the mean ± SEM. The statistical significance was calculated by student´s t-test or Mann-Whitney U test, no significant differences between groups could be detected.

3.2.3 The influence of a prenatally stress challenged lung on asthma susceptibility and severity in the murine offspring

Based on the findings described above, it became evident that mice harboring a prenatally stress challenged immune system and control lungs share a similarly mild asthmatic phenotype with mice carrying control lungs and immune system, following experimental asthma induction. Hence, the effect of prenatal stress challenge on the developing immune system alone can only slightly account for the stress-related high risk and severity of asthma early in life.

On the contrary, susceptibility to asthma and disease manifestation are significantly aggravated when prenatally stress challenged immune system and lungs coexist in one individual. For example, female bone marrow chimeras with prenatally stress challenged lungs and immune system exhibited the highest airway hyperresponsiveness compared to all other female groups (Figure 9A, 9B).

Similarly, peribronchial inflammation, mucus production as well as peribronchial fibrosis were significantly higher in female mice harboring prenatally stress challenged lungs and immune system compared to mice with control lungs and immune system (Figure 9C-F). Interestingly, a prenatally stress challenged lung alone could be sufficiently associated with enhanced asthma-related peribronchial inflammation and fibrosis regardless of the immune system (Figure 9C, 9 E-F).

Despite functional and histological findings indicating a significantly more severe disease manifestation in mice with prenatally stress challenged lungs and immune system, flow cytometry of lungs as well as analysis of leukocytes differentials in BAL cytospins revealed no difference in airway recruitment of alveolar macrophages, eosinophils and neutrophils among the groups (Figure 10). Additionally, the number of Treg cells in the lungs and lung draining lymph nodes was similar in all groups (Figure 11).

Taken together, these findings distinguish the two components of the pathogenesis of asthma, namely lung dysfunction and immunity and show that, while the latter remains unchanged, the former is aggravated in a prenatally stress challenged environment. Hence, although the stress-related higher asthma risk and severity may be attributed to a synergistic effect of prenatal stress on both organs, it is primarily the lung, and not the immune system, that crucially determines the manifestation of the disease following exposure to prenatal stress.

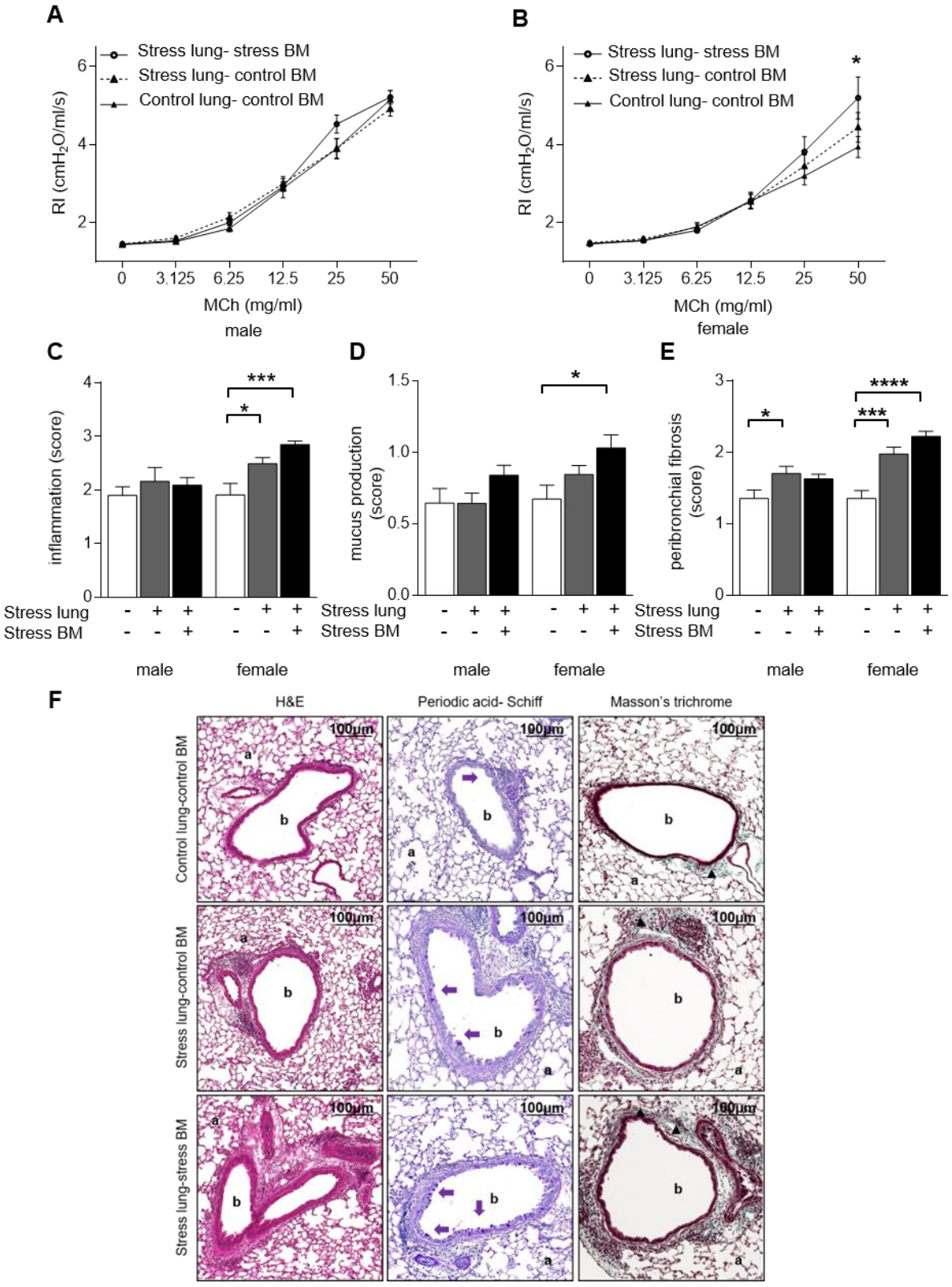

Figure 9. Asthma severity in the presence of prenatally stress challenged lungs and control or prenatally stress challenged immune system. (A, B) Airway response to increasing MCh doses in (A) male and (B) female OVA-treated mice with prenatally stress challenged or control lungs and bone marrow (BM). (C-E) Semiquantative analysis of peribronchial inflammation (C), the abundance of PAS-positive mucus-containing bronchial cells (D), and peribronchial fibrosis (E) in the lungs of mice harboring prenatally stress challenged or control lungs and BM. (F) Representative lung sections from OVA-treated mice with control lungs and control BM (top) and of mice with prenatally stress challenged lungs and control (middle) or stress challenged (bottom) BM for analysis of peribronchial inflammation

(left), mucus production (middle), and peribronchial fibrosis (right). Purple arrows show PAS-positive bronchial cells and triangles point to fibrotic areas around the bronchi. a, alveoli; b, bronchi. Sample size: 10 mice/group. Bars represent the mean ± SEM. *: p ≤0.05;**:p ≤ 0.01; ***:p ≤0.001; ****:p ≤0.0001 as assessed by one-way ANOVA. Non-significant differences (p > 0.05) are not explicitly stated.

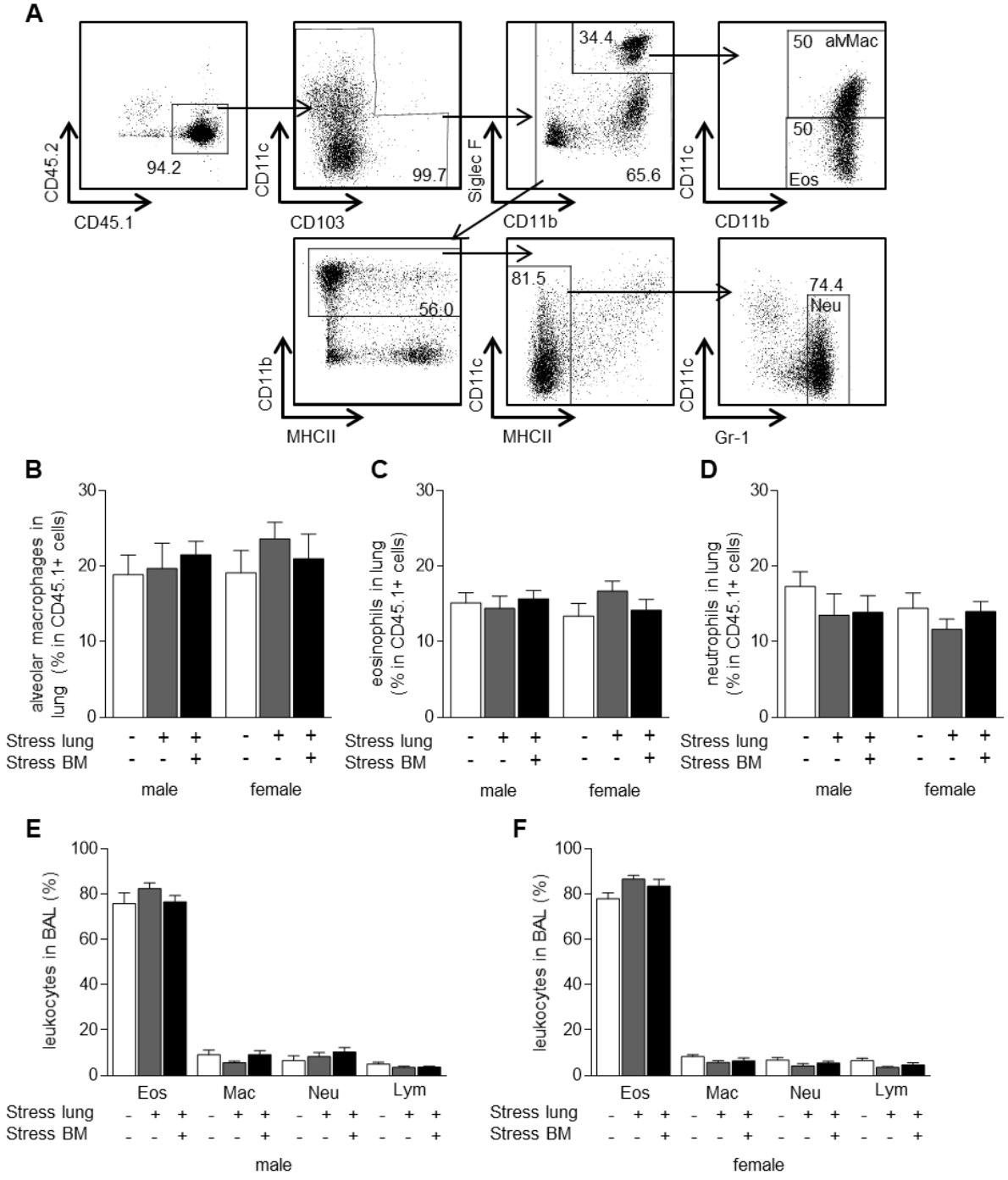

Figure 10. Airway immune cell recruitment in bone marrow chimeras upon experimental asthma induction. (A) Gating strategy to characterize immune cell recruitment in the murine lung following experimental asthma induction. Alveolar macrophages (alvMac; $CD45.1^{+}CD11c^{+}CD11b^{neg}SiglecF^{+}$), eosinophils (Eos; $CD45.1^{+}CD11c^{neg}CD11b^{+}SiglecF^{+}$) and neutrophils (neu; $CD45.1^{+}CD11b^{+}MHCII^{neg}Gr1^{hi}$) were distinguished by flow cytometry based on the characterization published in (158, 159). (B-D) Flow cytometric analysis of (B) alveolar macrophages, (C) eosinophils and (D) neutrophils in the lungs of male and female OVA-treated mice with prenatally stress challenged or control lungs and bone marrow (BM). Cell frequencies are provided as percentages within $CD45.1^{+}$ cells (D,E) Morphological differentiation of leukocytes in BAL cytospins from (E) male and (F) female

OVA-treated mice with prenatally stress challenged or control lungs and BM. Eos, eosinophils; Mac, macrophages; Neu, neutrophils; Lym, lymphocytes. Sample size: 10 mice/group. Bars represent the mean ± SEM. The statistical significance was calculated by one-way ANOVA, no significant differences among groups could be detected.

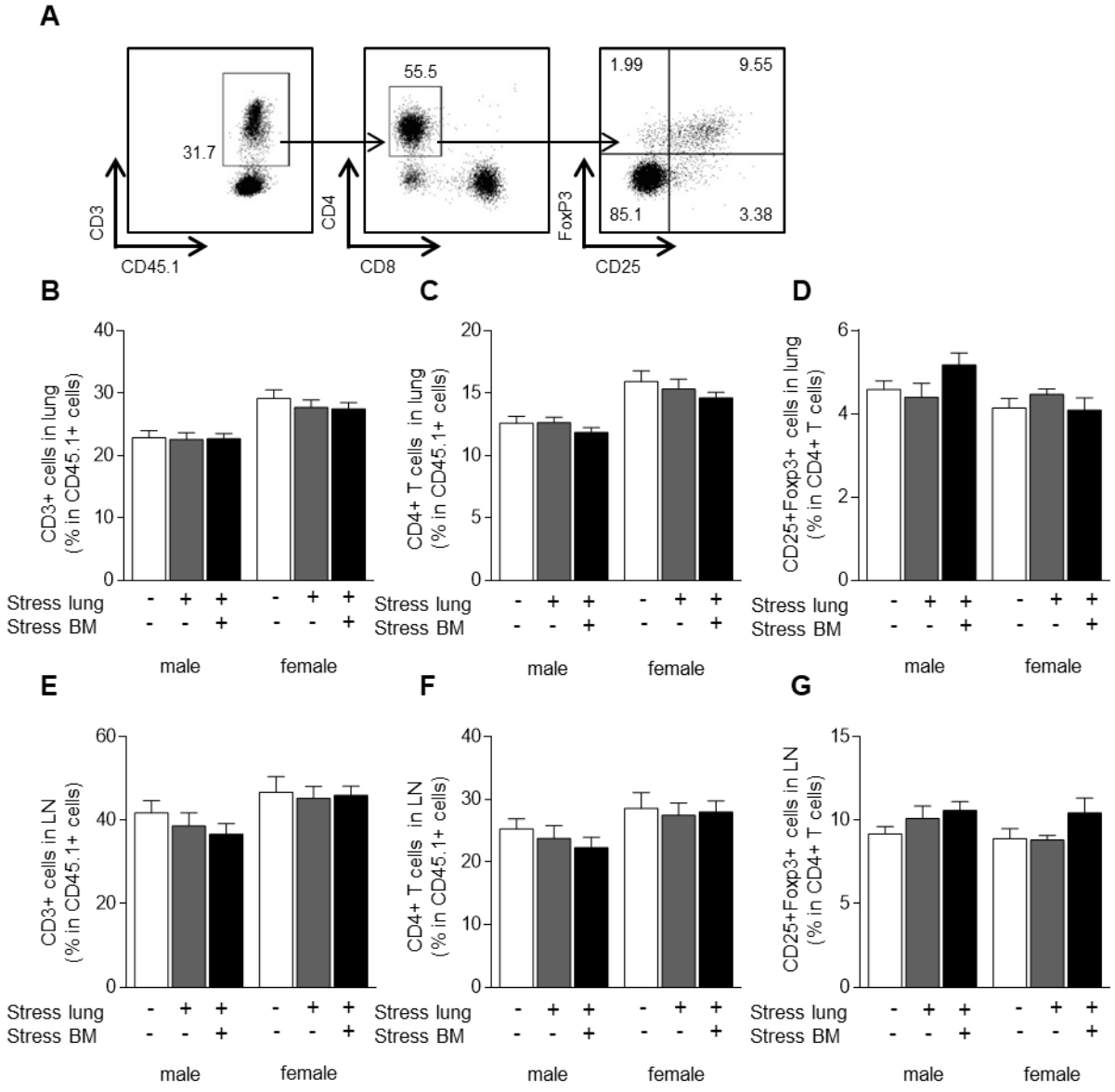

Figure 11. Regulatory T cells in the lungs and lung draining lymph nodes of bone marrow chimeras upon experimental asthma induction. (A) Gating strategy to identify $CD25^+FoxP3^+CD4^+$ Tregs in lung draining lymph nodes of OVA-treated mice. (B-G) Flow cytometric analysis of (B, E) $CD3^+$ cells, (C,F) $CD4^+$ T cells and (D,G) $CD25^+FoxP3^+CD4^+$ Tregs in the (B,C,D) lungs and (E,F,G) lung draining lymph nodes of male and female OVA-treated mice with prenatally stress challenged or control lungs and bone marrow (BM). Cell frequencies are provided as percentages within $CD45.1^+$cells (B,C,E,F) or $CD.4^+$ T cells (D,G). Sample size: 10 mice/group. Bars represent the mean ± SEM. The statistical significance was calculated by one-way ANOVA, no significant differences among groups could be detected.

3.3 The impact of prenatal stress challenge on the developing lung

3.3.1 Impaired lung development upon prenatal stress challenge

Based on our findings associating the presence of a prenatally stress challenged lung with an increased asthma severity, we hypothesized that prenatal stress interferes with crucial steps of lung development, thereby setting the ground for postnatal lung dysfunction and asthma in early life. To test this hypothesis, we used our model for prenatal stress challenge and assessed lung development histologically just before birth, on gd 18.5, and postnatally, throughout the first month of life. Additionally, mRNA expression of genes associated with lung development, cellular differentiation and glucocorticoid signaling in prenatally stress challenged and control lungs was evaluated on several prenatal and postnatal time points throughout the developmental process (Figure 12).

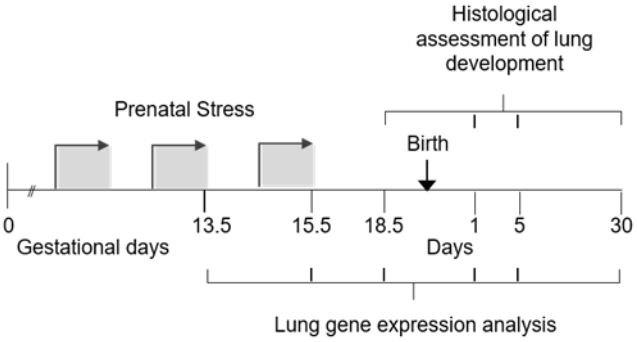

Figure 12. Experimental setup for assessment of fetal and postnatal lung development. Following prenatal stress challenge, lung development was histologically assessed on gd 18.5 and postnatal days (pd) 1, 5 and 30. mRNA expression of genes associated with lung development, differentiation and glucocorticoid signaling in the lungs was analyzed on gd 13.5,15.5,18.5 and pd 1,5 and 30.

Histological analysis of H&E stained lung sections on gd 18.5 revealed pronounced morphological differences between control and stress challenged tissues. While control lungs were appropriately developed, with extensive terminal sacs and thin intersaccular, or interalveolar, walls, as expected just before birth, the lungs of stress challenged fetuses appeared immature, with morphological traits corresponding to earlier developmental stages. Following sex-specific analysis, we observed that the lungs of male stress challenged fetuses were moderately affected, with properly formed terminal sacs, increased surrounding mesenchymal tissue and significantly thicker interalveolar walls, as compared to the respective controls (Figure 13). On the other hand, the lungs of female stress challenged fetuses were severely affected with structural signs pointing to significant developmental delay. Specifically, despite intact branching initiation from the primary lung buds, further branching morphogenesis was

disrupted, thereby resulting in limited airspace expansion and significantly smaller terminal sacs, as compared to the respective controls (Figure 13A, 13C). Additionally, impaired decomposition of the surrounding mesenchymal tissue resulted in hypercellular thick interalveolar walls (Figure 13B, 13C). Due to the limited airspaces and the surrounding hypercellular mesenchyme, the lung parenchyma of female stress challenged fetuses exhibited a dense gland-like structure, which is normally not expected at such a late developmental stage (Figure 13).

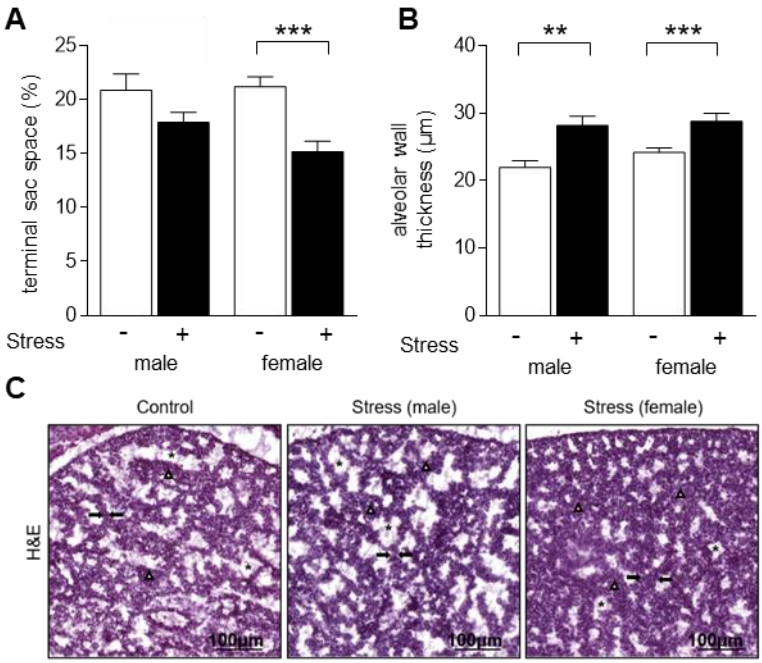

Figure 13. Sex-specific impact of prenatal stress challenge on fetal lung development. (A) Volume fraction of terminal sac spaces estimated by point counting, and (B) mean alveolar wall thickness estimated by point and intersection counting in the lungs of male and female control and stress challenged fetuses on gd 18.5. (C) Representative images from lungs of control (left), male stress challenged (middle) and female stress challenged (right) fetuses, after H&E staining. Arrows point to interalveolar walls, triangles and asterisks show mesenchymal tissue and terminal sac spaces, respectively. Sample size: 10 mice/group. Bars represent the mean ± SEM. **:$p \leq 0.01$; ***:$p \leq 0.001$ as assessed by student's t-test or Mann-Whitney U test. Non-significant differences ($p > 0.05$) are not explicitly stated. Data were pulished in (171).

Interestingly, the effect of prenatal stress challenge on lung development persisted postnatally. In mice, the postnatal phase of lung development comprises the formation of alveoli, also known as alveolarization, and it is completed within the first month of life. Alveolarization requires the generation of interalveolar septa, which subdivide preexisting terminal sacs into smaller alveoli. Continuous septum formation gives rise to a gradually growing number of smaller alveoli, thereby increasing lung parenchyma complexity. The progress of alveolarization following prenatal stress challenge was assessed based on serial histological analysis of the airspace size throughout the first month of life. To this end, we measured the

mean linear intercept (MLI), which describes the mean free distance in the airspaces and is, therefore, commonly used to quantify their size, on postnatal days (pd) 1, 5 and 30. A gradual MLI reduction is expected during postnatal lung development since the ongoing alveolarization comprises the formation of gradually increasing in number but decreasing in size airspaces.

Indeed, a gradually decreasing MLI and thus, airspace size was observed in both control and prenatally stress challenged mice throughout the first month of life. However, a late onset of alveolarization, as indicated by the high MLI one day after birth, was found in both male and female prenatally stress challenged mice, as compared to the respective controls (Figure 14A, 14B). Although the male mice managed to quickly catch up with the respective controls with subsequent normal progression of the alveolar stage of lung development, the female prenatally stress challenged offspring exhibited consistently delayed alveolarization, as shown by the significantly higher MLI and its slower decrease to normal values on pd 30, as compared to female controls (Figure 14).

Hence, prenatal stress disturbs both prenatal and postnatal milestones of lung development, especially in the female offspring.

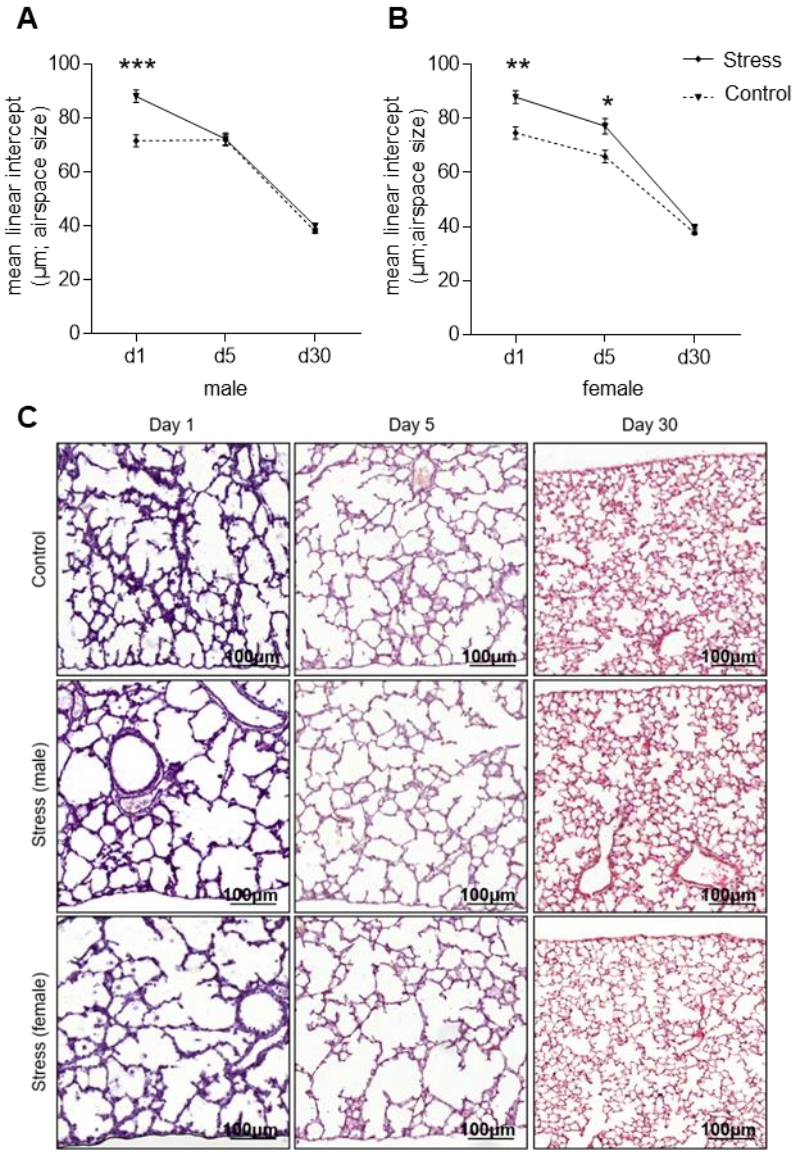

Figure 14. Prenatal stress challenge affects alveolarization, especially in the female murine offspring. (A,B) Mean linear intercept (MLI), as measure of the airspace size, in the lungs of male (A) and female (B) control and prenatally stress challenged mice on days (d) 1, 5 and 30 after birth. Note that, upon prenatal stress challenge, a slowly decreasing MLI indicates a delayed alveolarization during the first month of life. (C) Representative images from lungs of control (top), male stress challenged (middle) and female stress challenged (bottom) mice, on postnatal days 1(left), 5 (middle) and 30 (right) after H&E staining. Sample size: 10 mice/group. Bars represent the mean ± SEM. *:$p \leq 0.05$;**:$p \leq 0.01$; ***:$p \leq 0.001$ as assessed by student's t-test or Mann-Whitney U test. Non-significant differences ($p > 0.05$) are not explicitly stated.

3.3.2 Sex-specific alterations in lung gene expression upon prenatal stress challenge

To further characterize the effect of prenatal stress challenge on the developing lung and elucidate the mechanisms underlying the stress-induced arrest in development, the mRNA expression of factors associated with development, differentiation and glucocorticoid signaling was evaluated in prenatally stress challenged and control lungs throughout the developmental process. Specifically, to assess the progress of lung development, we analyzed the expression

pattern of *Igf1* and *Igf1r*, two well-known promoters of the developmental process, *Sox9*, whose expression is related to branching morphogenesis, and *Adam33*, an asthma susceptibility gene associated with lung development (66). Due to the role of *Sox9* in the transition from branching morphogenesis to alveolar epithelial terminal differentiation and its reported downregulation starting from gd 16.5 (146), its expression was analyzed on gd 15.5 and 18.5. To evaluate the differentiation state of type I and II AEC, the expression of *Aqp5* as well as *Sftpc* and *Sftpa* was measured, respectively. As alveolarization progresses, analysis of *Sftpc* expression provides sufficient insight into the maturation of type II AEC. Therefore, *Sftpa* expression was not determined postnatally. Assessment of the glucocorticoid-related signaling in the lung was based on the expression of *Hsd11b1* and *Hsd11b2*, two enzymes responsible for activation and inactivation of corticosterone in rodents, respectively, as well as the expression of *Nr3c1*, coding for the glucocorticoid receptor and of glucocorticoid-induced leucine zipper *(Gilz*), whose expression is stimulated by glucocorticoids (164).

Interestingly, sex-specific alterations in the expression of several of the above mentioned markers were observed upon prenatal stress challenge, with female stress challenged lungs exhibiting a more profoundly disturbed expression pattern both prenatally and postnatally, as compared to the respective controls (Figure 15).

Importantly, *Igf1* and *Igf1r* were significantly downregulated prenatally, on gd15.5 and 18.5, in the lungs of female stress challenged fetuses, while, at the same time, being slightly upregulated in the male ones, as compared to the respective controls. An upregulation of both markers was observed in both male and female prenatally stress challenged mice after birth, on pd 1. Similarly, genes involved in the glucocorticoid signaling pathway, namely *Nr3c1* and *Gilz,* were prenatally upregulated in the male stress challenged fetuses, whereas both genes and especially *Gilz* were downregulated in female stress challenged fetal lungs. Additionally, a slight downregulation of *Aqp5, Sftpc* and *Sftpa* was observed in female stress challenged fetal lungs just before birth, thereby suggesting a potential delay in AEC differentiation (Figure 15).

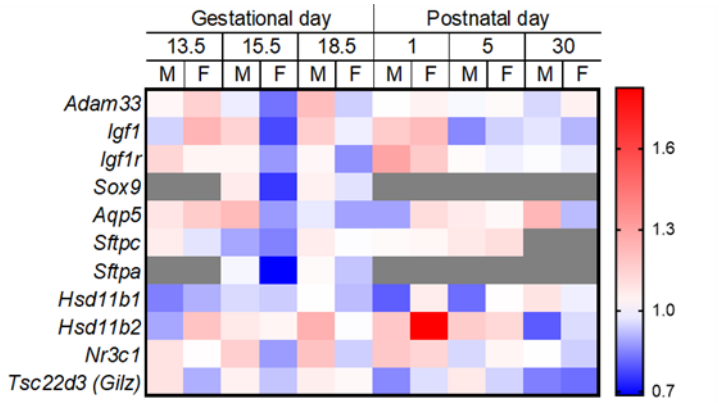

Figure 15. Altered lung gene expression upon prenatal stress challenge. Heat map depicting the differential lung mRNA expression of genes associated with lung development, cellular differentiation and glucocorticoid signaling between prenatally stress challenged and control mice. Red shades indicate higher and blue shades lower expression. Color key indicates the intensity associated with normalized expression values (fold change). Grey color: not applicable; M, males; F, females.

In summary, prenatal stress challenge affects the developing lung in a sex-specific manner, with especially the female offspring showing signs of profound lung immaturity, namely impaired branching morphogenesis and delayed postnatal alveolarization. This developmental arrest may be – at least partially- attributed to stress-induced sex-specific alterations in lung gene expression, and especially to IGF1/IGF1R signaling defects, as seen in the female offspring.

4 Discussion

Fetal programming encompasses the role of intrauterine environment in shaping postnatal health and disease. Specifically, prenatal maternal stress perception emerges as a crucial determinant of the offspring's health later in life. Indeed, recent epidemiological studies demonstrate an association between prenatal maternal stress and an increased risk for childhood asthma (43, 165), which, in some cases, appears to be sex-specific, with prenatal stress favoring asthma manifestation mainly in girls or boys in different settings (42, 44). In agreement to such clinical observations, using our well-established mouse models for midgestational stress challenge and postnatal experimental asthma induction, we managed to identify a sex-specific link between prenatal stress challenge and increased asthma severity in early life. Specifically, following OVA-mediated sensitization and challenge, female prenatally stress challenged mice exhibited a severe asthma-like phenotype, characterized by increased AHR, airway inflammation, mucus production and airway remodeling, whereas the male prenatally stress challenged offspring were only mildly affected, as compared to the respective controls.

Upon increased maternal stress perception, activation of the maternal HPA axis boosts glucocorticoid secretion, which subsequently disturb maternal immune adaptation to pregnancy thereby threatening fetal growth and development. Additionally, excessive maternal circulating glucocorticoids directly affect the developing fetus, as they manage to overcome 11β-HSD2-mediated inactivation in the placenta and enter the fetal circulation (53), thereby critically disturbing fetal homeostasis.

Despite its well-recognized association with poor postnatal health, the exact target of prenatal stress challenge and in turn, excessive maternal glucocorticoids in the developing fetus remains elusive. Mounting evidence supports a strong link between prenatal maternal stress and impaired immunity in the offspring and therefore, a potential stress-induced detrimental effect on the developing immune system cannot be neglected (166). On the other hand, prenatal challenges such as maternal stress perception and high glucocorticoid may also affect the developing lung, thereby predisposing to postnatal lung dysfunction and disease.

Since both lung dysfunction and impaired immunity are implicated in the pathogenesis of asthma, we next aimed to determine which of the two developing organs is mostly targeted by prenatal stress thereby increasing the risk for disease manifestation. To this end, we successfully generated bone marrow chimeras harboring prenatally stress challenged or control lungs and immune system. After experimental asthma induction, mice harboring a prenatally stress challenged lung and control bone marrow exhibited significantly higher allergic airway inflammation and remodeling as compared to mice with control lungs. On the other hand, mice

carrying a prenatally stress challenged immune system and control lungs presented a mild asthma-like phenotype, similar to the respective controls. Importantly, the highest asthma severity, translated in increased AHR, peribronchial immune cell infiltration, mucus production and fibrosis, was observed in mice harboring both prenatally stress challenged lungs and immune system. However, morphological analysis of BAL cytospins and flow cytometry revealed no differences in the frequency of asthma-related immune cell populations in the BAL, lungs and lung draining lymph nodes among the OVA-treated groups. Taken together, these observations suggest that the lung is the main culprit for enhanced asthma severity upon prenatal stress challenge. A similar immune response in the presence or absence of a prenatally stress challenged lung or immune system further supports the main role of lung dysfunction and remodeling in asthma development in this context. However, a synergy of both organs cannot be excluded, since a prenatally stress challenged immune system seems to have an additive effect thereby aggravating asthma severity only when combined with a prenatally stress challenged lung.

Based on our results identifying the lung as the key target of prenatal stress challenge and the main mechanistic link with an increased risk for postnatal asthma in this context, we hypothesized that prenatal stress challenge interferes with crucial steps of lung development thereby programming postnatal lung function and health. Since lung development is a tightly regulated multistage process, any intrauterine adversity challenging its homeostasis may severely affect its outcome. In our experiments, maternal exposure to stress coincided with the critical embryonic and pseudoglandular developmental stages. Hence, a detrimental effect on the developing lung could be expected. Indeed, serial histological assessment of lung development together with analysis of mRNA expression of selected genes associated with development, differentiation and glucocorticoid signaling revealed a sex-specific impact of prenatal stress challenge on the developing lung. Although the male lungs were only mildly affected upon prenatal stress challenge, the female stress challenged offspring exhibited a significantly impaired lung development both prenatally and postnatally, as evidenced by disrupted branching and delayed alveolarization, respectively. Interestingly, this observation was complemented by stress-induced sex differences in lung gene expression, with the downregulation of *Igf1* and *Igf1r* in females proposing a defective IGF1/IGF1R signaling as a plausible mechanistic explanation for the reported developmental arrest, especially in the female lung. In agreement to our findings, sex-specific alterations in *Igf1* and *Igf1r* expression in fetal murine lungs were reported as a consequence of prenatal tobacco smoking exposure and

therefore, both factors seem to be commonly targeted by prenatal challenges and programming agents (167).

Overall, our findings support a sex-specific association between prenatal stress challenge and increased asthma susceptibility and severity in early life and identify a direct detrimental effect of stress on the developing lung, especially in the female offspring, as a potential underlying mechanism. The reported impact of stress on lung development could be related with a stress-induced decrease in maternal progesterone, a hormone crucially involved in pregnancy maintenance and fetal development. Such a reduction in maternal progesterone could be attributed to the so-called "pregnenolone steal", a term describing how pregnenolone, a precursor hormone for both cortisol and progesterone, is diverted towards cortisol production and away from progesterone production upon stress exposure. Strikingly, low maternal progesterone, as seen in stress challenged pregnancies, has been associated with poor fetal growth and development in mice (26), and, in human studies, with an increased risk for atopic dermatitis, allergic asthma and rhinitis in girls during childhood (10). Importantly, administration of the progesterone derivative, dihydrodydrogesterone, to stress challenged pregnant mice ameliorated the prenatal stress-related asthma-like symptoms only in the female offspring (45). Based on our findings describing a stress-mediated programming of lung development and postnatal asthma manifestation, one could attribute the association between low maternal progesterone and childhood asthma to a similar progesterone-mediated effect on the developing lung. Indeed, progesterone is centrally involved in lung development, as it appears to enhance alveolarization and surfactant production (168, 169). Therefore, differential expression of the progesterone receptor in the male and female lung might account for the observed sex-specific effect of both prenatal stress challenge and maternal progesterone levels. Indeed, higher mRNA expression of the progesterone receptor in distal lung epithelial cells from female rat fetuses was recently reported, as compared to male fetal cells (170). Upregulation of the progesterone receptor may render the female fetal lung more sensitive and thus, more susceptible to a stress-induced reduction in progesterone levels, as compared to the male one, with dramatic consequences for its development and postnatal function.

Apart from their potential effect on maternal progesterone, prenatal stress and stress-triggered high glucocorticoid levels may directly interfere with the developing lung. Under physiological conditions, glucocorticoids play a key role in fetal lung maturation. To exert their function, glucocorticoids bind to the intracellular glucocorticoid receptor (GR), encoded by *NR3C1* gene in humans and mice. Upon glucocorticoid-induced GR activation, the receptor-glucocorticoid complex regulates gene transcription either directly by translocating into the nucleus or

indirectly via interaction with transcription factors in the cytoplasm (171). In early stages of lung development, GR expression is mainly found in the bronchial branching epithelium, but as gestation, and thus, lung development progress, all cell types and especially the airway and alveolar epithelium as well as the bronchial vessels express increasing GR levels (172-174). An upregulation of GR and therefore, a higher sensitivity to glucocorticoids is essential during late gestation, when endogenous glucocorticoids increase and exert their main function as promoters of fetal lung maturation. At this time, glucocorticoids induce significant morphological alterations in the pulmonary architecture, including decomposition of the mesenchymal tissue compartment and alignment of terminal sacculi with surrounding vessels thereby facilitating interalveolar wall formation and gas exchange after birth (175). Importantly, glucocorticoids also stimulate alveolar epithelial cell differentiation and surfactant production in late gestation, and therefore prepare the lung for the first breath. Due to their stimulatory effect on fetal lung maturation, synthetic glucocorticoids are broadly administered to women at risk for preterm delivery to reduce neonatal respiratory morbidity and mortality (176).

Despite their well-established beneficial role in late stages of lung maturation, untimely exposure to excessive glucocorticoids in early or mid-gestation may disturb the ongoing developmental process and negatively affect the developing lung. Indeed, adverse effects of high glucocorticoids on lung development have been reported in several human and animal studies. Specifically, epidemiological studies associate early and late postnatal dexamethasone administration to preterm infants with an increased risk for respiratory hospital readmission and poor lung function in later life and therefore, raise concerns about the impact of such drugs on the developing lung (177, 178). Similarly, studies in rats link prenatal dexamethasone treatment with inhibited secondary septation and thus, impaired alveolarization after birth (179-181). These findings go in line with our results revealing a stress- or glucocorticoid-induced delay in alveolarization, especially in the female offspring.

Our observations linking increased maternal stress perception and thus, high glucocorticoids, in mid-gestation with an impaired lung development and maturation, might be attributed to a glucocorticoid-induced negative feedback regulation of GR expression with a subsequent reduction in tissue sensitivity to glucocorticoids (174). An increased glucocorticoid resistance would then be detrimental, especially in late gestation, when fetal lung maturation depends mostly on glucocorticoid-mediated signaling. Indeed, previous studies in adult rodents indicate that administration of glucocorticoids leads to reduced GR mRNA expression and protein levels, and thus, to glucocorticoid resistance, in several tissues (182-184). On the other hand, upon glucocorticoid stimulation, GR expression may be differentially modulated depending on

the developmental stage and cell type. For example, although glucocorticoids were shown to induce a reduction in GR mRNA levels in rat brain and liver postnatally, no alteration was observed in the respective fetal organs (185). Similarly, the simultaneous increase of glucocorticoids and GR abundancy in the fetal lung during late gestation may indicate absence of a glucocorticoid-induced negative feedback regulation of GR expression in the lung at this time point. However, *in vivo* and *in vitro* studies focusing on GR ontogeny in late stages of lung development show that such a glucocorticoid-stimulated negative GR regulation may conditionally exist, in a cell-dependent manner. Specifically, incubation of fetal lung fibroblasts with cortisol *in vitro* increased GR protein levels whereas same treatment of distal airway epithelial cells resulted in lower GR protein concentration. Interestingly, in both cases, no changes in GR mRNA expression were observed, a finding suggesting that glucocorticoid-induced regulation of GR expression in the fetal lung takes place at a post-transcriptional level (174). Hence, slight or no changes in GR mRNA expression upon stress challenge, as observed in our setting, do not exclude a post-transcriptional glucocorticoid-mediated GR repression and an increased glucocorticoid resistance, especially in female lungs. Such an effect would then hamper the stimulatory effect of glucocorticoids on fetal lung maturation thereby resulting in developmental arrest, as seen in our female fetuses.

This sex-biased effect of glucocorticoids on lung development might be attributed to potentially differential exposure of male and female lungs to circulating glucocorticoids. As previously mentioned, fetal exposure to maternal glucocorticoids is tightly regulated in the placenta, where 11β-HSD2 and 11β-HSD1 are responsible for inactivation or activation of glucocorticoids, respectively. Based on mounting evidence suggesting that prenatal challenges modulate placental gene expression in a sex-specific manner (155, 186) one can assume that, upon stress exposure, an altered 11β-HSD2/11β-HSD1 ratio in the female placenta might increase

transplacental flow of glucocorticoids thereby augmenting their effect on the developing female fetus.

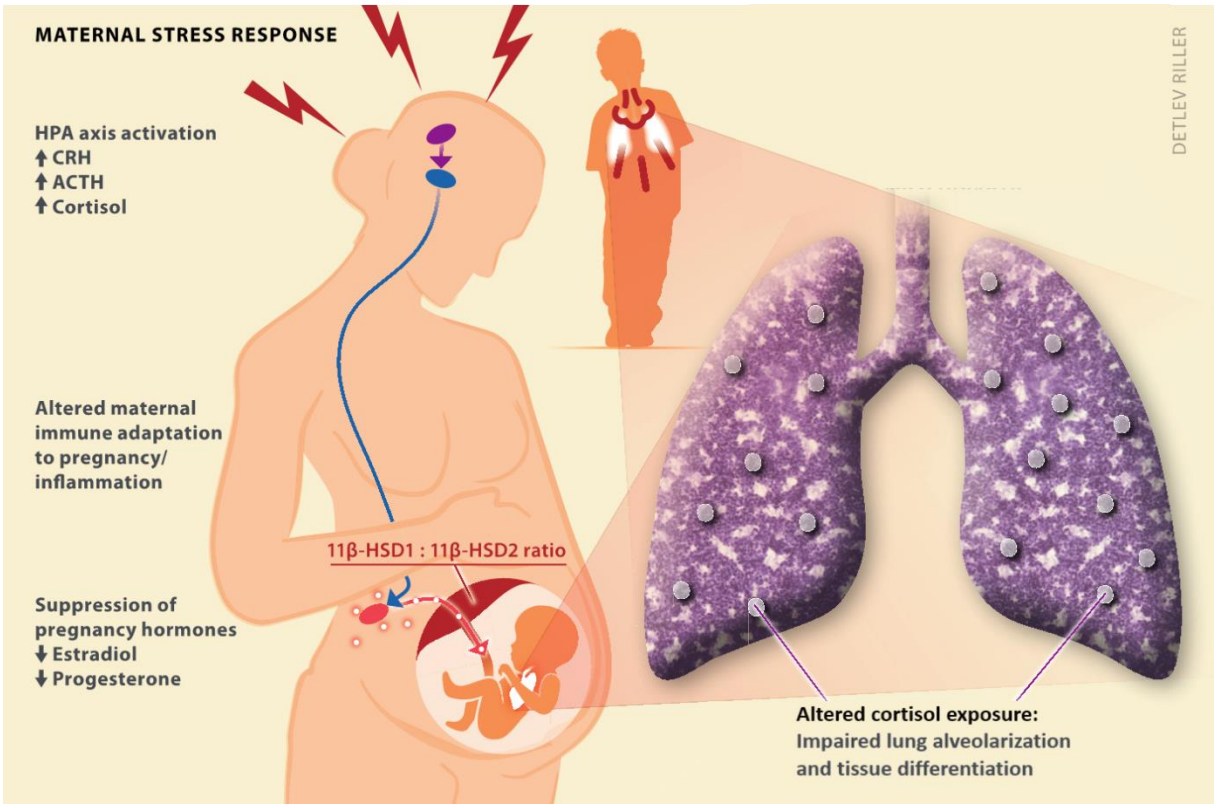

Figure 16. Hypothetical scenario on prenatal stress-induced altered fetal lung development. Stress challenge activates the hypothalamic-pituitary-adrenal (HPA) axis, which results in the secretion of neuroendocrine hormones. Here, the corticotropin-releasing hormone (CRH) stimulates the maternal pituitary gland, leading to increasing levels of adrenocorticotropic hormone (ACTH). In turn, ACTH activates the release of cortisol (corticosterone in mice) from the adrenal gland. Cortisol can transfer across the placenta into the fetus. This transfer is regulated by two placental enzymes, 11β-hydroxysteroid dehydrogenase (HSD) type 1 (11β-HSD1) and type 2. 11β-HSD1 converts largely inert cortisone into active cortisol, whereas 11β-HSD2 converts active glucocorticoids into inactive glucocorticoids. Placental 11β-HSD2 may also protect the fetus from an excessive maternal glucocorticoid surge, e.g. in response to stress. Maternal progesterone levels contribute to the maintenance of 11β-HSD2 activity. Conversely, prenatal stress can reduce levels of progesterone, subsequently interfering with 11β-HSD2 activity. Moreover, low levels of progesterone during pregnancy have been linked to an altered maternal immune adaptation to pregnancy, mirrored by increased inflammation. Overall, an untimely aberrant fetal glucocorticoid exposure may negatively interfere with the developing lung thereby resulting in impaired lung alveolarization, postnatal lung dysfunction, and subsequently, in a higher risk for airway diseases such as asthma in childhood.

The developmental defects described here seem to be associated with poor postnatal lung function and an increased risk for airway diseases such as asthma. Due to prenatal stress challenge, the final crucial milestones of prenatal lung development are not timely reached and thus, the lung seems inadequately prepared for postnatal life. The pivotal role of an impaired lung growth in asthma development is also supported by the well-recognized link among prematurity, its most common respiratory complication, namely bronchopulmonary dysplasia,

and an increased risk for asthma later in life (187, 188). Our findings highlighting the primary role of a poorly developed lung in the pathogenesis of asthma upon prenatal stress challenge support the theory of Holgate, who claims that the lung, and specifically the airway epithelium, is mainly responsible for the aberrant immune response and increased allergen sensitivity driving asthma manifestation (189). An impaired bronchial epithelial barrier function caused by tight junction disruption, as seen in our female prenatally stress challenged OVA-treated mice, results in increased epithelial permeability. A highly permeable airway epithelium allows inhaled agents to pass into the airway wall and attract immune and inflammatory cells. This feature, together with defects in antioxidant defense, leads to a status of chronic epithelial injury, inflammation and incomplete repair thereby giving rise to the hallmarks of asthma, namely AHR, inflammation and airway remodeling. Importantly, a disordered epithelial function may predispose the affected individual to early-life respiratory infections, which have been independently associated with an increased risk for allergic asthma in childhood (190).

Importantly, pulmonary factors, including lung development and function, might also partially explain the sex differences in asthma prevalence and severity throughout life. While preadolescent boys are more likely to suffer from asthma, as compared to age-matched girls (191), this sex bias reverses during puberty and adulthood, when females are at increased risk of developing asthma and also suffer from more severe disease compared to men (192, 193). Interestingly, studies in mice also support a female preponderance for asthma in adulthood (194-196). In accordance to previous findings in unchallenged mice, we demonstrated that female prenatally stress challenged OVA-treated mice exhibit more pronounced allergic airway inflammation and airway remodeling as well as reduced local Treg accumulation, as compared to similar males, which seem to be intrinsically more responsive to MCh and to recruit Tregs as a defensive mechanism against asthma development (155). The age - and sex - dependent predominance of asthma may be attributed to biological sex differences, including pulmonary and immunological aspects, which are largely determined by sex hormones, as evident by the switch in prevalence seen in puberty, a period of intense hormone production (197).

As previously mentioned, lung growth, maturation and function are affected by sex hormones and may account for differences in asthma susceptibility and severity between males and females. During gestation, lung maturation seems to progress faster in female fetuses compared to male ones. This difference can be attributed to the inhibitory effects of androgens, which delay the onset of surfactant production in male fetal lungs, while, at the same time, estrogens stimulate tissue differentiation and surfactant secretion in females (168, 169). As gestation progresses, male fetuses quickly catch up and, when born full-term, no difference in lung

maturity and surfactant levels can be found between sexes. However, adult female mice lacking the estrogen receptor β (ERβ) exhibit reduced number of alveoli as well as surfactant accumulation (198). Interestingly, SFTPA, one of the main components of surfactant, was found to suppress allergic responses in a murine model for asthma induction (199). Although further research is required, these observations imply that estrogens via ERβ-mediated signaling inhibit SFTPA production and therefore, can increase susceptibility to allergic asthma in adult females.

A second factor associated with sex-specific lung maturation and likely asthma severity is epidermal growth factor (EGF). During fetal lung development, EGF facilitates the crosstalk between lung fibroblasts and AEC type II thereby promoting maturation of the latter as well as surfactant production (200). Interestingly, EGF activity can be modulated by androgens, which induced a downregulation of EGF receptor (EGFR) in the lung thereby further disrupting fetal lung maturation in a mouse model (201). Importantly, increased EGFR expression and activation is a typical feature of the asthmatic airways and has been associated with airway epithelial barrier dysfunction and subsequent inflammation and remodeling (202, 203). Therefore, one can assume that lack of an androgen-mediated EGFR downregulation may contribute to the enhanced asthma severity in women.

Sex-specific differences in lung growth across the lifespan may also provide a plausible explanation for the reported sex bias in asthma development. At birth, males have bigger lungs with more respiratory bronchioles compared to females. However, during childhood, female airways and lung parenchyma grow proportionately and therefore, girls have overall lower airway resistance and better lung function. On the other hand, a disproportionate growth of airways and lung parenchyma in boys results in long, narrow airways, which may predispose to asthma development. After puberty, this trend reverses and therefore, women have narrower airways in proportion to lung parenchyma and are at higher risk for asthma (204).

The association between these physiological sex differences in lung development and function and the sex-specific predominance of asthma further supports our hypothesis that the lung is a key determinant of asthma development. Prenatal stress challenge disturbs the fine hormonal balance required for an uneventful lung development and therefore, exacerbates or rather reverses existing sex differences in the developing lung. The female fetal lung, likely due to differential exposure to high glucocorticoids, may respond poorly to the late gestational stimulatory effects of glucocorticoids and therefore, may fail to mature sufficiently in order to adjust to postnatal changes. An immature airway epithelial barrier is likely dysfunctional and thus, highly susceptible to inhaled irritants. An aberrant airway epithelial function, potentially

aggravated by sex hormone interactions, perpetuates a vicious cycle of chronic injury, inflammation and incomplete repair thereby leading to asthma manifestation. Further studies are required in order to uncover the molecular mechanisms connecting prenatal challenges, lung development and postnatal respiratory health and disease. An early detection of potential aberrations in lung development, which could subsequently lead to postnatal lung dysfunction and disease, would allow the design of efficient prediction, disease prevention and treatment strategies.

5 Summary

The intrauterine environment can shape postnatal health and disease. Prenatal exposure to adverse conditions, such as maternal medication, nutritional insults, smoking and increased stress perception, has been associated with an increased risk for diseases later in life. Specifically, several epidemiological studies underline a connection between prenatal maternal stress and childhood asthma. However, the exact mechanisms underlying this link, remain unknown.

Here, we hypothesized that prenatal stress increases the risk of the offspring to develop asthma in early life by affecting fetal lung development. To test this hypothesis, we first aimed to identify the effect of prenatal stress challenge on postnatal susceptibility to asthma in mice. To this end, pregnant dams were exposed to sound stress for 24h on gestational days 10.5, 12.5 and 14.5 and 6 weeks after birth, experimental asthma was induced in the offspring following sensitization and challenge with ovalbumin. Interestingly, prenatal stress increased susceptibility to asthma and disease severity in a sex-specific manner. Specifically, female prenatally stress challenged mice exhibited enhanced airway hyperresponsiveness, airway inflammation, mucus production and airway remodeling, as compared to the respective controls. In agreement with current theories placing the airway epithelium in the center of asthma pathogenesis, a significantly disrupted airway epithelial barrier integrity was observed in the lungs of female prenatally stress challenged mice.

Since asthma is characterized by both lung and immune dysfunction, prenatal stress may predispose to asthma by affecting either the developing lung, immune system, or both. To conclusively determine the target of prenatal stress, bone marrow chimeras harboring prenatally stress challenged lungs, immune system or both were generated and, following experimental asthma induction, the severity of the asthmatic phenotype was assessed. Interestingly, mice harboring a prenatally stress challenged immune system and control lungs exhibited a similarly mild asthmatic phenotype with mice carrying control lungs and immune system. However, asthma severity was significantly exacerbated when prenatally stress challenged immune system and lungs coexisted. Importantly, a prenatally stress challenged lung alone could also be sufficiently associated with enhanced airway inflammation and fibrosis regardless of the immune system. Hence, although the stress-related higher asthma severity may be attributed to a synergistic effect of prenatal stress on both organs, it is primarily the lung, and not the immune system, that crucially determines the manifestation of the disease following prenatal stress exposure. Based on these findings, we hypothesized that prenatal stress interferes with fetal lung development thereby predisposing to asthma in early life. Indeed, histological assessment revealed a sex-specific impact of prenatal stress on the developing lung. Specifically, stress challenged female offspring exhibited significantly smaller airspaces and thicker alveolar walls before birth, followed by impaired alveolarization in early life. Sex-specific alterations in the expression pattern of markers involved in lung development and differentiation, such as Igf1 and Igf1r, were also observed.

In conclusion, prenatal stress challenge affects the developing lung sex-specifically, with especially the female offspring showing signs of developmental arrest which may be explained, at least in part, by stress-induced sex-specific alterations in lung gene expression, such as IGF1/IGF1R signaling defects. An immature lung fails, in turn, to adjust to postnatal changes and is, therefore, susceptible to environmental insults. Among others, a dysfunctional airway epithelial barrier may be vulnerable to inhaled irritants and, hence, may emerge as a trigger for a series of events which collectively lead to asthma manifestation.

6 Zusammenfassung

Einflüsse während der Pränatalzeit spielen eine entscheidende Rolle für Gesundheit und Krankheit im Verlauf des späteren Lebens. Epidemiologische Studien assoziieren eine mütterliche Stressbelastung während der Schwangerschaft mit dem Auftreten von Asthma bei Kindern. Der genaue Mechanismus, der diesem Zusammenhang zugrunde liegt, ist jedoch noch nicht bekannt.
In der vorliegenden Arbeit wird untersucht, ob eine pränatale Stressbelastung bei Mäusen die postnatale Anfälligkeit für Asthma durch eine Beeinträchtigung der fötalen Lungenentwicklung erhöhen kann. Um diese Hypothese zu testen, wollten wir zuerst die Konsequenz einer pränatalen Stressbelastung auf die postnatale Anfälligkeit für Asthma bei Mäusen untersuchen. Zu diesem Zweck wurden tragende Weibchen 24 Stunden an den Gestationstagen 10.5, 12.5 und 14.5 einer Stressbelastung durch Lärm ausgesetzt. 6 Wochen nach der Geburt wurde experimentelles Asthma mittels Ovalbumin in den Nachkommen induziert. Interessanterweise erhöhte die pränatale Stressbelastung geschlechtsspezifisch die Anfälligkeit für Asthma und den Schweregrad der Erkrankung. Weibliche Nachkommen gestresster Mütter zeigten eine ausgeprägte bronchiale Hyperreaktivität, Entzündung der Atemwege, vermehrte Mukusproduktion und Umbau der Atemwege. In Übereinstimmung mit aktuellen Theorien, die das Atemwegsepithel in den Mittelpunkt der Asthma-Pathogenese stellen, wurde in den Lungen von pränatal gestressten weiblichen Mäusen eine signifikant verminderte Integrität der Atemwegsepithelbarriere beobachtet.
Asthma wird ausgelöst durch eine Dysfunktion der Lunge sowie des Immunsystems. Daher untersuchten wir, ob eine pränatale Stressbelastung durch eine Beeinträchtigung der fötalen Entwicklung der Lunge oder des Immunsystems zu Asthma führt. Hierfür wurden Knochenmarks-Chimäre erzeugt, die ein pränatal gestresstes Immunsystem, eine pränatal gestresste Lunge oder beides aufwiesen, und nach experimenteller Asthma-Induktion wurde der Schweregrad des asthmatischen Phänotyps bewertet. Interessanterweise zeigten Mäuse, die lediglich ein pränatal gestresstes Immunsystem aufwiesen, einen ähnlich milden asthmatischen Phänotyp wie Kontrollmäuse, die kein gestresstes Organ erhielten. Der Schweregrad von Asthma war jedoch am höchsten in Mäusen mit pränatal gestresster Lunge und gestresstem Immunsystem. Eine pränatal stressbelastete Lunge allein könnte auch unabhängig vom Immunsystem mit einer verstärkten Atemwegsentzündung und Fibrose in Verbindung gebracht werden. Obwohl der stressbedingte höhere Asthma-Schweregrad auf einen synergistischen Effekt von pränatalem Stress in beiden Organen zurückzuführen ist, ist vor allem die Lunge und nicht das Immunsystem, das Organ, welches die Manifestation der Krankheit nach einer pränatalen Stressbelastung entscheidend bestimmt. Aufgrund dieser Ergebnisse stellten wir die Hypothese auf, dass pränataler Stress die fötale Lungenentwicklung beeinträchtigt und somit zu Asthma im frühen Leben führt. Die histologische Auswertung der Lunge zeigte, dass eine pränatale Stressbelastung die Lungenentwicklung geschlechtsspezifisch beeinflusst. Kurz vor der Geburt wiesen weibliche Nachkommen gestresster Mütter signifikant kleinere Lufträume und dickere Alveolarwände auf. Außerdem zeigten sie eine stärkere Beeinträchtigung der Alveolarentwicklung im frühen Leben. Es wurden weiterhin geschlechtsspezifische Veränderungen im Expressionsmuster von Faktoren beobachtet, wie z.B. Igf1 und Igf1r, welche in der Lungenentwicklung und Differenzierung involviert sind.
In dieser Arbeit konnten wir zeigen, dass eine pränatale Stressbelastung die Lungenentwicklung geschlechtsspezifisch beeinflusst. Eine unreife Lunge kann sich nicht an postnatale Veränderungen anpassen und ist daher anfällig für Umweltbelastungen. Eine Dysfunktion der Atemwegsepithelbarriere kann eine Reihe von Konsequenzen haben, die gemeinsam zur Manifestation von Asthma führen.

7 Abbreviations

11β-HSD1	11β-hydroxysteroid dehydrogenase type 1
11β-HSD2	11β-hydroxysteroid dehydrogenase type 2
µg	Microgram
µm	Micrometer
µl	Microliter
a	alveoli
ACTH	Adrenocorticotropic hormone
ADAM33	ADAM Metallopeptidase Domain 33
AEC	Alveolar epithelial cells
AHR	Airway hyperresponsiveness
alvMac	Alveolar macrophage
Alum	Aluminium hydroxide
APC	Allophycocyanin
AQP5	Aquaporin 5
ASF	Volume fraction of alveolar walls
ATP5B	ATP synthase F1 subunit beta
b	bronchi
BAL	Bronchoalveolar lavage
bp	Base pairs
BM	Bone marrow
BMT	Bone marrow transplantation
BSA	Bovine serum albumin
BV	Brilliant Violet
BW	Body weight
CD	Cluster of differentiation
CRH	Corticotropin-releasing hormone
dB	Desibel
DMSO	Dimethyl sulfoxide
DNA	Deoxyribonucleic acid
dNTP	Deoxynucleotide phosphate
E	Gestational day

EDTA	Ethylene diamine tetraacetic acid
EGF	Epidermal growth factor
Eos	Eosinophils
ERβ	Estrogen receptor β
FACS	Fluorescence activated cell sorting
FCS	Fetal calf serum
Fc	Fragment, crystallizable
FITC	Fluorescein isothiocyanate
FMO	Fluorescence minus one
FoxP3	Forkhead box protein 3
FSC	Forward scatter
g	grams
gd	Gestational day
Gapdh	Glycerinaldehyd-3-phosphat-dehydrogenase
Gilz	Glucocorticoid-induced leucine zipper
GR	Glucocorticoid receptor
Gy	Gray
h	hour
H&E	Hematoxylin and Eosin
HPA	Hypothalamic-pituitary-adrenocortical axis
HSC	Hematopoietic stem cells
Hz	Herz
I_o	Number of intersections of alveolar walls with test line
i.p.	Intraperitoneal
i.v.	Intravenous
Ig	Immunoglobulin
IGF-1	Insulin-like growth factor-1
IGF-1R	Insulin-like growth factor-1 receptor
IL	Interleukin
intMac	Interstitial macrophages
L_r	Length of test line
Lym	Lymphocytes
kg	kilograms

Mac	Macrophages
MGG	May-Grünwald Giemsa
MCh	Metacholine
MHC	Major histocompatibility complex
mg	Milligram
min	minutes
ml	Milliliter
MLI	Mean linear intercept
mRNA	Messenger RNA
NaCl	Sodium chloride
Neu	Neutrophils
NR3C1	Nuclear Receptor Subfamily 3 Group C Member 1
NRS	Normal rat serum
OVA	Ovalbumin
P_i	Number of points on structure of interest
P_t	Total number of points on reference field
PacO	Pacific orange
PAS	Periodic acid-Schiff
PBS	Phosphate-buffered saline
(q)PCR	(quantitative) Polymerase chain reaction
pd	Postnatal day
PE	Phycoerythrin
PerCP	Peridinin-Chlorophyll Protein
PFA	Paraformaldehyde
pn	Postnatal day
RBC	Red blood cell
RI	Airway resistance
(m)RNA	(messenger) Ribonucleic acid
Rpm	Rounds per minute
RPMI	Roswell Park Memorial Institute medium
RT	Room temperature
sec	seconds
SEM	Standard error of the mean

SFTP(A,B,C,D)	Surfactant protein (A,B,C,D)
SOX9	SRY-related high-mobility group (HMG) box 9
SP-(A,B)	Surfactant protein (A,B)
SSC	Side scatter
TD	Alveolar wall thickness
TGF	Transforming growth factor
Th1	T helper cells 1
Th2	T helper cells 2
TNF	Tumor necrosis factor
Tregs	Regulatory T cells
UV	Ultaviolet
XEM	Xylol replacement medium
ZO-1	Zonula occludens-1

8 List of figures and tables

8.1. List of figures

8.2. List of tables

9 References

1. Barker DJ. 1995. The fetal and infant origins of disease. *Eur J Clin Invest* 25: 457-63
2. Hanson MA, Gluckman PD. 2014. Early developmental conditioning of later health and disease: physiology or pathophysiology? *Physiological reviews* 94: 1027-76
3. Arck PC, Hecher K. 2013. Fetomaternal immune cross-talk and its consequences for maternal and offspring's health. *Nature Medicine* 19: 548
4. Gluckman PD, Hanson MA, Cooper C, Thornburg KL. 2008. Effect of in utero and early-life conditions on adult health and disease. *N Engl J Med* 359: 61-73
5. Solano ME, Jago C, Pincus MK, Arck PC. 2011. Highway to health; or How prenatal factors determine disease risks in the later life of the offspring. *J Reprod Immunol* 90: 3-8
6. Fisher RE, Steele M, Karrow NA. 2012. Fetal programming of the neuroendocrine-immune system and metabolic disease. *J Pregnancy* 2012: 792934
7. Brunst KJ, Leung YK, Ryan PH, Khurana Hershey GK, Levin L, Ji H, Lemasters GK, Ho SM. 2013. Forkhead box protein 3 (FOXP3) hypermethylation is associated with diesel exhaust exposure and risk for childhood asthma. *J Allergy Clin Immunol* 131: 592-4 e1-3
8. Burbank AJ, Sood AK, Kesic MJ, Peden DB, Hernandez ML. 2017. Environmental determinants of allergy and asthma in early life. *J Allergy Clin Immunol* 140: 1-12
9. Eder W, Ege MJ, von Mutius E. 2006. The asthma epidemic. *N Engl J Med* 355: 2226-35
10. Hartwig IR, Sly PD, Schmidt LA, van Lieshout RJ, Bienenstock J, Holt PG, Arck PC. 2014. Prenatal adverse life events increase the risk for atopic diseases in children, which is enhanced in the absence of a maternal atopic predisposition. *J Allergy Clin Immunol* 134: 160-9
11. Henriksen RE, Thuen F. 2015. Marital Quality and Stress in Pregnancy Predict the Risk of Infectious Disease in the Offspring: The Norwegian Mother and Child Cohort Study. *PLoS One* 10: e0137304
12. Nielsen NM, Hansen AV, Simonsen J, Hviid A. 2011. Prenatal stress and risk of infectious diseases in offspring. *Am J Epidemiol* 173: 990-7
13. Bach J-F. 2002. The Effect of Infections on Susceptibility to Autoimmune and Allergic Diseases. *New England Journal of Medicine* 347: 911-20
14. Lundback B, Backman H, Lotvall J, Ronmark E. 2016. Is asthma prevalence still increasing? *Expert Rev Respir Med* 10: 39-51
15. PrabhuDas M, Bonney E, Caron K, Dey S, Erlebacher A, Fazleabas A, Fisher S, Golos T, Matzuk M, McCune JM, Mor G, Schulz L, Soares M, Spencer T, Strominger J, Way SS, Yoshinaga K. 2015. Immune mechanisms at the maternal-fetal interface: perspectives and challenges. *Nat Immunol* 16: 328-34
16. Thorburn AN, McKenzie CI, Shen S, Stanley D, Macia L, Mason LJ, Roberts LK, Wong CH, Shim R, Robert R, Chevalier N, Tan JK, Marino E, Moore RJ, Wong L, McConville MJ, Tull DL, Wood LG, Murphy VE, Mattes J, Gibson PG, Mackay CR. 2015. Evidence that asthma is a developmental origin disease influenced by maternal diet and bacterial metabolites. *Nat Commun* 6: 7320
17. Macpherson AJ, de Aguero MG, Ganal-Vonarburg SC. 2017. How nutrition and the maternal microbiota shape the neonatal immune system. *Nat Rev Immunol* 17: 508-17
18. Engels G, Hierweger AM, Hoffmann J, Thieme R, Thiele S, Bertram S, Dreier C, Resa-Infante P, Jacobsen H, Thiele K, Alawi M, Indenbirken D, Grundhoff A, Siebels S, Fischer N, Stojanovska V, Muzzio D, Jensen F, Karimi K, Mittrucker HW, Arck PC, Gabriel G. 2017. Pregnancy-Related Immune Adaptation Promotes the Emergence of

Highly Virulent H1N1 Influenza Virus Strains in Allogenically Pregnant Mice. *Cell Host Microbe* 21: 321-33

19. Altfeld M, Bunders MJ. 2016. Impact of HIV-1 infection on the feto-maternal crosstalk and consequences for pregnancy outcome and infant health. *Seminars in Immunopathology* 38: 727-38
20. Laake I, Tunheim G, Robertson AH, Hungnes O, Waalen K, Haberg SE, Mjaaland S, Trogstad L. 2018. Risk of pregnancy complications and adverse birth outcomes after maternal A(H1N1)pdm09 influenza: a Norwegian population-based cohort study. *BMC Infect Dis* 18: 525
21. Karimi K, Kessler T, Thiele K, Ramisch K, Erhardt A, Huebener P, Barikbin R, Arck P, Tiegs G. 2015. Prenatal acetaminophen induces liver toxicity in dams, reduces fetal liver stem cells, and increases airway inflammation in adult offspring. *J Hepatol* 62: 1085-91
22. Thiele K, Solano ME, Huber S, Flavell RA, Kessler T, Barikbin R, Jung R, Karimi K, Tiegs G, Arck PC. 2015. Prenatal acetaminophen affects maternal immune and endocrine adaptation to pregnancy, induces placental damage, and impairs fetal development in mice. *Am J Pathol* 185: 2805-18
23. Arck PC, Rücke M, Rose M, Szekeres-Bartho J, Douglas AJ, Pritsch M, Blois SM, Pincus MK, Bärenstrauch N, Dudenhausen JW, Nakamura K, Sheps S, Klapp BF. 2008. Early risk factors for miscarriage: a prospective cohort study in pregnant women. *Reproductive BioMedicine Online* 17: 101-13
24. Nepomnaschy PA, Welch KB, McConnell DS, Low BS, Strassmann BI, England BG. 2006. Cortisol levels and very early pregnancy loss in humans. *Proceedings of the National Academy of Sciences of the United States of America* 103: 3938
25. Entringer S, Buss C, Wadhwa PD. 2010. Prenatal stress and developmental programming of human health and disease risk: concepts and integration of empirical findings. *Current opinion in endocrinology, diabetes, and obesity* 17: 507-16
26. Solano ME, Kowal MK, O'Rourke GE, Horst AK, Modest K, Plosch T, Barikbin R, Remus CC, Berger RG, Jago C, Ho H, Sass G, Parker VJ, Lydon JP, DeMayo FJ, Hecher K, Karimi K, Arck PC. 2015. Progesterone and HMOX-1 promote fetal growth by CD8+ T cell modulation. *J Clin Invest* 125: 1726-38
27. Markham JA, Koenig JI. 2011. Prenatal stress: role in psychotic and depressive diseases. *Psychopharmacology (Berl)* 214: 89-106
28. Gilman SE, Cherkerzian S, Buka SL, Hahn J, Hornig M, Goldstein JM. 2016. Prenatal immune programming of the sex-dependent risk for major depression. *Translational psychiatry* 6: e822-e
29. Kim DR, Bale TL, Epperson CN. 2015. Prenatal programming of mental illness: current understanding of relationship and mechanisms. *Current psychiatry reports* 17: 5-
30. Kundakovic M, Jaric I. 2017. The Epigenetic Link between Prenatal Adverse Environments and Neurodevelopmental Disorders. *Genes* 8: 104
31. Walder DJ, Laplante DP, Sousa-Pires A, Veru F, Brunet A, King S. 2014. Prenatal maternal stress predicts autism traits in 6(1/2) year-old children: Project Ice Storm. *Psychiatry Res* 219: 353-60
32. Plana-Ripoll O, Liu X, Momen NC, Parner E, Olsen J, Li J. 2016. Prenatal exposure to maternal stress following bereavement and cardiovascular disease: A nationwide population-based and sibling-matched cohort study. *Eur J Prev Cardiol* 23: 1018-28
33. Ho H, Lhotak S, Solano ME, Karimi K, Pincus MK, Austin RC, Arck P. 2013. Prenatal stress enhances severity of atherosclerosis in the adult apolipoprotein E-deficient mouse offspring via inflammatory pathways. *J Dev Orig Health Dis* 4: 90-7

34. Entringer S, Wadhwa PD. 2013. Developmental programming of obesity and metabolic dysfunction: role of prenatal stress and stress biology. *Nestle Nutr Inst Workshop Ser* 74: 107-20
35. Virk J, Li J, Vestergaard M, Obel C, Lu M, Olsen J. 2010. Early life disease programming during the preconception and prenatal period: making the link between stressful life events and type-1 diabetes. *PLoS One* 5: e11523
36. Bale TL, Epperson CN. 2015. Sex differences and stress across the lifespan. *Nat Neurosci* 18: 1413-20
37. Brunton PJ, Sullivan KM, Kerrigan D, Russell JA, Seckl JR, Drake AJ. 2013. Sex-specific effects of prenatal stress on glucose homoeostasis and peripheral metabolism in rats. *J Endocrinol* 217: 161-73
38. Cheong JN, Cuffe JS, Jefferies AJ, Anevska K, Moritz KM, Wlodek ME. 2016. Sex-Specific Metabolic Outcomes in Offspring of Female Rats Born Small or Exposed to Stress During Pregnancy. *Endocrinology* 157: 4104-20
39. Chang HY, Suh DI, Yang SI, Kang MJ, Lee SY, Lee E, Choi IA, Lee KS, Shin YJ, Shin YH, Kim YH, Kim KW, Ahn K, Won HS, Choi SJ, Oh SY, Kwon JY, Kim YH, Park HJ, Lee KJ, Jun JK, Yu HS, Lee SH, Jung BK, Kwon JW, Choi YK, Do N, Bae YJ, Kim H, Chang WS, Kim EJ, Lee JK, Hong SJ. 2016. Prenatal maternal distress affects atopic dermatitis in offspring mediated by oxidative stress. *J Allergy Clin Immunol* 138: 468-75 e5
40. Andersson NW, Hansen MV, Larsen AD, Hougaard KS, Kolstad HA, Schlünssen V. 2016. Prenatal maternal stress and atopic diseases in the child: a systematic review of observational human studies. *Allergy* 71: 15-26
41. Pincus-Knackstedt MK, Joachim RA, Blois SM, Douglas AJ, Orsal AS, Klapp BF, Wahn U, Hamelmann E, Arck PC. 2006. Prenatal Stress Enhances Susceptibility of Murine Adult Offspring toward Airway Inflammation. *The Journal of Immunology* 177: 8484
42. Lee A, Mathilda Chiu YH, Rosa MJ, Jara C, Wright RO, Coull BA, Wright RJ. 2016. Prenatal and postnatal stress and asthma in children: Temporal- and sex-specific associations. *J Allergy Clin Immunol* 138: 740-7 e3
43. Rosa MJ, Just AC, Tamayo YOM, Schnaas L, Svensson K, Wright RO, Tellez Rojo MM, Wright RJ. 2016. Prenatal and postnatal stress and wheeze in Mexican children: Sex-specific differences. *Ann Allergy Asthma Immunol* 116: 306-12 e1
44. Turcotte-Tremblay AM, Lim R, Laplante DP, Kobzik L, Brunet A, King S. 2014. Prenatal maternal stress predicts childhood asthma in girls: project ice storm. *Biomed Res Int* 2014: 201717
45. Hartwig IR, Bruenahl CA, Ramisch K, Keil T, Inman M, Arck PC, Pincus M. 2014. Reduced levels of maternal progesterone during pregnancy increase the risk for allergic airway diseases in females only. *J Mol Med (Berl)* 92: 1093-104
46. Zazara DE, Arck PC. 2018. Developmental origin and sex-specific risk for infections and immune diseases later in life. *Semin Immunopathol*
47. Blois SM, Joachim R, Kandil J, Margni R, Tometten M, Klapp BF, Arck PC. 2004. Depletion of CD8+ cells abolishes the pregnancy protective effect of progesterone substitution with dydrogesterone in mice by altering the Th1/Th2 cytokine profile. *J Immunol* 172: 5893-9
48. Blois S, Tometten M, Kandil J, Hagen E, Klapp BF, Margni RA, Arck PC. 2005. Intercellular adhesion molecule-1/LFA-1 cross talk is a proximate mediator capable of disrupting immune integration and tolerance mechanism at the feto-maternal interface in murine pregnancies. *Journal of Immunology* 174: 1820-9

49. Entringer S, Buss C, Swanson JM, Cooper DM, Wing DA, Waffarn F, Wadhwa PD. 2012. Fetal programming of body composition, obesity, and metabolic function: the role of intrauterine stress and stress biology. *J Nutr Metab* 2012: 632548
50. Manti S, Marseglia L, D'Angelo G, Cuppari C, Cusumano E, Arrigo T, Gitto E, Salpietro C. 2016. "Cumulative Stress": The Effects of Maternal and Neonatal Oxidative Stress and Oxidative Stress-Inducible Genes on Programming of Atopy. *Oxid Med Cell Longev* 2016: 8651820
51. Seckl JR, Holmes MC. 2007. Mechanisms of Disease: glucocorticoids, their placental metabolism and fetal 'programming' of adult pathophysiology. *Nature Clinical Practice Endocrinology &Amp; Metabolism* 3: 479
52. Cottrell EC, Seckl JR. 2009. Prenatal stress, glucocorticoids and the programming of adult disease. *Frontiers in behavioral neuroscience* 3: 19-
53. Solano ME, Holmes MC, Mittelstadt PR, Chapman KE, Tolosa E. 2016. Antenatal endogenous and exogenous glucocorticoids and their impact on immune ontogeny and long-term immunity. *Seminars in Immunopathology* 38: 739-63
54. Fowden AL, Giussani DA, Forhead AJ. 2005. Endocrine and metabolic programming during intrauterine development. *Early Hum Dev* 81: 723-34
55. Chen M, Zhang L. 2011. Epigenetic mechanisms in developmental programming of adult disease. *Drug Discov Today* 16: 1007-18
56. Moisiadis VG, Matthews SG. 2014. Glucocorticoids and fetal programming part 2: Mechanisms. *Nat Rev Endocrinol* 10: 403-11
57. Moisiadis VG, Matthews SG. 2014. Glucocorticoids and fetal programming part 1: Outcomes. *Nat Rev Endocrinol* 10: 391-402
58. O'Donnell KJ, Glover V. 2016. Chapter 7 - Maternal Prenatal Stress and the Developmental Origins of Mental Health: The Role of Epigenetics. In *The Epigenome and Developmental Origins of Health and Disease*, ed. CS Rosenfeld, pp. 103-26. Boston: Academic Press
59. Custovic A. 2015. To what extent is allergen exposure a risk factor for the development of allergic disease? *Clinical & Experimental Allergy* 45: 54-62
60. Loftus PA, Wise SK. 2016. Epidemiology of asthma. *Curr Opin Otolaryngol Head Neck Surg* 24: 245-9
61. Asher MI, Montefort S, Bjorksten B, Lai CK, Strachan DP, Weiland SK, Williams H, Group IPTS. 2006. Worldwide time trends in the prevalence of symptoms of asthma, allergic rhinoconjunctivitis, and eczema in childhood: ISAAC Phases One and Three repeat multicountry cross-sectional surveys. *Lancet* 368: 733-43
62. Butland BK, Strachan DP. 2007. Asthma onset and relapse in adult life: the British 1958 birth cohort study. *Ann Allergy Asthma Immunol* 98: 337-43
63. Amelink M, de Groot JC, de Nijs SB, Lutter R, Zwinderman AH, Sterk PJ, ten Brinke A, Bel EH. 2013. Severe adult-onset asthma: A distinct phenotype. *Journal of Allergy and Clinical Immunology* 132: 336-41
64. Holgate ST, Wenzel S, Postma DS, Weiss ST, Renz H, Sly PD. 2015. Asthma. *Nat Rev Dis Primers* 1: 15025
65. Peters SP, Jones CA, Haselkorn T, Mink DR, Valacer DJ, Weiss ST. 2007. Real-world Evaluation of Asthma Control and Treatment (REACT): Findings from a national Web-based survey. *Journal of Allergy and Clinical Immunology* 119: 1454-61
66. Haitchi HM, Bassett DJ, Bucchieri F, Gao X, Powell RM, Hanley NA, Wilson DI, Holgate ST, Davies DE. 2009. Induction of a disintegrin and metalloprotease 33 during embryonic lung development and the influence of IL-13 or maternal allergy. *J Allergy Clin Immunol* 124: 590-7, 7 e1-11

67. Haitchi HM, Powell RM, Shaw TJ, Howarth PH, Wilson SJ, Wilson DI, Holgate ST, Davies DE. 2005. ADAM33 expression in asthmatic airways and human embryonic lungs. *Am J Respir Crit Care Med* 171: 958-65
68. Van Eerdewegh P, Little RD, Dupuis J, Del Mastro RG, Falls K, Simon J, Torrey D, Pandit S, McKenny J, Braunschweiger K, Walsh A, Liu Z, Hayward B, Folz C, Manning SP, Bawa A, Saracino L, Thackston M, Benchekroun Y, Capparell N, Wang M, Adair R, Feng Y, Dubois J, FitzGerald MG, Huang H, Gibson R, Allen KM, Pedan A, Danzig MR, Umland SP, Egan RW, Cuss FM, Rorke S, Clough JB, Holloway JW, Holgate ST, Keith TP. 2002. Association of the ADAM33 gene with asthma and bronchial hyperresponsiveness. *Nature* 418: 426-30
69. Holgate ST. 2007. Epithelium dysfunction in asthma. *J Allergy Clin Immunol* 120: 1233-44; quiz 45-6
70. Reuter S, Stassen M, Taube C. 2010. Mast cells in allergic asthma and beyond. *Yonsei Med J* 51: 797-807
71. Fehrenbach H, Wagner C, Wegmann M. 2017. Airway remodeling in asthma: what really matters. *Cell Tissue Res* 367: 551-69
72. Holgate ST. 2008. Pathogenesis of asthma. *Clin Exp Allergy* 38: 872-97
73. Kay AB. 2005. The role of eosinophils in the pathogenesis of asthma. *Trends Mol Med* 11: 148-52
74. Hammad H, Lambrecht BN. 2006. Recent progress in the biology of airway dendritic cells and implications for understanding the regulation of asthmatic inflammation. *Journal of Allergy and Clinical Immunology* 118: 331-6
75. Smit JJ, Lukacs NW. 2006. A closer look at chemokines and their role in asthmatic responses. *European Journal of Pharmacology* 533: 277-88
76. Jayaram L, Pizzichini MM, Cook RJ, Boulet LP, Lemière C, Pizzichini E, Cartier A, Hussack P, Goldsmith CH, Laviolette M, Parameswaran K, Hargreave FE. 2006. Determining asthma treatment by monitoring sputum cell counts: effect on exacerbations. *European Respiratory Journal* 27: 483
77. Grünig G, Warnock M, Wakil AE, Venkayya R, Brombacher F, Rennick DM, Sheppard D, Mohrs M, Donaldson DD, Locksley RM, Corry DB. 1998. Requirement for IL-13 independently of IL-4 in experimental asthma. *Science (New York, N.Y.)* 282: 2261-3
78. Hallstrand TS, Henderson WR, Jr. 2010. An update on the role of leukotrienes in asthma. *Current opinion in allergy and clinical immunology* 10: 60-6
79. Tan SYS, Krasnow MA. 2016. Developmental origin of lung macrophage diversity. *Development* 143: 1318
80. Balhara J, Gounni AS. 2012. The alveolar macrophages in asthma: a double-edged sword. *Mucosal Immunology* 5: 605
81. Lloyd CM, Hawrylowicz CM. 2009. Regulatory T cells in asthma. *Immunity* 31: 438-49
82. Hawrylowicz CM, O'Garra A. 2005. Potential role of interleukin-10-secreting regulatory T cells in allergy and asthma. *Nature Reviews Immunology* 5: 271
83. O'Garra A, Vieira P. 2004. Regulatory T cells and mechanisms of immune system control. *Nature Medicine* 10: 801
84. Gambineri E, Torgerson TR, Ochs HD. 2003. Immune dysregulation, polyendocrinopathy, enteropathy, and X-linked inheritance (IPEX), a syndrome of systemic autoimmunity caused by mutations of FOXP3, a critical regulator of T-cell homeostasis. *Curr Opin Rheumatol* 15: 430-5
85. Grindebacke H, Wing K, Andersson AC, Suri-Payer E, Rak S, Rudin A. 2004. Defective suppression of Th2 cytokines by CD4+CD25+ regulatory T cells in birch allergics during birch pollen season. *Clinical & Experimental Allergy* 34: 1364-72

86. Karlsson MR, Rugtveit J, Brandtzaeg P. 2004. Allergen-responsive CD4+CD25+ regulatory T cells in children who have outgrown cow's milk allergy. *The Journal of experimental medicine* 199: 1679-88
87. Ling EM, Smith T, Nguyen XD, Pridgeon C, Dallman M, Arbery J, Carr VA, Robinson DS. 2004. Relation of CD4+CD25+ regulatory T-cell suppression of allergen-driven T-cell activation to atopic status and expression of allergic disease. *The Lancet* 363: 608-15
88. Hartl D, Koller B, Mehlhorn AT, Reinhardt D, Nicolai T, Schendel DJ, Griese M, Krauss-Etschmann S. 2007. Quantitative and functional impairment of pulmonary CD4+CD25hi regulatory T cells in pediatric asthma. *Journal of Allergy and Clinical Immunology* 119: 1258-66
89. Godfrey RW. 1997. Human airway epithelial tight junctions. *Microsc Res Tech* 38: 488-99
90. Gon Y, Hashimoto S. 2018. Role of airway epithelial barrier dysfunction in pathogenesis of asthma. *Allergology International* 67: 12-7
91. Xiao C, Puddicombe SM, Field S, Haywood J, Broughton-Head V, Puxeddu I, Haitchi HM, Vernon-Wilson E, Sammut D, Bedke N, Cremin C, Sones J, Djukanović R, Howarth PH, Collins JE, Holgate ST, Monk P, Davies DE. 2011. Defective epithelial barrier function in asthma. *Journal of Allergy and Clinical Immunology* 128: 549-56.e12
92. Kirkham P, Rahman I. 2006. Oxidative stress in asthma and COPD: antioxidants as a therapeutic strategy. *Pharmacol Ther* 111: 476-94
93. Barbato A, Turato G, Baraldo S, Bazzan E, Calabrese F, Panizzolo C, Zanin ME, Zuin R, Maestrelli P, Fabbri LM, Saetta M. 2006. Epithelial damage and angiogenesis in the airways of children with asthma. *Am J Respir Crit Care Med* 174: 975-81
94. Fedorov IA, Wilson SJ, Davies DE, Holgate ST. 2005. Epithelial stress and structural remodelling in childhood asthma. *Thorax* 60: 389-94
95. Saglani S, Malmstrom K, Pelkonen AS, Malmberg LP, Lindahl H, Kajosaari M, Turpeinen M, Rogers AV, Payne DN, Bush A, Haahtela T, Makela MJ, Jeffery PK. 2005. Airway remodeling and inflammation in symptomatic infants with reversible airflow obstruction. *Am J Respir Crit Care Med* 171: 722-7
96. Turner S. 2012. Perinatal programming of childhood asthma: early fetal size, growth trajectory during infancy, and childhood asthma outcomes. *Clin Dev Immunol* 2012: 962923
97. Canoy D, Pekkanen J, Elliott P, Pouta A, Laitinen J, Hartikainen A-L, Zitting P, Patel S, Little MP, Järvelin M-R. 2007. Early growth and adult respiratory function in men and women followed from the fetal period to adulthood. *Thorax* 62: 396-402
98. Aysola RS, Hoffman EA, Gierada D, Wenzel S, Cook-Granroth J, Tarsi J, Zheng J, Schechtman KB, Ramkumar TP, Cochran R, Xueping E, Christie C, Newell J, Fain S, Altes TA, Castro M. 2008. Airway remodeling measured by multidetector CT is increased in severe asthma and correlates with pathology. *Chest* 134: 1183-91
99. Haland G, Carlsen KC, Sandvik L, Devulapalli CS, Munthe-Kaas MC, Pettersen M, Carlsen KH, Oraacle. 2006. Reduced lung function at birth and the risk of asthma at 10 years of age. *N Engl J Med* 355: 1682-9
100. Hancox RJ, Poulton R, Greene JM, McLachlan CR, Pearce MS, Sears MR. 2009. Associations between birth weight, early childhood weight gain and adult lung function. *Thorax* 64: 228-32
101. Shi W, Bellusci S, Warburton D. 2007. Lung development and adult lung diseases. *Chest* 132: 651-6
102. Jaddoe VW, Verburg BO, de Ridder MA, Hofman A, Mackenbach JP, Moll HA, Steegers EA, Witteman JC. 2007. Maternal smoking and fetal growth characteristics in different periods of pregnancy: the generation R study. *Am J Epidemiol* 165: 1207-15

103. Gilliland FD, Berhane K, Li YF, Rappaport EB, Peters JM. 2003. Effects of early onset asthma and in utero exposure to maternal smoking on childhood lung function. *Am J Respir Crit Care Med* 167: 917-24
104. Noel A, Xiao R, Perveen Z, Zaman H, Le Donne V, Penn A. 2017. Sex-specific lung functional changes in adult mice exposed only to second-hand smoke in utero. *Respir Res* 18: 104
105. Bjerg A, Hedman L, Perzanowski M, Lundback B, Ronmark E. 2011. A strong synergism of low birth weight and prenatal smoking on asthma in schoolchildren. *Pediatrics* 127: e905-12
106. Burke H, Leonardi-Bee J, Hashim A, Pine-Abata H, Chen Y, Cook DG, Britton JR, McKeever TM. 2012. Prenatal and passive smoke exposure and incidence of asthma and wheeze: systematic review and meta-analysis. *Pediatrics* 129: 735-44
107. Duijts L, Jaddoe VWV, van der Valk RJP, Henderson JA, Hofman A, Raat H, Steegers EAP, Moll HA, de Jongste JC. 2012. Fetal exposure to maternal and paternal smoking and the risks of wheezing in preschool children: the Generation R Study. *Chest* 141: 876-85
108. Thacher JD, Gruzieva O, Pershagen G, Neuman A, Wickman M, Kull I, Melen E, Bergstrom A. 2014. Pre- and postnatal exposure to parental smoking and allergic disease through adolescence. *Pediatrics* 134: 428-34
109. Wu P. 2012. Maternal smoking during pregnancy and its effect on childhood asthma: understanding the puzzle. *Am J Respir Crit Care Med* 186: 941-2
110. Hsu HH, Chiu YH, Coull BA, Kloog I, Schwartz J, Lee A, Wright RO, Wright RJ. 2015. Prenatal Particulate Air Pollution and Asthma Onset in Urban Children. Identifying Sensitive Windows and Sex Differences. *Am J Respir Crit Care Med* 192: 1052-9
111. Brunst KJ, Ryan PH, Brokamp C, Bernstein D, Reponen T, Lockey J, Khurana Hershey GK, Levin L, Grinshpun SA, LeMasters G. 2015. Timing and Duration of Traffic-related Air Pollution Exposure and the Risk for Childhood Wheeze and Asthma. *Am J Respir Crit Care Med* 192: 421-7
112. Fedulov AV, Leme A, Yang Z, Dahl M, Lim R, Mariani TJ, Kobzik L. 2008. Pulmonary exposure to particles during pregnancy causes increased neonatal asthma susceptibility. *Am J Respir Cell Mol Biol* 38: 57-67
113. Hamada K, Suzaki Y, Leme A, Ito T, Miyamoto K, Kobzik L, Kimura H. 2007. Exposure of pregnant mice to an air pollutant aerosol increases asthma susceptibility in offspring. *J Toxicol Environ Health A* 70: 688-95
114. Mauad T, Rivero DH, de Oliveira RC, Lichtenfels AJ, Guimaraes ET, de Andre PA, Kasahara DI, Bueno HM, Saldiva PH. 2008. Chronic exposure to ambient levels of urban particles affects mouse lung development. *Am J Respir Crit Care Med* 178: 721-8
115. Yoshida S, Takano H, Nishikawa M, Miao H, Ichinose T. 2012. Effects of fetal exposure to urban particulate matter on the immune system of male mouse offspring. *Biol Pharm Bull* 35: 1238-43
116. Yang Q, Wen SW, Smith GN, Chen Y, Krewski D, Chen XK, Walker MC. 2006. Maternal cigarette smoking and the risk of pregnancy-induced hypertension and eclampsia. *Int J Epidemiol* 35: 288-93
117. Kajekar R. 2007. Environmental factors and developmental outcomes in the lung. *Pharmacol Ther* 114: 129-45
118. Chen T, Yan YE, Liu S, Liu HX, Yan HY, Hou LF, Qu W, Ping J. 2016. Increased Fetal Thymocytes Apoptosis Contributes to Prenatal Nicotine Exposure-induced Th1/Th2 Imbalance in Male Offspring Mice. *Sci Rep* 6: 39013
119. Land SC, Wilson SM. 2004. Redox Regulation of Lung Development and Perinatal Lung Epithelial Function. *Antioxidants & Redox Signaling* 7: 92-107

120. Breton CV, Byun HM, Wenten M, Pan F, Yang A, Gilliland FD. 2009. Prenatal tobacco smoke exposure affects global and gene-specific DNA methylation. *Am J Respir Crit Care Med* 180: 462-7
121. Chhabra D, Sharma S, Kho AT, Gaedigk R, Vyhlidal CA, Leeder JS, Morrow J, Carey VJ, Weiss ST, Tantisira KG, DeMeo DL. 2014. Fetal lung and placental methylation is associated with in utero nicotine exposure. *Epigenetics* 9: 1473-84
122. Nielsen CH, Larsen A, Nielsen AL. 2016. DNA methylation alterations in response to prenatal exposure of maternal cigarette smoking: A persistent epigenetic impact on health from maternal lifestyle? *Arch Toxicol* 90: 231-45
123. Perera F, Tang WY, Herbstman J, Tang D, Levin L, Miller R, Ho SM. 2009. Relation of DNA methylation of 5'-CpG island of ACSL3 to transplacental exposure to airborne polycyclic aromatic hydrocarbons and childhood asthma. *PLoS One* 4: e4488
124. Hellstrom A, Ley D, Hansen-Pupp I, Hallberg B, Lofqvist C, van Marter L, van Weissenbruch M, Ramenghi LA, Beardsall K, Dunger D, Hard AL, Smith LE. 2016. Insulin-like growth factor 1 has multisystem effects on foetal and preterm infant development. *Acta Paediatr* 105: 576-86
125. Meyer KF, Krauss-Etschmann S, Kooistra W, Reinders-Luinge M, Timens W, Kobzik L, Plosch T, Hylkema MN. 2017. Prenatal exposure to tobacco smoke sex dependently influences methylation and mRNA levels of the Igf axis in lungs of mouse offspring. *Am J Physiol Lung Cell Mol Physiol* 312: L542-L55
126. Meyer KF, Verkaik-Schakel RN, Timens W, Kobzik L, Plosch T, Hylkema MN. 2017. The fetal programming effect of prenatal smoking on Igf1r and Igf1 methylation is organ- and sex-specific. *Epigenetics* 12: 1076-91
127. Devereux G, Litonjua AA, Turner SW, Craig LC, McNeill G, Martindale S, Helms PJ, Seaton A, Weiss ST. 2007. Maternal vitamin D intake during pregnancy and early childhood wheezing. *Am J Clin Nutr* 85: 853-9
128. Devereux G, Turner SW, Craig LC, McNeill G, Martindale S, Harbour PJ, Helms PJ, Seaton A. 2006. Low maternal vitamin E intake during pregnancy is associated with asthma in 5-year-old children. *Am J Respir Crit Care Med* 174: 499-507
129. Whitrow MJ, Moore VM, Rumbold AR, Davies MJ. 2009. Effect of supplemental folic acid in pregnancy on childhood asthma: a prospective birth cohort study. *Am J Epidemiol* 170: 1486-93
130. Haberg SE, London SJ, Stigum H, Nafstad P, Nystad W. 2009. Folic acid supplements in pregnancy and early childhood respiratory health. *Arch Dis Child* 94: 180-4
131. Mikkola HK, Orkin SH. 2006. The journey of developing hematopoietic stem cells. *Development* 133: 3733-44
132. Holladay SD, Smialowicz RJ. 2000. Development of the murine and human immune system: differential effects of immunotoxicants depend on time of exposure. *Environ Health Perspect* 108 Suppl 3: 463-73
133. Perdiguero EG, Geissmann F. 2016. The development and maintenance of resident macrophages. *Nat Immunol* 17: 2-8
134. Palmer AC. 2011. Nutritionally mediated programming of the developing immune system. *Adv Nutr* 2: 377-95
135. Holsapple MP, West LJ, Landreth KS. 2003. Species comparison of anatomical and functional immune system development. *Birth Defects Res B Dev Reprod Toxicol* 68: 321-34
136. Morrisey EE, Hogan BL. 2010. Preparing for the first breath: genetic and cellular mechanisms in lung development. *Dev Cell* 18: 8-23
137. Schittny JC. 2017. Development of the lung. *Cell Tissue Res* 367: 427-44
138. Metzger RJ, Klein OD, Martin GR, Krasnow MA. 2008. The branching programme of mouse lung development. *Nature* 453: 745-50

139. Yang J, Hernandez BJ, Martinez Alanis D, Narvaez del Pilar O, Vila-Ellis L, Akiyama H, Evans SE, Ostrin EJ, Chen J. 2016. The development and plasticity of alveolar type 1 cells. *Development (Cambridge, England)* 143: 54-65
140. Flodby P, Li C, Liu Y, Wang H, Rieger ME, Minoo P, Crandall ED, Ann DK, Borok Z, Zhou B. 2017. Cell-specific expression of aquaporin-5 (Aqp5) in alveolar epithelium is directed by GATA6/Sp1 via histone acetylation. *Sci Rep* 7: 3473
141. Rozycki HJ, Hendricks-Muñoz KD. 2017. 81 - Structure and Development of Alveolar Epithelial Cells. In *Fetal and Neonatal Physiology (Fifth Edition)*, ed. RA Polin, SH Abman, DH Rowitch, WE Benitz, WW Fox, pp. 809-13: Elsevier
142. Whitsett JA, Weaver TE. 2015. Alveolar development and disease. *American journal of respiratory cell and molecular biology* 53: 1-7
143. Alcorn JL. 2017. Chapter 4 - Pulmonary Surfactant Trafficking and Homeostasis. In *Lung Epithelial Biology in the Pathogenesis of Pulmonary Disease*, ed. VK Sidhaye, M Koval, pp. 59-75. Boston: Academic Press
144. Desai TJ, Brownfield DG, Krasnow MA. 2014. Alveolar progenitor and stem cells in lung development, renewal and cancer. *Nature* 507: 190-4
145. Okubo T, Knoepfler PS, Eisenman RN, Hogan BLM. 2005. Nmyc plays an essential role during lung development as a dosage-sensitive regulator of progenitor cell proliferation and differentiation. 132: 1363-74
146. Rockich BE, Hrycaj SM, Shih HP, Nagy MS, Ferguson MA, Kopp JL, Sander M, Wellik DM, Spence JR. 2013. Sox9 plays multiple roles in the lung epithelium during branching morphogenesis. *Proc Natl Acad Sci U S A* 110: E4456-64
147. Rawlins EL, Clark CP, Xue Y, Hogan BLM. 2009. The Id2+ distal tip lung epithelium contains individual multipotent embryonic progenitor cells. *Development (Cambridge, England)* 136: 3741-5
148. Perl A-KT, Kist R, Shan Z, Scherer G, Whitsett JA. 2005. Normal lung development and function after Sox9 inactivation in the respiratory epithelium. *genesis* 41: 23-32
149. Nagata K, Masumoto K, Uesugi T, Yamamoto S, Yoshizaki K, Fukumoto S, Nonaka K, Taguchi T. 2007. Effect of insulin-like-growth factor and its receptors regarding lung development in fetal mice. *Pediatr Surg Int* 23: 953-9
150. Pais RS, Moreno-Barriuso N, Hernandez-Porras I, Lopez IP, De Las Rivas J, Pichel JG. 2013. Transcriptome analysis in prenatal IGF1-deficient mice identifies molecular pathways and target genes involved in distal lung differentiation. *PLoS One* 8: e83028
151. Wang Z, Li W, Guo Q, Wang Y, Ma L, Zhang X. 2018. Insulin-Like Growth Factor-1 Signaling in Lung Development and Inflammatory Lung Diseases. *BioMed research international* 2018: 6057589-
152. McEvoy CT, Spindel ER. 2017. Pulmonary Effects of Maternal Smoking on the Fetus and Child: Effects on Lung Development, Respiratory Morbidities, and Life Long Lung Health. *Paediatric respiratory reviews* 21: 27-33
153. Veras MM, de Oliveira Alves N, Fajersztajn L, Saldiva P. 2017. Before the first breath: prenatal exposures to air pollution and lung development. *Cell and Tissue Research* 367: 445-55
154. Lunding LP, Webering S, Vock C, Behrends J, Wagner C, Holscher C, Fehrenbach H, Wegmann M. 2015. Poly(inosinic-cytidylic) acid-triggered exacerbation of experimental asthma depends on IL-17A produced by NK cells. *J Immunol* 194: 5615-25
155. Zazara DE, Perani CV, Solano ME, Arck PC. 2018. Prenatal stress challenge impairs fetal lung development and asthma severity sex-specifically in mice. *J Reprod Immunol* 125: 100-5
156. Chen J, Li H, Addabbo F, Zhang F, Pelger E, Patschan D, Park H-C, Kuo M-C, Ni J, Gobe G, Chander PN, Nasjletti A, Goligorsky MS. 2009. Adoptive transfer of syngeneic

bone marrow-derived cells in mice with obesity-induced diabetes: selenoorganic antioxidant ebselen restores stem cell competence. *The American journal of pathology* 174: 701-11

157. Pfaffl MW. 2001. A new mathematical model for relative quantification in real-time RT-PCR. *Nucleic Acids Res* 29: e45
158. Stevens WW, Kim TS, Pujanauski LM, Hao X, Braciale TJ. 2007. Detection and quantitation of eosinophils in the murine respiratory tract by flow cytometry. *J Immunol Methods* 327: 63-74
159. Misharin AV, Morales-Nebreda L, Mutlu GM, Budinger GR, Perlman H. 2013. Flow cytometric analysis of macrophages and dendritic cell subsets in the mouse lung. *Am J Respir Cell Mol Biol* 49: 503-10
160. Hsia CC, Hyde DM, Ochs M, Weibel ER, Structure AEJTFoQAoL. 2010. An official research policy statement of the American Thoracic Society/European Respiratory Society: standards for quantitative assessment of lung structure. *Am J Respir Crit Care Med* 181: 394-418
161. Willet KE, McMenamin P, Pinkerton KE, Ikegami M, Jobe AH, Gurrin L, Sly PD. 1999. Lung morphometry and collagen and elastin content: changes during normal development and after prenatal hormone exposure in sheep. *Pediatr Res* 45: 615-25
162. Triantaphyllopoulos K, Hussain F, Pinart M, Zhang M, Li F, Adcock I, Kirkham P, Zhu J, Chung KF. 2011. A model of chronic inflammation and pulmonary emphysema after multiple ozone exposures in mice. *American journal of physiology. Lung cellular and molecular physiology* 300: L691-L700
163. Myou S, Leff AR, Myo S, Boetticher E, Tong J, Meliton AY, Liu J, Munoz NM, Zhu X. 2003. Blockade of inflammation and airway hyperresponsiveness in immune-sensitized mice by dominant-negative phosphoinositide 3-kinase-TAT. *J Exp Med* 198: 1573-82
164. Ronchetti S, Migliorati G, Riccardi C. 2015. GILZ as a Mediator of the Anti-Inflammatory Effects of Glucocorticoids. *Front Endocrinol (Lausanne)* 6: 170
165. Douros K, Moustaki M, Tsabouri S, Papadopoulou A, Papadopoulos M, Priftis KN. 2017. Prenatal Maternal Stress and the Risk of Asthma in Children. *Frontiers in pediatrics* 5: 202-
166. Laplante DP, Luheshi G, King S. 2014. Prenatal maternal stress exposure and immune function in the offspring AU - Veru, Franz. *Stress* 17: 133-48
167. Dehmel S, Nathan P, Bartel S, El-Merhie N, Scherb H, Milger K, John-Schuster G, Yildirim AO, Hylkema M, Irmler M, Beckers J, Schaub B, Eickelberg O, Krauss-Etschmann S. 2018. Intrauterine smoke exposure deregulates lung function, pulmonary transcriptomes, and in particular insulin-like growth factor (IGF)-1 in a sex-specific manner. *Sci Rep* 8: 7547
168. Sathish V, Prakash YS. 2016. Chapter 6 - Sex Differences in Pulmonary Anatomy and Physiology: Implications for Health and Disease A2 - Neigh, Gretchen N. In *Sex Differences in Physiology*, ed. MM Mitzelfelt, pp. 89-103. Boston: Academic Press
169. Seaborn T, Simard M, Provost PR, Piedboeuf B, Tremblay Y. 2010. Sex hormone metabolism in lung development and maturation. *Trends Endocrinol Metab* 21: 729-38
170. Kaltofen T, Haase M, Thome UH, Laube M. 2015. Male Sex is Associated with a Reduced Alveolar Epithelial Sodium Transport. *PLoS One* 10: e0136178
171. Beato M. 1989. Gene regulation by steroid hormones. *Cell* 56: 335-44
172. Adcock IM, Gilbey T, Gelder CM, Chung KF, Barnes PJ. 1996. Glucocorticoid receptor localization in normal and asthmatic lung. *American Journal of Respiratory and Critical Care Medicine* 154: 771-82

173. Condon J, Gosden C, Gardener D, Nickson P, Hewison M, Howie AJ, Stewart PM. 1998. Expression of type 2 11beta-hydroxysteroid dehydrogenase and corticosteroid hormone receptors in early human fetal life. *J Clin Endocrinol Metab* 83: 4490-7
174. Sweezey N, Mawdsley C, Ghibu F, Song L, Buch S, Moore A, Antakly T, Post M. 1995. Differential regulation of glucocorticoid receptor expression by ligand in fetal rat lung cells. *Pediatr Res* 38: 506-12
175. Bird AD, McDougall ARA, Seow B, Hooper SB, Cole TJ. 2015. Glucocorticoid regulation of lung development: lessons learned from conditional GR knockout mice. *Molecular endocrinology (Baltimore, Md.)* 29: 158-71
176. Scott SM, Rose SR. 2018. Use of Glucocorticoids for the Fetus and Preterm Infant. *Clinics in Perinatology* 45: 93-102
177. Harris C, Crichton S, Zivanovic S, Lunt A, Calvert S, Marlow N, Peacock JL, Greenough A. 2018. Effect of dexamethasone exposure on the neonatal unit on the school age lung function of children born very prematurely. *PloS one* 13: e0200243-e
178. Qin G, Lo JW, Marlow N, Calvert SA, Greenough A, Peacock JL. 2017. Postnatal dexamethasone, respiratory and neurodevelopmental outcomes at two years in babies born extremely preterm. *PloS one* 12: e0181176-e
179. Massaro GD, Massaro D. 1992. Formation of alveoli in rats: postnatal effect of prenatal dexamethasone. *American Journal of Physiology-Lung Cellular and Molecular Physiology* 263: L37-L41
180. Vyas J, Kotecha S. 1997. Effects of antenatal and postnatal corticosteroids on the preterm lung. *Arch Dis Child Fetal Neonatal Ed* 77: F147-50
181. Bolt RJ, van Weissenbruch MM, Lafeber HN, Delemarre-van de Waal HA. 2001. Glucocorticoids and lung development in the fetus and preterm infant. *Pediatr Pulmonol* 32: 76-91
182. Okret S, Dong Y, Brönnegård M, Gustafsson JÅ. 1991. Regulation of glucocorticoid receptor expression. *Biochimie* 73: 51-9
183. Gross KL, Lu NZ, Cidlowski JA. 2009. Molecular mechanisms regulating glucocorticoid sensitivity and resistance. *Molecular and cellular endocrinology* 300: 7-16
184. Ramamoorthy S, Cidlowski JA. 2013. Ligand-induced repression of the glucocorticoid receptor gene is mediated by an NCoR1 repression complex formed by long-range chromatin interactions with intragenic glucocorticoid response elements. *Molecular and cellular biology* 33: 1711-22
185. Kalinyak JE, Griffin CA, Hamilton RW, Bradshaw JG, Perlman AJ, Hoffman AR. 1989. Developmental and hormonal regulation of glucocorticoid receptor messenger RNA in the rat. *The Journal of clinical investigation* 84: 1843-8
186. Rosenfeld CS. 2015. Sex-Specific Placental Responses in Fetal Development. *Endocrinology* 156: 3422-34
187. Pérez Tarazona S, Solano Galán P, Bartoll Alguacil E, Alfonso Diego J. 2018. Bronchopulmonary dysplasia as a risk factor for asthma in school children and adolescents: A systematic review. *Allergologia et Immunopathologia* 46: 87-98
188. Voge GA, Katusic SK, Qin R, Juhn YJ. 2015. Risk of Asthma in Late Preterm Infants: A Propensity Score Approach. *The journal of allergy and clinical immunology. In practice* 3: 905-10
189. Holgate ST. 2011. The sentinel role of the airway epithelium in asthma pathogenesis. *Immunological Reviews* 242: 205-19
190. Beigelman A, Bacharier LB. 2016. Early-life respiratory infections and asthma development: role in disease pathogenesis and potential targets for disease prevention. *Current opinion in allergy and clinical immunology* 16: 172-8

191. Osman M, Tagiyeva N, Wassall HJ, Ninan TK, Devenny AM, McNeill G, Helms PJ, Russell G. 2007. Changing trends in sex specific prevalence rates for childhood asthma, eczema, and hay fever. *Pediatr Pulmonol* 42: 60-5
192. Pignataro FS, Bonini M, Forgione A, Melandri S, Usmani OS. 2017. Asthma and gender: The female lung. *Pharmacol Res* 119: 384-90
193. Ridolo E, Incorvaia C, Martignago I, Caminati M, Canonica GW, Senna G. 2018. Sex in Respiratory and Skin Allergies. *Clin Rev Allergy Immunol*
194. Melgert BN, Postma DS, Kuipers I, Geerlings M, Luinge MA, van der Strate BWA, Kerstjens HAM, Timens W, Hylkema MN. 2005. Female mice are more susceptible to the development of allergic airway inflammation than male mice. *Clinical & Experimental Allergy* 35: 1496-503
195. Corteling R, Trifilieff A. 2004. Gender comparison in a murine model of allergen-driven airway inflammation and the response to budesonide treatment. *BMC pharmacology* 4: 4-
196. Hayashi T, Adachi Y, Hasegawa K, Morimoto M. 2003. Less Sensitivity for Late Airway Inflammation in Males than Females in BALB/c Mice. *Scandinavian Journal of Immunology* 57: 562-7
197. Melgert BN, Ray A, Hylkema MN, Timens W, Postma DS. 2007. Are there reasons why adult asthma is more common in females? *Curr Allergy Asthma Rep* 7: 143-50
198. Patrone C, Cassel TN, Pettersson K, Piao Y-S, Cheng G, Ciana P, Maggi A, Warner M, Gustafsson J-A, Nord M. 2003. Regulation of postnatal lung development and homeostasis by estrogen receptor beta. *Molecular and cellular biology* 23: 8542-52
199. Madan T, Kishore U, Singh M, Strong P, Clark H, Hussain EM, Reid KB, Sarma PU. 2001. Surfactant proteins A and D protect mice against pulmonary hypersensitivity induced by Aspergillus fumigatus antigens and allergens. *The Journal of clinical investigation* 107: 467-75
200. Nielsen HC. 1989. Epidermal growth factor influences the developmental clock regulating maturation of the fetal lung fibroblast. *Biochim Biophys Acta* 1012: 201-6
201. McCants DD, Nielsen HC, Pham LD, Ramadurai SM, Dammann CEL. 2000. Androgen Regulation of Signaling Pathways in Late Fetal Mouse Lung Development*. *Endocrinology* 141: 2923-9
202. Hamilton LM, Torres-Lozano C, Puddicombe SM, Richter A, Kimber I, Dearman RJ, Vrugt B, Aalbers R, Holgate ST, Djukanović R, Wilson SJ, Davies DE. 2003. The role of the epidermal growth factor receptor in sustaining neutrophil inflammation in severe asthma. *Clinical & Experimental Allergy* 33: 233-40
203. Habibovic A, Hristova M, Heppner DE, Danyal K, Ather JL, Janssen-Heininger YMW, Irvin CG, Poynter ME, Lundblad LK, Dixon AE, Geiszt M, van der Vliet A. 2016. DUOX1 mediates persistent epithelial EGFR activation, mucous cell metaplasia, and airway remodeling during allergic asthma. *JCI insight* 1: e88811-e
204. Becklake MR, Kauffmann F. 1999. Gender differences in airway behaviour over the human life span. *Thorax* 54: 1119-38

10 Acknowledgement

First and foremost, I would like to express my heartfelt gratitude to my supervisor Prof. Petra Arck for giving me the opportunity to work on this project. I thank you for your support, constant mentoring and the motivation you inspired in me. With your guidance and advice, I was able to grow as a person and scientist. I would also like to thank Maria Emilia Solano, who guided me during my research study with her scientific knowledge, patience and natural generosity. I thank you for all the fruitful discussions and advice that broadened my skills and knowledge, and for proofreading my thesis. I am deeply grateful for meeting you and learning from both of you.

I would like also to thank Prof. Ania Muntau and Prof. Gisa Tiegs for participating in my Thesis Committee. I am grateful for your insightful comments, support, advice and mentoring that allowed me to progress and complete my studies in the best way possible.

I thank Prof. Udo Markert for accepting to be the second reviewer of this thesis and part of the evaluating committee at the defense.

Next, I would like to thank all my colleagues, former and current members of the Arck group: Géraldine, Hendrik, Ina, Janina, Kathrin, Lesley, Lilja, Mayumi, Roswitha, Sophie, Steven and Veronika. I would also like to thank Clara for her advice and support, Kristin for providing me with her flow cytometry expertise, and Detlev Riller for his excellent graphic art. Special thanks goes to Thomas, Agnes and Christopher for their assistance on the experiments, for supporting me during long working days and for all the happy moments that we shared during the past years.

Many thanks I owe to Alexandra Hierweger for all the productive discussions, advice and especially, for her valuable assistance not only with experiments but also with the german language. Thank you for your patience and time.

Finally, I would like to express my deepest gratitude to my beloved parents for being there for me throughout life, for encouraging me all the time and for supporting my dreams. Many thanks to my brother John, for his friendship, love and support.

Last but not least, I would like to thank you, Tasos, my husband, friend and colleague, for always being there for me, supporting me and encouraging me. Your guidance and help kept me going during my studies and I thank you for that. Thank you for believing in me.

11 Curriculum vitae

“ Der Lebenslauf wurde aus datenschutzrechtlichen Gründen entfernt”.

12 Affidavit

Ich versichere ausdrücklich, dass ich die Arbeit selbständig und ohne fremde Hilfe verfasst, andere als die von mir angegebenen Quellen und Hilfsmittel nicht benutzt und die aus den benutzten Werken wörtlich oder inhaltlich entnommenen Stellen einzeln nach Ausgabe (Auflage und Jahr des Erscheinens), Band und Seite des benutzten Werkes kenntlich gemacht habe.

Ferner versichere ich, dass ich die Dissertation bisher nicht einem Fachvertreter an einer anderen Hochschule zur Überprüfung vorgelegt oder mich anderweitig um Zulassung zur Promotion beworben habe.

Ich erkläre mich einverstanden, dass meine Dissertation vom Dekanat der Medizinischen Fakultät mit einer gängigen Software zur Erkennung von Plagiaten überprüft werden kann.

Unterschrift: